PHYTOSTEROL ADSORPTION: RESINS AND SYNTHESIZED MOLECULAR IMPRINTED SILICA

CHINAKRIT LADADOK

A THESIS SUBMITTED IN PARTIAL FULFILLMENT
OF THE REQUIREMENT FOR THE DEGREE OF
DOCTOR OF ENGINEERING IN CHEMICAL ENGINEERING
FACULTY OF ENGINEERING
KING MONGKUT'S INSTITUTE OF TECHNOLOGY LADKRABANG
2019

KMITL-2019-EN-D-228-006

PHYTOSTEROL ADSORPTION: RESINS AND SYNTHESIZED MOLECULAR IMPRINTED SILICA

CHINAKRIT LADADOK

A THESIS SUBMITTED IN PARTIAL FULFILLMENT
OF THE REQUIREMENT FOR THE DEGREE OF
DOCTOR OF ENGINEERING IN CHEMICAL ENGINEERING
FACULTY OF ENGINEERING

หัวข้อวิทยานิพนธ์	การดูดซับไฟโตสเตอรอล: ตัวดูดซับแบบเรซินและตัวดูดซับลอกแบบโมเลกุล
นักศึกษา	นายชินกฤต ละดาดก
รหัสประจำตัว	55610351
ปริญญา	วิศวกรรมศาสตรดุษฎีบัณฑิต
สาขาวิชา	วิศวกรรมเคมี
พ.ศ.	2562
อาจารย์ที่ปรึกษาวิทยานิพนธ์	รศ.ดร. ดวงกมล ณ ระนอง

บทคัดย่อ

งานวิจัยนี้มุ่งเน้นไปที่การใช้การดูดซับและการคายซับในสภาวะที่ไม่รุนแรงในกระบวนการนำกลับสารไฟโตสเตอรอล โดยตัวดูดซับทางการค้า 3 ชนิดคือ เรซินที่มีคุณสมบัติเป็นกรดแก่ เรซินที่มีคุณสมบัติเป็นเบสแก่และเรซินที่มีคุณสมบัติเป็นเบสอ่อนได้ถูกนำมาใช้ในการศึกษาประสิทธิภาพการดูดซับไฟโตสเตอรอล และตัวดูดซับซิลิกาลอกแบบโมเลกุลได้ถูกสังเคราะห์ขึ้นเพื่อใช้เป็นตัวดูดซับทางเลือกสำหรับใช้ในกระบวนการนำกลับไฟโตสเตอรอล โดยเพื่อให้ได้ข้อมูลที่เป็นประโยชน์สำหรับใช้ออกแบบกระบวนการดูดซับ การทดลองสมดุลการดูดซับของไฟโตสเตอรอลบนเรซินทางการค้าได้ถูกทำขึ้นโดยใช้สารละลายสติกมาสเตอรอลในนอร์มอลเฮปเทน การศึกษาพฤติกรรมการดูดซับของไฟโตสเตอรอลบนเรซินเกรดการค้าแสดงให้เห็นว่า อัตราการดูดซับของไฟโตสเตอรอลบนเรซินทั้ง 3 ชนิดสามารถอธิบายได้ดีโดยใช้สมการอัตราเร็วปฏิกิริยาเทียมอันดับสอง ข้อมูลสมดุลการดูดซับสามารถอธิบายได้โดยสมการสมดุลการดูดซับของฟรุนดลิช ตัวแปรทางอุณหพลศาสตร์แสดงให้เห็นว่าการดูดซับเป็นกระบวนการคายความร้อนและเกิดขึ้นได้เอง ในการแสดงให้เห็นถึงศักยภาพของกระบวนการที่นำเสนอ การดูดซับไฟโตสเตอรอลในนอร์มอลเฮปเทนและการคายซับไฟโตสเตอรอลในเอทานอลได้ถูกใช้เพื่อประเมินประสิทธิภาพของตัวดูดซับในระบบแบบกะ โดยเรซินที่มีคุณสมบัติเป็นเบสแก่และเรซินที่มีคุณสมบัติเป็นเบสอ่อนได้ถูกเลือกมาใช้ในกระบวนการเนื่องจากมีปริมาณการดูดซับไฟโตสเตอรอลสูงกว่าเรซินที่มีคุณสมบัติเป็นกรดแก่ ในขั้นตอนการดูดซับพบว่า เรซินที่มีคุณสมบัติเป็นเบสอ่อนมีปริมาณการดูดซับไฟโตสเตอรอลเท่ากับ 43.75 มิลลิกรัมต่อกรัมตัวดูดซับ มากกว่าเรซินที่มีคุณสมบัติเป็นเบสแก่ 1.1 เท่า ในขั้นตอนการคายซับพบว่า เรซินที่มีคุณสมบัติเป็นเบสแก่แสดงร้อยละการคายซับเท่ากับร้อยละ 79.94 มากกว่าเรซินที่มีคุณสมบัติเป็นเบสอ่อน 1.3 เท่า โดยเรซินทั้ง 2 ชนิดนี้แสดงร้อยละการนำกลับไฟโตสเตอรอลระหว่างร้อยละ 30 ถึง 37 ส่วนในกรณีของตัวดูดซับซิลิกาลอกแบบโมเลกุล ผลการทดลองแสดงให้เห็นว่าตัวดูดซับซิลิกาลอกแบบโมเลกุลมีปริมาณการดูดซับไฟโตสเตอรอลถึง 68.01 มิลลิกรัมต่อกรัมตัวดูดซับ มากกว่าตัวดูดซับซิลิกาไม่ลอกแบบโมเลกุล 1.4 เท่า และยังแสดงร้อยละการนำกลับไฟโตสเตอรอลมากกว่าตัวดูดซับซิลิกาไม่ลอกแบบโมเลกุลถึง 2.0 เท่า นอกจากนี้ตัวดูดซับซิลิกาลอกแบบโมเลกุลยังแสดงประสิทธิภาพในการนำกลับไฟโตสเตอรอลสูงกว่าเรซินที่

มีคุณสมบัติเป็นเบสแก่และเรซินที่มีคุณสมบัติเป็นเบสอ่อนอีกด้วย ในการศึกษาผลของตัวแปรในการสังเคราะห์ตัวดูดซับซิลิกาลอกแบบโมเลกุลต่อพื้นที่ผิวจำเพาะและปริมาณการดูดซับไฟโตสเตอรอล พบว่า ค่าความเป็นกรด-เบสของสารละลายส่งผลต่อพื้นที่ผิวจำเพาะและปริมาณการดูดซับไฟโตสเตอรอลของตัวดูดซับซิลิกาลอกแบบโมเลกุลมากที่สุด

Thesis	Phytosterol adsorption: Resins and synthesized molecular imprinted silica
Student	Mr. Chinakrit Ladadok
Student ID.	55610351
Degree	Doctor of Engineering
Program	Chemical Engineering
Year	2019
Thesis Advisor	Assoc. Prof. Dr. Duangkamol Na-Ranong

ABSTRACT

This study focused on the selection of adsorption and desorption processes under mild condition for phytosterol recovery. Three types of ion-exchange resins (strong acid resin: SA-R, strong base resin: SB-R, and weak base resin: WB-R) were used to study the efficiency of phytosterol adsorption, and molecular imprinted silica was synthesized and used as an alternative adsorbent for phytosterol recovery. In order to obtain useful information for the design of an adsorption process, an experiment on the adsorption of phytosterol on three resins was performed by using a model solution of stigmasterol in n-heptane. The study of behavior of phytosterol adsorption on three resins showed that the adsorption rate could be well described by pseudo-second-order kinetics model. The equilibrium adsorption data fitted better with a Freundlich isotherm. The thermodynamic parameters indicated that the adsorption was an exothermic and spontaneous process. To investigate the potential of the proposed two-step process, adsorption of phytosterol in n-heptane and desorption of phytosterol in ethanol were performed by using a batch system. SB-R and WB-R were selected as the promising adsorbents to be used in the proposed process due to they showed a higher adsorption capacity than that of SA-R. In the adsorption step, the adsorption capacity of phytosterol on WB-R was 43.75 mg/g-adsorbent which was 1.1 times of that achieved by SB-R. In the desorption step, the desorption percentage of SB-R was 78.94 % which was 1.3 times of that achieved by WB-R, and the recovery

percentage of both SB-R and WB-R were in the range of 30-37 %. In the case of molecular imprinted silica (MIS). The results showed that the adsorption capacity of MIS was 68.01 mg/g-adsorbent which was 1.4 times of that achieved by non imprinted silica (NIS), and the recovery percentage of phytosterol from MIS was 2.0 times higher than that from NIS. In addition, MIS showed a higher efficiency in phytosterol recovery than those achieved by SB-R and WB-R. The effects of synthesis factors on the BET surface area and the adsorption capacity of MIS were studied. An analysis of response surface showed that the pH of solution was found to have the largest effect on the BET surface area and the adsorption capacity of MIS.

Acknowledgement

I would like to thank all of the people who have contributed to this work. First, I sincerely thank Assoc. Prof. Dr. Duangkamol Na-Ranong for giving me an opportunity to improve myself as a researcher and for her valuable suggestions.

I would also like to thank Thailand Research Fund (TRF) and King Mongkut's Institute of Technology Ladkrabang (KMITL) for offering their Royal Golden Jubilee Ph.D. program (PHD/0021/2555) as well as the National Research Council of Thailand (NRCT) for providing the financial support.

I would also like to thank Mr. Sarawut Sinpichai for his assistance in the surface analysis of silica.

In addition, I would like to thank the officers of the Department of Chemical Engineering, King Mongkut's Institute of Technology Ladkrabang for their research support.

Finally, I sincerely thank my family for giving me an opportunity to study and supporting me to the fullest extent.

Chinakrit Ladadok

Table of Contents

Table of Contents (cont.)

List of Tables

List of Figures

List of Figures (cont.)

Nomenclatures

$a_{s,BET}$	BET surface area (m^2/g)
%Ad	Adsorption percentage of phytosterol (%)
C_0	Liquid phase concentration of phytosterol at initial (mg/g-solution)
C_e	Liquid phase concentration of phytosterol at equilibrium (mg/g-solution)
C_{HCl}	Concentration of hydrochloric acid in the sol-gel solution (mol/L)
C_t	Liquid phase concentration of phytosterol at time t (mg/g-solution)
% De	Desorption percentage of phytosterol (%)
$\triangle G$	Gibb's free energy change (kJ/mol)
$\triangle H$	Enthalpy change (kJ/mol)
k_1	The adsorption rate constant of pseudo-first-order (min^{-1})
k_2	The adsorption rate constant of pseudo-second-order (g-adsorbent/(mg·min))
K_F	Adsorption equilibrium constant in Freundlich model (mg/(g-adsorbent(mg/g-solution)$^{1/n}$))
K_{La}	Adsorption equilibrium constant in Langmuir model (g-solution/mg)
K_{Li}	Adsorption equilibrium constant in linear model (g-solution/g-adsorbent)
n	Freundlich adsorption isotherm constant
q_e	Adsorption capacity at equilibrium (mg/g-adsorbent)
q_m	The monolayer capacity of the adsorbent (mg/g-adsorbent)
q_t	The adsorption capacity at time t (mg/g-adsorbent)
R^2	Coefficient of determination (%)
%Re	Recovery percentage of phytosterol (%)
$\triangle S$	Entropy change (kJ/(mol·K))
t	time (min)
T	Temperature (K)
W_{Ads}	Weight of adsorbent used (g)
W_{Sol}	Weight of the solution (g)
$W_{St,Ad}$	Weight of phytosterol adsorbed on adsorbent (mg)
$W_{St,De}$	Weight of phytosterol desorbed from adsorbent (mg)
W_T	Total weight of phytosterol in the solution (mg)

Chapter 1
Introduction

1.1 Rationale and problem

Deodorizer distillate (DD) is a major byproduct from vegetable oil refining process. It consists of various hydrocarbons including free fatty acids (FFA), monoglycerides (MG), diglycerides (DG), triglycerides (TG), and small amount of some bioactive compounds [1]. The amount of FFA in DD varies around 25 to 82.5 wt% depending on type of vegetable oil, refining method, and condition [2]. In recent years, large amount of DD has been annually generated due to high demand of biodiesel. Based on the amount of crude palm oil produced in 2014 to 2016 in Thailand, Indonesia and Malaysia (53 million ton per year), the annually generated amount of palm fatty acid distillate (PFAD) was about 3 million ton per year [3-9]. To make overall process of biodiesel production become more economical, reasonable, and environmental friendly, DD has been utilized as a low cost raw material for production of biodiesel [9] and as a natural resource of phytonutrients such as tocopherols, squalene, and phytosterols [2]. Therefore, the use of deodorizer distillate as a source of phytosterols may increase the economical value of vegetable oil production.

Phytosterols have several beneficial bioactivities and have been widely used in food, cosmetics, and pharmaceutical industries. As summarized in an excellent review [10], phytosterols have been successfully recovered from DD by several methods. In general, these methods consist of several steps of chemical and physical treatments. Since removal of undesired compounds (FFA and glycerides) from DD by distillation requires relatively high temperature and extremely low pressure, it is necessary to transform these undesired compounds into the forms that can be separated more easily. There are two main approaches to recover phytosterol from DD. In one approach, FFA in DD was saponified and the resulted soap was removed from the obtained mixture by simple solid-liquid separation. In the last step, phytosterols were separated from the liquid mixture of unsaponifiable components by using either vacuum distillation or cold crystallization [11-13]. In the other

approach, FFA and glycerides were chemically transformed to fatty acid alkyl esters (FAAE) by esterification and transesterification, respectively [14-18]. Then, either vacuum distillation or molecular distillation was applied to remove large fraction of FAAE. In this phytosterol pre-concentration step, physical treatments were usually applied to obtain high yield of phytosterol recovery and to reduce the size of the equipment used in the downstream process. Similar to the former approach, cold crystallization was also applied as the last step of phytosterol isolation. Although these approaches have been successfully applied to recover phytosterol from DDs, the processes face a major problem of extensive energy requirement; vacuum distillation usually operates at 1×10^{-3} to 1.33 mbar and 413 to 623 K to vaporize large quantity of the undesired compounds [11, 15-17, 19], and cold crystallization usually operates at low temperature in the range of 253 to 288 K [12-18, 20-22]. Therefore, a method with higher efficiency and more economical use of energy should be developed to serve the rapid growth of recent phytosterol demand. Adsorption is widely used in separation of minor components from liquid or gas mixture. In recent years, adsorption and desorption processes have been used to recovery of phytosterol from tall oil. Barder [23] described adsorption and desorption processes that used activated carbon as an adsorbent. In desorption step, monochlorobenzene was used as a desorbent to separate phytosterol from activated carbon at 423 K. This method yielded a phytosterol recovery of 89 wt% and a purity of 77.6 wt%. Barder et al. [24] reported adsorption and desorption processes that used carbonaceous pyropolymer as an adsorbent. In desorption step, toluene was used as a desorbent to separate phytosterol from carbonaceous pyropolymer at 397 K. This proposed method yielded a phytosterol product that had a recovery of 90 wt% and a purity of 50 wt%. In addition, Barder et al. [25] used magnesium silicate as an adsorbent for adsorption of phytosterol. In desorption step, Methyl-t-butyl ether (MTBE) was used as a desorbent to separate phytosterol from magnesium silicate at the temperature range of 293-503 K. The obtained phytosterol had a high recovery of 50-95 wt% and purity of 80-95 wt%. These processes showed that activated carbon, carbonaceous pyropolymer, and magnesium silicate were effective adsorbents for recovery of phytosterol. However, the desorption step was necessary to use toxic solvents at very high temperature to obtain phytosterol with high recovery and purity.

Therefore, this study focused on the selection of adsorption and desorption processes under mild condition for phytosterol recovery. The proposed process consisted of adsorption of phytosterol at 303 K and desorption of phytosterol in non-toxic ethanol at 343 K. Based on chemical resistance and simplicity of operation, three types of commercial grade styrene-divinylbenzene copolymer ion-exchange resin (strong acid resin: SA-R, strong base resin: SB-R, and weak base resin: WB-R) were considered as attractive adsorbents in the physterol recovery process. SA-R was selected to use in this study due to the sulfonic acid groups on the surface of SA-R can be able to interact with bases by strong electrostatic interaction [26]. SB-R with quaternary amine groups and WB-R with both quaternary and tertiary amine groups were also selected to use in this study. As reported by Anasthas and Gaikar [27], alkylphenols adsorption on anion-exchange resin occurred through a weak hydrogen bond between amine group on anion-exchange resin and hydroxyl group in organic compound. To investigate behavior of physterol adsorption on SA-R, SB-R, and WB-R, isothermal batch adsorption was performed using a model solution of stigmasterol in n-heptane to evaluate adsorption capacity. Kinetics of phytosterol adsorption was evaluated based on pseudo-first-order and pseudo-second-order models. Adsorption data at equilibrium were analyzed based on Langmuir, Freundlich, and linear isotherms and three important thermodynamics parameters (i.e. Gibb's free energy change, enthalpy change, and entropy change) were calculated and the adsorption behavior was discussed based on the calculated thermodynamics parameters. This information can be useful for selection of the operating conditions of the adsorbent. In addition, Silica is also an interesting material to use as an alternative adsorbent for phytosterol recovery due to numerous remarkable properties such as high porosity, high specific surface area, high stability and easily synthesized. This study also focused on a synthesis of molecular imprinted silica with phytosterol as the template molecule and using the imprinting silica as an efficient adsorbent. The effect of synthesis factors were studied simultaneously by using a central composite design in order to obtain optimal conditions for the synthesis of a high adsorption-capacity molecular imprinted silica for phytosterol. The results of this study will demonstrate the feasibility of using adsorption and desorption process under mild condition for phytosterol recovery and indicate the efficiencies of adsorbents used for phytosterol recovery. In addition, this study will also demonstrate the feasibility

of synthesis of molecular imprinted silica by using phytosterol as a template molecule.

1.2 Objectives of the research

1.2.1 To study the feasibility of using an adsorption method under mild condition to recover phytosterol.

1.2.2 To study the feasibility of synthesis of molecular imprinted silica by using phytosterol as a template molecule and using the imprinting silica as an efficient adsorbent.

1.3 Scope of the study

1.3.1 Study behavior of phytosterol adsorption on ion-exchange resins by using isothermal batch adsorption of phytosterol in a model solution in order to evaluate the kinetics, equilibrium, and thermodynamics of phytosterol adsorption.

1.3.2 Study batch experiments for adsorption of phytosterol in model solution and for desorption of phytosterol from ion-exchange resins.

1.3.3 Synthesis of a molecular imprinted silica by using phytosterol as a template molecule.

1.3.4 Study the effect of synthesis factors of molecular imprinted silica on the adsorption of phytosterol.

1.4 Research expectations

1.4.1 The proposed process can demonstrate the feasibility of phytosterol recovery by an adsorption process.

1.4.2 The experimental data can be used for process design as well as development of a high efficiency adsorbent for separation of phytosterol.

Chapter 2
Literature Review

2.1 Phytosterols

2.1.1 Introduction of phytosterols

Phytosterols are members of triterpenes compounds with similar chemical structure as cholesterol [28]. Both consist of steroid nucleus, a hydroxyl group and a double bond between carbons number 5 and 6. While cholesterol has an alkyl side chain consisted of 8 carbon atoms, most phytosterol s' alkyl side chains contain 9 or 10 carbon atoms. Over 200 different types of phytosterols have been reported. The most abundant of them are brassicasterol, campesterol, stigmasterol, and beta-sitosterol [29]. The most commonly found phytosterols in all vegetable oils and fats have the structures shown in Figure 2.1.

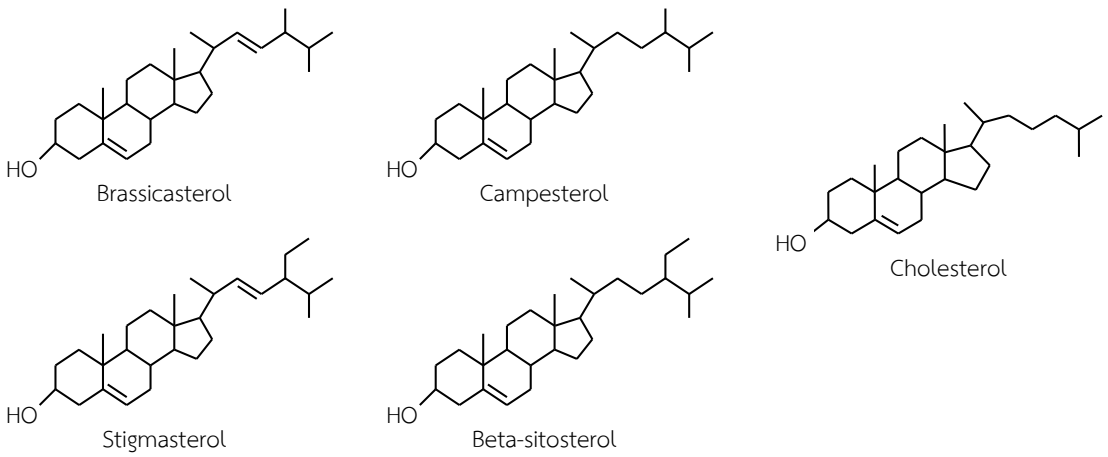

Figure 2.1 Structures of triterpenes compounds

Phytosterols in nature are either in a free form or in a conjugated form such as fatty-acid esters, steryl glycosides, and acylated steryl glycosides [28]. Phytosterols are potentially very valuable due to their desirable bioactive properties. They reduce blood cholesterol level, particularly low-density lipoprotein (LDL) which is the main cause of cardiovascular disease [30]. In addition, phytosterols also have been proven to have anti-inflammatory [31], and anti cancer efficacies [28].

2.1.2 Sources of phytosterols

Phytosterols in esterified and free alcohol forms are commonly found in plants. Verleyen el al. [32] stated that more than half of phytosterols in many edible plant oils are esterified while Phillips et al. [29] reported that 32 to 94 % of the total phytosterol content of edible oils are free phytosterols.

In the refinery process of vegetable oils, deodorizer distillates (DDs) are obtained as by-products of the deodorization step. DDs are good raw materials for tocopherols, free phytosterols, FASEs, fatty acids, and squalene productions [2]. DDs are usually obtained from soybean, palm, corn, sunflower, and rapseed oils. Minor constituents of DDs are shown in Table 2.1.

Table 2.1 Minor constituents (wt %) of deodorizer distillates

DD Type	Tocopherols	Free phytosterols	Steryl ester	Squalene	References
Soybean	16.48	17.06	2.59	1.28	[1]
Soybean	18.02	18.81	2.33	2.09	[1]
Soybean	7.51	6.32	4.45	0.65	[1]
Soybean	6.40	5.36	3.91	1.83	[34]
Soybean	10.40	10.30	12.80	-	[35]
Corn	1.42	2.71	0.62	0.21	[1]
Corn	3.31	5.42	-	0.99	[1]
Sunflower	1.28	4.29	0.09	1.00	[1]
Sunflower	5.06	13.90	0.30	0.73	[1]
Sunflower	6.00	5.10	-	-	[16]
Rapseed	4.19	13.36	5.33	0.40	[1]
Rapseed	3.67	8.63	1.35	0.07	[1]
Palm	1.00	0.30	0.50	-	[36]
Palm	0.5	0.24	-	1.03	[37]
Palm	0.50	0.40	-	0.80	[38]
Olive	-	4.60	-	28.00	[39]

Another source of phytosterols is tall oil which is obtained from black liquor from alkaline digestion of wood in pulp industry. Black liquor is a complex mixture of sodium salts of fatty acids, sodium salts of resin acids, fatty alcohols, free phytosterols, steryl esters, and fatty acid esters [33].

2.2 Adsorption process

Adsorption is a process that a molecular species in gas phase or liquid phase gets attached on the surfaces or pores of a solid. Adsorption occurs in two types: physical adsorption and chemical adsorption. Physical adsorption occurs via weak van der Waals forces between molecular species and solid while chemical adsorption occurs via chemical bonds between molecular species and solid.

2.2.1 Adsorption isotherms

Adsorption isotherms are important for the description of the interaction between molecules of adsorbate and adsorbent surface. Two isotherm models Langmuir and Freundlich isotherms are commonly used to describe adsorption of a molecular species on surface of a solid.

2.2.1.1 Langmuir isotherm

Langmuir equation assumes that there is no interaction between the adsorbate molecules, and adsorption is limited to a monolayer. Langmuir equation can be derived based on fundamental assumptions [40]. A general form and a linear form of the Langmuir isotherm are shown in Equation 2.1 and 2.2, respectively,

$$q_e = \frac{q_m K_{La} C_e}{1 + K_{La} C_e}, \tag{2.1}$$

$$\frac{C_e}{q_e} = \frac{1}{K_{La} q_m} + \frac{1}{q_m} C_e . \tag{2.2}$$

A plot of C_e/q_e versus C_e gives a straight line and the values of q_m and K_{Li} can be evaluated from the slope and y-intercept, respectively.

2.2.1.2 Freundlich isotherm

Freundlich isotherm is an empirical equation that is commonly used to describe the adsorption characteristics of adsorbate on a heterogeneous adsorbent surface. This isotherm explains non-ideal adsorption as well as the formation of multilayer adsorption. A general form and a linear form of Freundlich isotherm are shown in Equation 2.3 and 2.4, respectively,

$$q_e = K_F C_e^{1/n}, \tag{2.3}$$

$$\log q_e = \log K_F + \frac{1}{n}\log C_e . \tag{2.4}$$

The plot of logq_e versus logC_e gives a straight line and the values of 1/n and K_F can be evaluated from the slope and y-intercept, respectively. The constant K_F related to the strength of the adsorption bond, and n is constant that can be related to the favorability of adsorption. The value of $n < 1$ indicates the increase of the interactions between adsorbate and adsorbent that causes with favorable adsorbate and adsorbate interactions on the adsorbent surface. The value of $n > 1$ indicates the decrease of the interactions between adsorbent and adsorbate due to the presence of unfavorable interactions between adsorbate and adsorbate on the surface of adsorbent [41].

2.2.2 Adsorption kinetics

In order to investigate the mechanism of adsorption, characteristic constants of adsorption are estimated by using a kinetic model. Lagergren introduced a pseudo-first-order model for the adsorption of solute from liquid solution [42]. A pseudo-first-order model is expressed by Equation 2.5,

$$\frac{dq_t}{dt} = k_1(q_e - q_t). \tag{2.5}$$

Integrating Equation 2.5 for boundary conditions of $t = 0$ to $t = t$ and $q_t = 0$ to $q_t = q_t$, it becomes

$$\ln(q_e - q_t) = \ln q_e - k_1 t . \tag{2.6}$$

Another model for analysis of adsorption kinetics is pseudo-second-order model [43]. The rate law for this system is expressed by equation 2.7,

$$\frac{dq_t}{dt} = k_2(q_e - q_t)^2 . \tag{2.7}$$

Integrating Equation 2.7, for boundary conditions of t = 0 to t = t and q_t = 0 to q_t = q_t, it becomes

$$\frac{t}{q_t} = \frac{1}{k_2 q_e^2} + \frac{1}{q_e} t . \quad (2.8)$$

Equation 2.8 can be rearranged to obtain a linear form below

$$\frac{t}{q_t} = \frac{1}{k_2 q_e^2} + \frac{1}{q_e} t . \quad (2.9)$$

A plot of t/q_t versus t gives a straight line with a slope of $1/k_2 q^2_e$ and a y-intercept of $1/q_e$, so q_e and k_2 can be evaluated from the slope and y-intercept, respectively.

Two kinetic models for adsorption of solute from liquid solution (first- and second-order models) were derived and used by Azizian [44]. The kinetic models were derived by a general and a specific method to identify the real meaning of their observed rate coefficients.

2.2.3 Adsorption thermodynamics

Thermodynamics of adsorption is a key to understand the nature of adsorption. A negative value of ΔG indicates that the adsorption is spontaneous and feasible. An adsorption equilibrium constant (K) is used to calculate ΔG as shown in Equation 2.10 below,

$$\Delta G = -RT \ln K . \quad (2.10)$$

Equation 2.11 shows a relation between adsorption equilibrium constant and temperature of adsorption,

$$\ln K = \frac{\Delta S}{R} - \frac{\Delta H}{RT} . \quad (2.11)$$

By performing linear regression analysis of the plot between ln$K$ and 1/T, ΔH and ΔS can be calculated from the slope and the y-intercept of the obtained straight line.

2.3 Molecular imprinted silica

2.3.1 Sol-gel process

A sol-gel process has been used to prepare solid silica-based materials through hydrolysis and condensation of an alkoxide precusor [45]. The process starts with hydrolysis of an alkoxide precursor (metal alkoxide $M(OR)_n$ to produce a reactive hydroxyl group on the metal molecule, where M represents a network-forming element such as Si, Ti, Zr, Al, and B, and R is typically an alkyl group (C_xH_{2x+1}) and water) [46]. This step is followed by formation of metal hydroxyl group by condensation. An elementary sol-gel process involves hydrolysis and condensation of tetraalkyl orthosilicates in the presence of a cosolvent to form SiO_2 networks as shown in Figure 2.2.

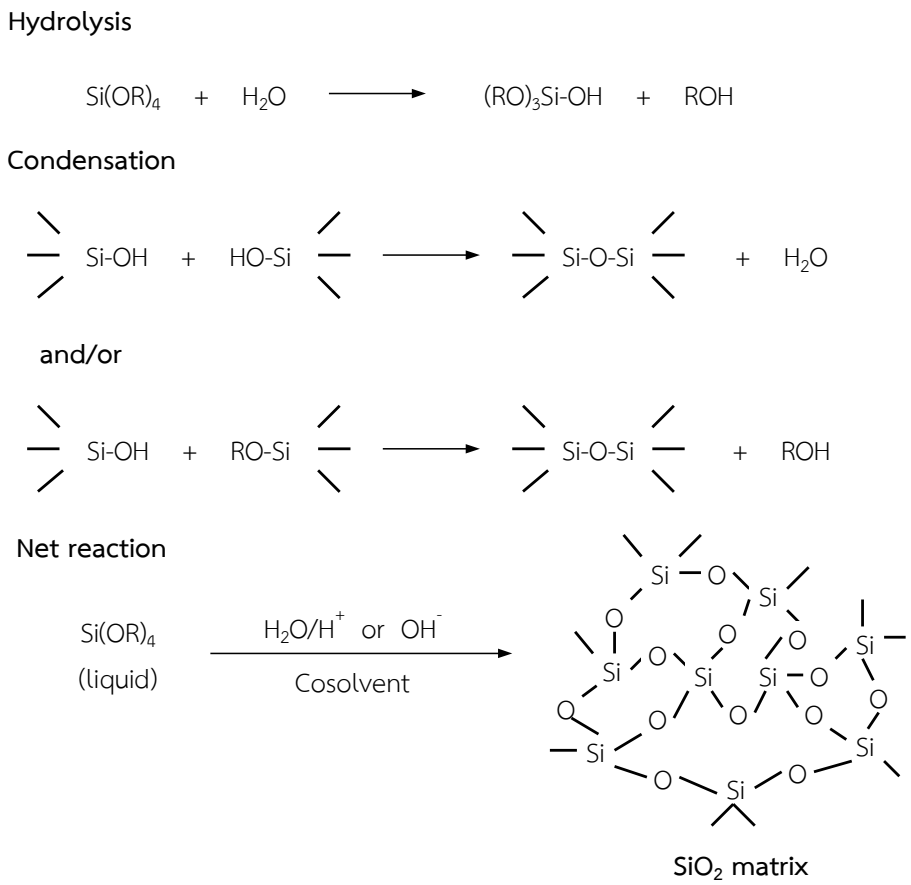

Figure 2.2 Processing steps involved in production of sol-gel derived silica matrix [47]

2.3.2 Molecular imprinting process

An imprinting process consists of three main steps. In the first step, a template molecule interacts with a functional monomer to produce a polymerizable ligand. The second step is polymerization of the polymerizable ligands to produce polymer networks. The final step is removal of the template molecule from the polymer matrix, leaving cavities that can be recognized by the target molecule. There are two main approaches to produce a molecularly imprinted material by sol-gel method. One approach has a template molecule reacts directly with a functional monomer. The other approach has a template reacts first with a derivatizating precursor prior to reacting to a functional monomer.

2.3.2.1 Self-assembly or non-covalent approach

A template molecule is directly added to a sol-gel solution prior to acid-catalysed hydrolysis and condensation by using a polar solvent such as ethanol or water. The imprinted sites are created by weak chemical interactions (van der Waals, π-stacking, electrostatic, etc.) between the template molecule and the sol-gel network [46]. Following the drying step, the gel is extracted by a suitable solvent to remove the template molecule as shown in Figure 2.3.

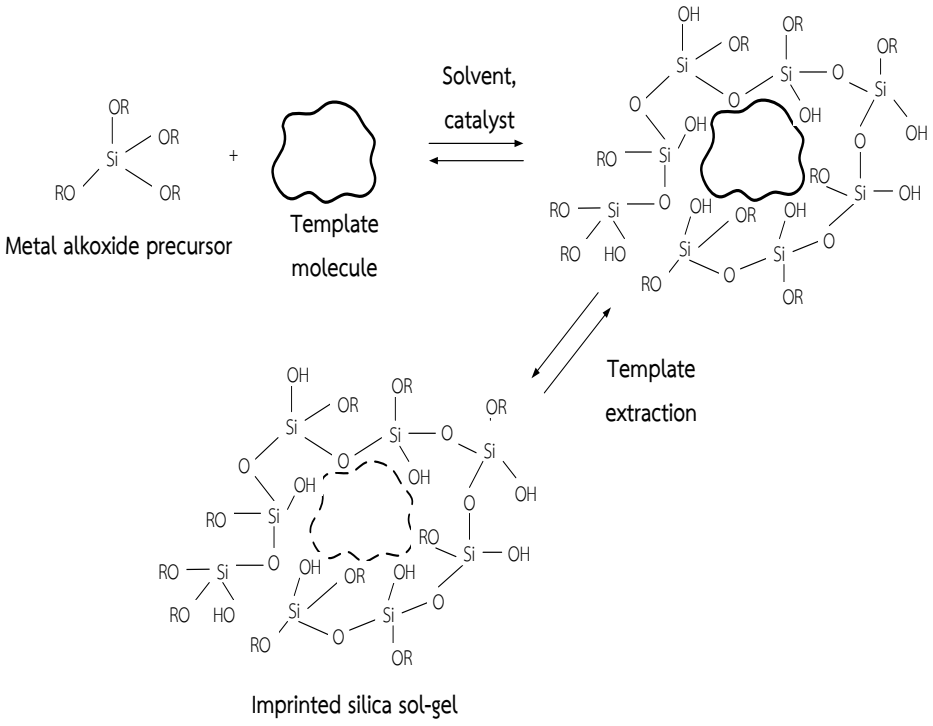

Figure 2.3 Non-covalent silica imprinting process [46]

2.3.2.2 Pre-organized or covalent approach employing reversible covalent bonds

Prior to a polymerization step, a chemical synthesis is used to link a derivatizating precursor to a template molecule to create a sacrificial spacer. Then, the polymerization step is used to combine a sacrificial spacer and a metal oxide precursor. After polymerization, the template molecule is removed by a suitable solvent to provide specific molecular binding sites as shown in Figure 2.4.

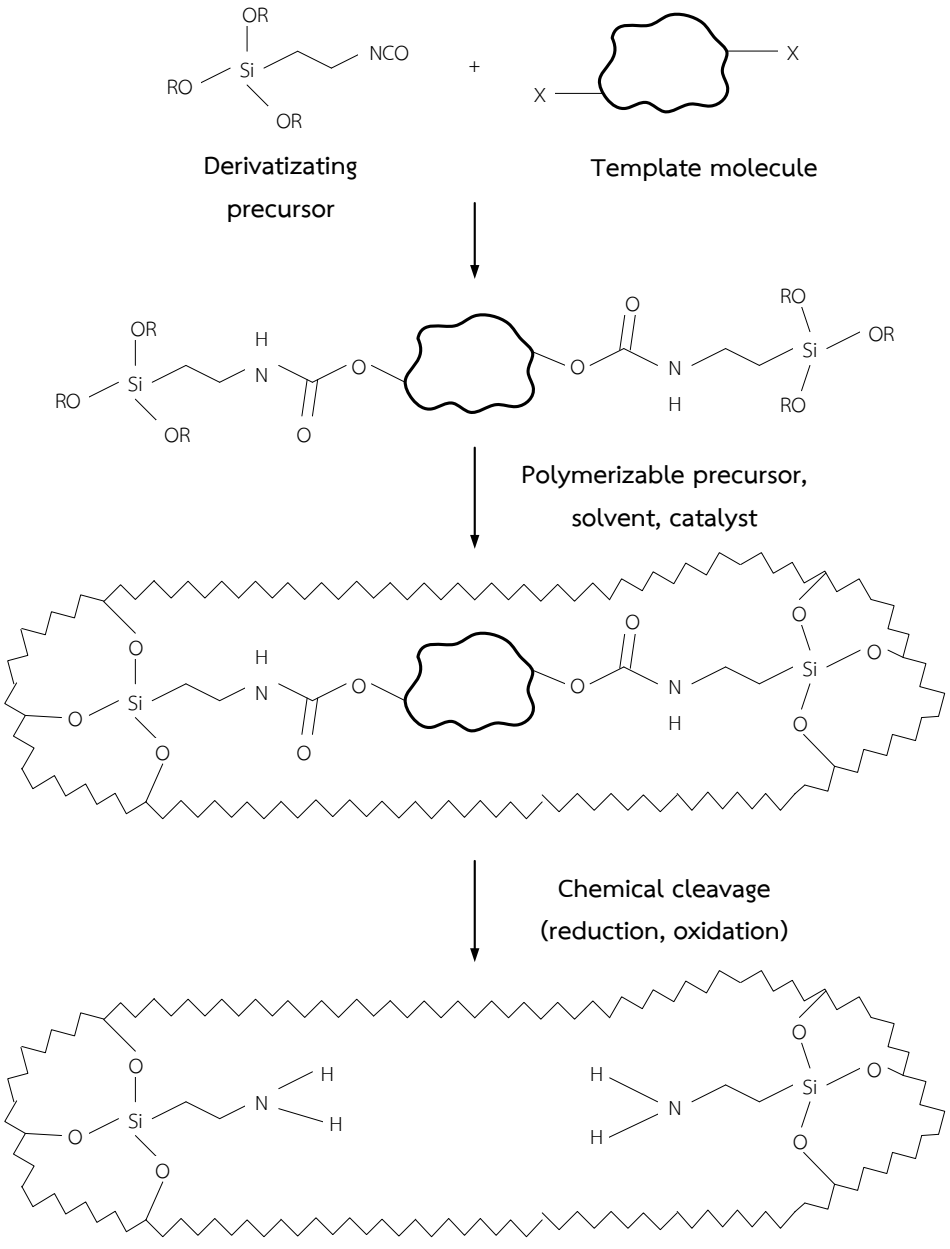

Figure 2.4 Covalent silica imprinting process [46]

2.4 Central composite design

A central composite design (CCD) is an effective method for fitting second-order model. The number of tests required for CCD including the center points, the factorial points (2^k), and the axial points fixed with the distance from center points (α). The value of α and the number of tests for CCD are expressed by equation 2.12 and 2.13, respectively.

$$\alpha = (2k)^{1/4}, \tag{2.12}$$

$$\text{The number of tests} = 2^k + 2k + n_0, \tag{2.13}$$

where k is the number of factors and n_0 is the number of center points. For exsample, a CCD for 3 factors, with 3 center points resulting in total number of tests $2^3 + 2(3) + 3 = 17$ runs as illustrated in Figure 2.5.

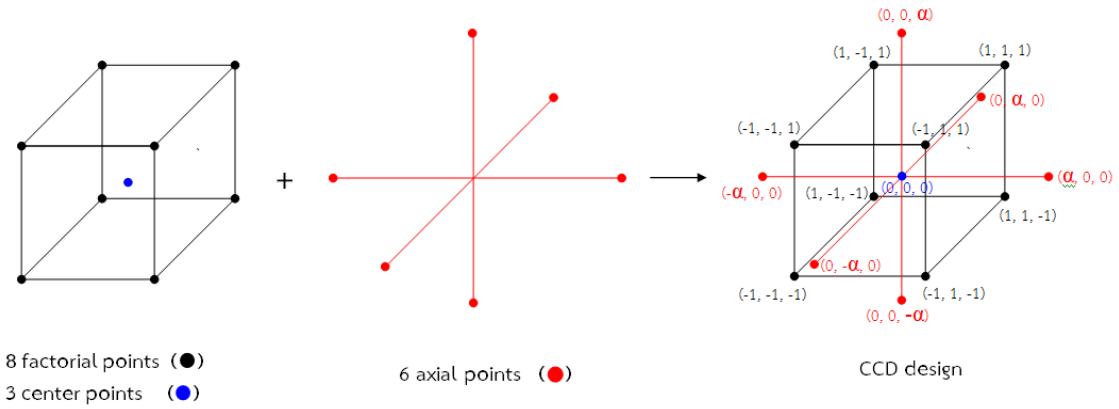

Figure 2.5 A central composite design for 3 factors, with 3 center points

Table 2.2 Relationship between the code of factor and the value of factor [48]

Code	The value of factor
-α	X_{min}
-1	$\frac{(\alpha-1)X_{max}+(\alpha+1)X_{min}}{2\alpha}$
0	$\frac{X_{max}+X_{min}}{2}$
+1	$\frac{(\alpha-1)X_{min}+(\alpha+1)X_{max}}{2\alpha}$
+α	X_{max}

*X_{min} and X_{max} are minimum and maximum value of X, respectively.

In addition, the desired value ranges of the factors have to defined, it is coded as ±1, 0, and ± α for the factorial poins, the center points, and the axial points, respectively. The code can be calculated based on the range of each factor, as shown in Table 2.2.

2.5 Recovery of phytosterols

Phytoterols have several beneficial bioactivities and have been widely used in food, cosmetics, and pharmaceutical industries [10]. Over the past several decades, deodorizer distillates (DDs) have become one of the most important sources of phytosterols due to an increase in the total global production of vegetable oils of about 17 % between 2012/13 and 2017/18 [4].

Phytosterols have been successfully recovered from DDs by several methods. In general, these methods consist of several steps of chemical and physical treatments. Since removal of undesired compounds (FFA and glycerides) from DDs by distillation requires relatively high temperature and extremely low pressure, it is necessary to transform these undesired compounds to the forms that can be separated more easily. In one approach, FFA in DD is saponified and the resulted soap is removed from the obtained mixture by a simple solid-liquid separation. Then, phytosterols are separated from the liquid mixture of the unsaponifiable components by using either vacuum distillation or cold crystallization. Rohr et al. [11] proposed a method for recovery of phytosterols from soybean oil deodorizer

distillate (SODD). In their process, SODD was saponified with sodium hydroxide solution and magnesium sulfate solution to remove FFA and glycerides. Next, the unsaponifiable product was distilled at 623 K and 1×10^{-3} mbar to obtain a residue and a distilled product. The yields of the residue and the distilled product taken from the first distillation were 63 wt% and 37 wt%, respectively. Tocopherols and phytosterols were concentrated in the distilled product and their concentrations were 8.0 wt% and 10.4 wt%. In the residue, tocopherols and phytosterols were found at concentrations of 0.4 wt% and 1.37 wt%, respectively. The first distilled product was submitted to a second distillation at 553 K in order to remove the remaining soap in the first distilled product. From the second distillation, the residue and distilled product yields were 2.6 wt% and 34.4 wt%, relative to the raw material. Total tocopherols and phytosterols concentrations in the distilled product were 8.5 wt% and 11.4 wt%, respectively. The concentrations of tocopherols and phytosterols in the residue product were 0.38 wt% and 0.24 wt%, respectively. The second distilled product was then distilled again at 413 K. In third distillation, the residue and distilled product yields were 21.6 wt% and 12.8 wt%, respectively relative to the raw material. The concentrations of tocopherols and phytosterols in the residue product were 13.0 wt% and 17.9 wt%, respectively. The concentrations of tocopherols and phytosterols in the distilled product were 0.93 wt% and 0.50 wt%, respectively. This shows that the recovery of tocopherols and phytosterols were 87.8 wt% and 80.5 wt%, respectively relative to the raw material. Yang et al. [12] described a catalytic decomposition and crystallization process for recovery of phytosterols from waste residue of soybean oil deodorizer distillate (WRSODD). In their work, WRSODD was chemically treated by saponification with an alkali solution to decompose WRSODD and transform steryl esters into phytosterols. Crystallization of phytosterols in the obtained preconcentrated mixture was optimized by varying the types of solvents (methanol, ethanol, n-propanol, n-hexane, cyclohexane, petroleum ether, acetone, butanone, cyclo-hexanone, benzene, toluene, acetone, and ethanol mixed (4/1, v/v)), mass ratios of preconcentrated mixture to solvent (from 1 to 4), the ripening temperatures (from 265 to 293 K), and ripening times (from 4 to 24 h). Based on their experimental results, the optimum crystallization conditions obtained were the following: a solvent to preconcentrated mixture mass ratio of 2.5, an acetone and ethanol solvent with a volume ratio of 4/1, a ripening time of 24 h, and a ripening

temperature of 279 K. Under these optimized crystallization conditions, phytosterols with a yield of 22.95 wt% and a purity of 91.82 wt% were obtained after the first crystallization. The purity of the phytosterols reached 92.73 and 97.17 wt% after the second and third crystallization, respectively. Khatoon et al. [13] reported a method for isolating phytosterols from soybean oil deodorizer distillate (SODD) by crystallization with hexane and water. In this method, SODD was saponified with potassium hydroxide to remove FFA and glycerides, followed by an organic solvent extraction that yielded an unsaponifiable matter containing phytosterols with a recovery of 74.6 wt%. After that, the unsaponifiable matter was purified by crystallization using a mixture of hexane and water as solvent at 253 K for 72 h. Then, the crude phytosterol mixture obtained from the first crystallization was recrystallized with hexane at 278 K for 2 h. This method yielded a phytosterols recovery of 65.8 wt% and a purity of 87 wt%. In addition, the process included saponification and esterification for pretreatment of DDs. Similarly, Smith [20] developed a method that included saponification, methyl esterification, and solvent crystallization for separation of phytosterols from deodorizer distillate (DD). In his process, DD was saponified with caustic soda, followed by double esterification of the unsaponifiable product with hydrochloric acid. Then, the resulting mixture was crystallized at 288 K to separate phytosterols, and the phytosterol-rich cake was recrystallized with acetone at 293 K. This method yielded a phytosterol recovery of 95 wt% and a purity of 97.5 wt%. In the same vein, Yan et al. [21] reported a process that included saponification, methyl esterification, and solvent crystallization for separation of phytosterols from soya oil deodorizer distillate (SODD). In their process, SODD was saponified with a sodium hydroxide solution to remove FFA and glycerides. The unsaponifiable product was then submitted to an acid-catalyzed esterification with methanol. In the last step, crystallization was performed by varying the types of a single solvent (methanol, ethanol, *n*-propanol, acetone, butanone, benzene, toluene, petroleum ether, and ethyl acetate) or a mixture with a co-solvent (water), the proportions of feed solution to solvent (1.32 to 4.00 g/ml), the ripening temperatures (269.86 to 286.41 K), and the ripening times (10.55 to 37.45 h). An optimum phytosterol product recovery of 6.64 wt% and a purity of 94.7 wt% were obtained by using a petroleum ether solvent with water as a co-solvent, a feed solution to solvent ratio of 3.41 g/ml, a ripening temperature of 277.48 K, and a

ripening time of 26.47 h. Deodorizer sludge (DS) which is the same as soybean deodorizer distillate (SODD) was used by Savinova et al. [22] for phytosterol separation. The process started with saponification of fatty acids contained in the DS with an aqueous sodium hydroxide solution, followed by esterification with sulfuric acid. The resulting phytosterol-containing phase was then dissolved by boiling in a mixture of solvents consisting of acetone, methanol, and water (41:8:1 by volume). The resulting solution was cooled to 278 K and kept at this temperature for 15 h. This proposed method yielded a phytosterol product that had a purity of 90.30 wt% and a recovery of 96.15 wt%.

In another method, FFA and other glycerides in DDs were transformed to fatty acid alkyl ester (FAEE) by esterification and transesterification, respectively. In the phytosterol preconcentration step, the FAEE fraction was removed by either a fractional liquid-liquid extraction or a vacuum distillation to obtain a high yield of phytosterols. Ghosh and Bhattacharyya [19] reported a combination of lipase catalyzed hydrolysis and esterification reaction, followed by a fraction distillation to recover tocopherols and phytosterols from sunflower deodorizer distillate (SODD). In their process, the neutral glycerides in SODD were hydrolyzed by *Candida cylindracea* lipase into free fatty acids (FFAs). The total FFAs were transformed to butyl ester by using *Mucor miehei* lipase, and the esterified product was then fractionally distillated. The fraction obtained from 453 to 503 K temperature range and 1.3 mbar for 45 min was the first fraction, and this fraction contained mainly butyl ester, hydrocarbons, several oxidized products and some free fatty acids. The distillation was continued at 503 to 533 K and 1.3 mbar for 15 min, and the second fraction was collected. The second fraction was rich in tocopherols (30.1 wt%) and phytosterols (36.4 wt%). Finally, the overall recovery of tocopherols and phytosterols from this process were 70.2 wt% and 41.9 wt% of the original content in the starting material, respectively. In addition, crystallization was applied as the last step for sterols separation. Brow and Smith [14] reported that processes for separating phytosterols from soybean oil deodorizer distillate (SODD) included esterification, fractional liquid-liquid extraction, and crystallization. FFA could be transformed into fatty acid methyl ester (FAME) by esterification. A fractional liquid-liquid extraction could be applied to separate FAME, glycerides, and other compounds from the resulting mixture from the esterification. These compounds would be found in the

raffinate fraction. The free phytosterols found in the extract fraction could be separated by crystallization in acetone at 253 K, and the total recovery of 73 wt% could be obtained in the final product. Fizet [15] developed a process including esterification, vacuum distillation, transesterification, and crystallization for separation of phytosterol from soya oil deodorizer distillate (SODD). In this process, FFA and glycerides in SODD were transformed into fatty acid alkyl ester (FAEE). The esterification product was then distilled at 418 to 433 K and 0.1 to 0.25 mbar, and the residue product was then distilled again at 438 to 483 K and 0.01 to 0.05 mbar to obtain a residue containing mostly steryl esters. Then, the enriched steryl esters in the residue would be submitted to an acid-catalyzed transesterification with methanol to produce free phytosterol. Finally, phytosterol products with a recovery percentage of 90 wt% and purity of 90 wt% would be obtained by crystallization at 273 K. Moreira and Baltanás [16] proposed an alternative method for separation of phytosterol from fatty acid ethyl ester (FAEE) matrices by using vacuum distillation. Crystallization was done to purify the phytosterol. They also investigated the effect of operating variables on the purity and yield of the phytosterol products. By this method, FFA and triglyceride in sunflower oil deodorizer distillate (SODD) were transformed into FAEE. After that, FAEE was removed from the resulting mixture by vacuum distillation at 1.3 mbar and ≤ 473 K. The optimized conditions for crystallization of phytosterols in the obtained pre-concentrated mixture was found by varying the types of solvents (hexane single solvent, hexane with co-solvent), the types of co-solvents (water, ethanol and both of them), the mass ratio of solvent-to-the pre-concentrated mixture (3 to 5 mass ratio), the cooling rate (253 K/h or brisk chilling from 313 to 268 K), the final ripening temperature (253 to 273 K), and the ripening time (4 to 96 h. Phytosterol products with a recovery percentage of 84 wt% and purity of 36 wt% were obtained by using this method with hexane and 2.5 wt% of ethanol as a co-solvent, a solvent-to-pre-concentrated mixture mass ratio of 4, a cooling rate of 293 K/h, a final ripening temperature of 268 K, and a ripening time of 22 h. Wollmann et al. [17] described a process for separation of phytosterols from soybean oil deodorizer distillate (SODD). In their process, FFA and glycerides in SODD were transformed into fatty acid methyl ester (FAME), and then FAME was removed by using vacuum distillation at 1.0 mbar and 453 K. After that, the sterol esters concentrated in the residue of the distillation was transformed into free phytosterols

by transesterification. Finally, phytosterol products with a purity of 93.9 wt% was obtained by crystallization at 288 K. Carmona et al. [18] pointed out that the pre-concentration step by vacuum distillation of phytosterol in FAME matrices required a large amount of energy and also destroyed some phytosterols present in the matrices. Therefore, they proposed an alternative method for isolation of phytosterols from FAME matrices with no requirement of vacuum distillation. Crystallization was performed to FAME, which was formed from esterification and/or transesterification without either addition of extra FAME or partial distillation. The obtained isolated solid was then washed with hexane and gave end-products of phytosterols. By using this proposed method, at the best conditions for crystallization (268 K, 24 h), 35 to 42 wt% of phytosterols were recovered from sunflower oil deodorizer distillate with a high purity of over 92 wt%. In addition, under some conditions, the method produced end-products of phytosterols with a purity higher than 99 wt%. A summary of phytosterol recovery by different methods is shown in Table 2.3.

Table 2.3 Phytosterol recovery by different methods

Feed stock	Process	Recovery (wt%)	Purity (wt%)	Ref.
Soybean oil deodorizer distillate (SODD)	SODD ⟶ saponification (NaOH + $MgSO_4$) ⟶ unsaponifiable product ⟶ first distillation (623 K and 1×10^{-3} mbar) ⟶ the first distilled product ⟶ second distillation (553 K) ⟶ the second distilled product ⟶ third distillation (413 K) ⟶ third residue product	80.5	-	[11]
Waste residue of soybean oil deodorizer distillate (WRSODD)	WRSODD ⟶ saponification (alkali solution + ethanol) ⟶ pre-concentrated mixture ⟶ crystallization (solvent-to-pre-con centrated mixture mass ratio of 2.5, acetone and ethanol (volume ratio = 4/1) as a solvent, ripening time of 24 h, and ripening temperature of 279 K)	22.95	97.17	[12]
Soybean oil deodorizer distillate (SODD)	SODD ⟶ saponification (KOH + ethanol) ⟶ unsaponifiable product ⟶ crystallization (a mixture of hexane and water as solvent, 253 K, 72 h) ⟶ crude phytosterol mixture ⟶ recrystallization (hexane, 278 K, 2 h)	65.8	87	[13]

Table 2.3 Phytosterol recovery by different methods (cont.)

Feed stock	Process	Recovery (wt%)	Purity (wt%)	Ref.
Deodorizer distillate (DD)	DD ⟶ saponification (caustic soda + methanol) ⟶ unsaponifiable product ⟶ first esterification (37% HCl) ⟶ second esterification (concentrated HCl + methanol) ⟶ esterified product ⟶ crystallization (288 K) ⟶ crude phytosterol mixture ⟶ recrystallization (acetone, 253 K)	95	97.5	[20]
Soya oil deodorizer distillate (SODD)	SODD ⟶ saponification (NaOH solution + ethanol) ⟶ unsaponifiable product ⟶ esterification (H_2SO_4 + methanol) ⟶ esterified product ⟶ crystallization (petroleum ether with water as co-solvent, a feed solution-to-solvent ratio of 3.41 g/ml, ripening temperature of 277.48 K, ripening time of 26.47 h)	6.64	94.7	[21]
Deodorizer sludge (DS)	DS ⟶ saponification (NaOH solution) ⟶ unsaponifiable product ⟶ esterification (H_2SO_4) ⟶ esterified product ⟶ crystallization (a mixture of solvents consisting of acetone, methanol, and water (41:8:1 by volume), ripening temperature of 278 K, ripening time of 15 h)	96.15	90.30	[22]

Table 2.3 Phytosterol recovery by different methods (cont.)

Feed stock	Process	Recovery (wt%)	Purity (wt%)	Ref.
Sunflower oil deodorizer distillate (SODD)	SODD ⟶ hydrolysis (*Candida cylindracea* lipase) ⟶ esterification (*Mucor miehei* lipase + butanol) ⟶ esterified product ⟶ fraction distillation (first fraction at 453 to 503 K and 1.3 mbar for 45 min, second fraction at 503 to 533 K and 1.3 mbar for 15 min)	41.9	-	[19]
Soybean oil deodorizer distillate (SODD)	SODD ⟶ esterification (HCl + methanol) ⟶ esterified product ⟶ fractional liquid-liquid extraction (hexane, methanol (98 %) + water (2%)) ⟶ the extract fraction ⟶ vacuum distillation ⟶ crystallization (acetone, 253 K)	-	73	[14]
Soya oil deodorizer distillate (SODD)	SODD ⟶ esterification ⟶ esterified product ⟶ first vacuum distillation (418 to 433 K, 0.1 to 0.25 mbar) ⟶ the residue product ⟶ second vacuum distillation (438 to 483 K, 0.01 to 0.05 mbar) ⟶ the residue product ⟶ tranesterification (H_2SO_4 + methanol) ⟶ crystallization	90	90	[15]

	(273 K)			

Table 2.3 Phytosterol recovery by different methods (cont.)

Feed stock	Process	Recovery (wt%)	Purity (wt%)	Ref.
Sunflower oil deodorizer distillate (SODD)	SODD ⟶ esterification (HCl + ethanol) ⟶ esterified product ⟶ vacuum distillation (1.3 mbar, ≤ 473 K) ⟶ the bottom product ⟶ crystallization (hexane and 2.5 wt% of ethanol as a co-solvent, a solvent-to-pre-concentrated mixture mass ratio of 4, cooling rate of 293 K/h, final ripening temperature of 268 K, ripening time of 22 h)	84	36	[16]
Soybean oil deodorizer distillate (SODD)	SODD ⟶ esterification (tin(2) isooctoate + glycerol) ⟶ esterified product ⟶ first transesterification (sodium methylate solution + methanol) ⟶ transesterified product ⟶ vacuum distillation (1.0 mbar, 453 K) ⟶ the bottom product ⟶ second transesterification (sodium methylate	-	93.9	[17]

	solution + methanol) ⟶ crystallization (288 K)			
Sunflower oil deodorizer distillate (SODD)	SODD ⟶ esterification (*p*-toluene sulphonic + methanol) ⟶ esterified product ⟶ crystallization (268 K, 24 h)	35-42	92-99	[18]

Chapter 3
Recovery of Phytosterol by Using Commercial Adsorbents

3.1 Description

In this study, three types of commercial grade styrene-divinylbenzene ion-exchange resins (strong acid resin: SA-R, strong base resin: SB-R, and weak base resin: WB-R) were used as adsorbents in a phytosterol recovery process. To investigate the performance of the selected ion-exchange resins (i.e. kinetics, equilibrium, and thermodynamics of phytosterol adsorption), in an experiment, batch adsorption was performed by using stigmasterol in n-heptane as a model solution in the range of initial stigmasterol concentration of 0.3 to 1.8 mg/g-solution and temperature in the range from 298 to 313 K. The adsorption was operated at the condition not far from ambient temperature and pressure to indicate that the adsorption can be performed at mild conditions. It is the goal to reduce large amount of overall energy consumption in phytosterol recovery. Two general kinetic models: pseudo-first-order and pseudo-second-order were used for analysis of kinetics of adsorption. Equilibrium adsorption data were analyzed based on Langmuir, Freundlich, and linear isotherms. From the obtained results, three important thermodynamics parameters (i.e., Gibb's free energy change, enthalpy change, and entropy change) were calculated. The adsorption behavior was discussed based on these calculated thermodynamics parameters.

In addition, a two-step process consisting of an adsorption step of phytosterol in model solution by using the selected ion-exchange resin and a desorption step of stigmasterol from the ion-exchange resin by using nontoxic ethanol was considered a low cost and simple method for recovery of phytosterol.

3.2 Materials and methods

3.2.1 Materials

Styrene-divinylbenzene copolymer based ion-exchange resins with different functional groups; Lewatit® Monoplus SP112H (strong acid resin: SA-R), Lewatit® Monoplus MP 800 (strong base resin: SB-R), and Lewatit® Monoplus MP 68

(weak base resin: WB-R) supplied by Lanxess, Germany, were used as adsorbents. Table 3.1 summarizes the characteristic properties of these three adsorbents. To remove moisture from the adsorbents, SA-R was dried in an oven at 383 K under vacuum condition for 360 min while the SB-R and WB-R were dried in an oven at 333 K under vacuum condition for 360 min. Before using in the adsorption experiment, SA-R was washed with methanol, n-propanol, and n-hexanein that order. SB-R and WB-R were washed with n-propanol and n-hexane in that order.

Table 3.1 Properties of adsorbents

Property	SA-R	SB-R	WB-R
Type	Strong acid	Strong base	Weak base
Functional group	Sulfonic acid	Quaternary amine, type I	Tertiary/quarternary Amine
Matrix structure	Crosslinked polystyrene	Crosslinked polystyrene	Crosslinked polystyrene
Structure	Macroporous	Macroporous	Macroporous
Ionic form as shipped	H+	OH-	free base/Cl^-
Bead size (mm)	0.67 (± 0.05)	0.65 (± 0.05)	0.54 (± 0.05)
Total exchange capacity (min.eq/l)	1.6	0.8	1.3
Operating pH range	0 - 14	0 – 12	0 – 7
Operating temperature (max. K)	393	343	343

Stigmasterol supplied by Tama Biochemical Co. Ltd. and n-heptane (AR grade) supplied by Apex Chemicals Co. Ltd., (Bangkok, Thailand) were used in the preparation of a model solution of stigmasterol. Cholesterol supplied from Sigma-aldrich chemical Co., Ltd., (Milwaukee, USA) was used as an internal standard (ISTD) in a quantitative analysis of stigmasterol. Methanol, Isopropanol, and n-Hexane used were commercial grade and supplied from Asian Scientific Co., Ltd., (Samutprakarn, Thailand). Ethanol used was AR grade and supplied from RCI Labscan Ltd., (Bangkok, Thailand). Methanol, acetonitrile, and water used were supplied by RCI Labscan Ltd.,

(Bangkok, Thailand) while the acetic acid used was supplied by Merck Ltd., (Darmstadt, Germany). It was HPLC grade and used without purification.

3.2.2 Methods

3.2.2.1 Kinetics, isotherm, and thermodynamics of phytosterol adsorption

To study the kinetics, isotherm, and thermodynamics of phytosterol adsorption with the three adsorbents, an isothermal batch adsorption experiment was performed by using the model solution of stigmasterol in n-heptane. Adsorption temperature and stigmasterol concentration were varied in the ranges of 298 to 313 K and 0.3 to 1.8 mg/g-solution, respectively. The model solution (50 ml) and the adsorbent (5 wt%) were heated and shaken in an orbital shaker (4000ic; IKA) at 200 rpm for 120 min. Point samples (200 µl) were taken at different time intervals for a quantitative analysis of stigmasterol content. The q_t was calculated according to Equation 3.1,

$$q_t = \frac{(C_0 - C_t)W_{Sol}}{W_{Ads}}. \quad (3.1)$$

3.2.2.2 Recovery of phytosterol by using ion-exchange resins

The adsorption experiment was carried out in n-heptane solution containing stigmasterol at 4.0 mg/g-solution as a model solution. In all tests, 2.5 g of the model solution was mixed with 0.133 g of adsorbent and then the mixture was shaken at 200 rpm and 303 K for 2 h. The q_e was calculated according to Equation 3.2,

$$q_e = \frac{(C_0 - C_e)W_{Sol}}{W_{Ads}}, \quad (3.2)$$

At the end of the adsorption process, the adsorbent was separated from the solution by filtration and the concentration of stigmasterol in liquid phase was analyzed by HPLC. The adsorbent separated from the solution was dried at room temperature. In the desorption experiment, ethanol was used as a desorbent to desorb stigmasterol from adsorbent. The dried adsorbent was mixed

with the desorbent at a ratio of 10 g-desorbent/g-adsorbent. The mixture was then shaken in an orbital shaker at 200 rpm, 333 K for 2 h. After 2 h of desorption, samples were taken and heated to 333 K for 3 h to evaporate the desorbent. The mixture obtained after desorbent evaporation were further used for analysis of stigmasterol. The *%De* and the *%Re* were quantified according to the following Equation, 3.3 and 3.4, respectively,

$$\%\mathrm{De} = \frac{W_{\mathrm{St,De}}}{W_{\mathrm{St,Ad}}} \times 100\,, \tag{3.3}$$

$$\%\,\mathrm{Re} = \left(\frac{W_{\mathrm{St,De}}}{W_{\mathrm{T}}} \right) \times 100\,, \tag{3.4}$$

3.2.3 Analytical method

Concentration of stigmasterol was measured by using a high performance liquid chromatography (HPLC) system connected with a UV detector. An injection valve with a 20-µl sample loop was used to introduce samples into the system. Peak separation was achieved by using a reverse-phase column (Inertsil C8-3; 5 µm particle diameter, 250 mm length, 4.6 mm i.d., GL Sciences Inc, Japan). Conditions and mobile phase were adapted from a work reported by Chang et al. [49]. The measurement conditions were: absorbance wavelength of 210 nm and a mobile phase of a mixture of acetonitrile (85%), methanol (5%), and water containing 1% of acetic acid (10%). The flow rate of the mobile phase was 1.3 ml/min. Cholesterol in methanol (4.0 mg/g-solution) was used as an internal standard (ISTD) in the quantification of stigmasterol. Since the sample did not dissolve well in the mobile phase, first, n-heptane was evaporated from the sample then 800 µl of methanol was added. The sample was shaken at 200 rpm for 1 h, and then 200 µl of ISTD was added. One hundred microliters of the prepared sample was then injected into the system through the injection valve.

3.3 Results and discussion

3.3.1 Kinetics, isotherm, and thermodynamics of phytosterol adsorption

To investigate the performances of the three selected ion-exchange resins (i.e. kinetics, equilibrium and thermodynamics of phytosterol adsorption), batch adsorption experiments were performed by using stigmasterol in n-heptane as a model solution. Two general kinetics models, pseudo-first-order and pseudo-second-order, were adopted for the analysis of kinetics of adsorption. Equilibrium adsorption data were analyzed based on Langmuir, Freundlich, and linear isotherms. In addition, from the obtained data, three important thermodynamics parameters (Gibb's free energy change, enthalpy change, and entropy change) were calculated. The adsorption behavior was discussed based on the calculated thermodynamic parameters.

3.3.1.1 Adsorption capacity

Figure 3.1 shows the time dependence of adsorption capacity at 303 K of the three ion-exchange resins at various initial concentrations of stigmasterol. The adsorption capacity increased with time until an equilibrium was reached within 30 min. A comparison of the profiles obtained at different initial concentrations reveals that the rates of adsorption on all three ion-exchange resins decreased with increasing concentration of stigmasterol. By increasing the initial concentration of stigmasterol from 0.3 to 1.8 mg/g-solution, in the case of SA-R (Figure 3.1 (a)), q_e increased from 2.44 to 9.17 mg/g-adsorbent.

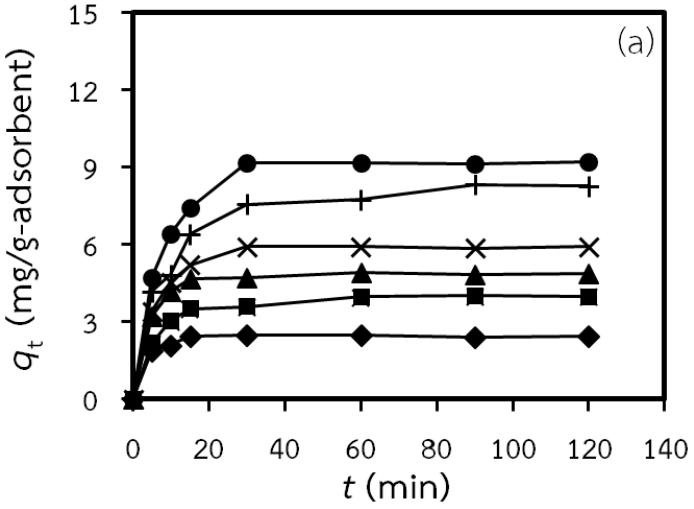

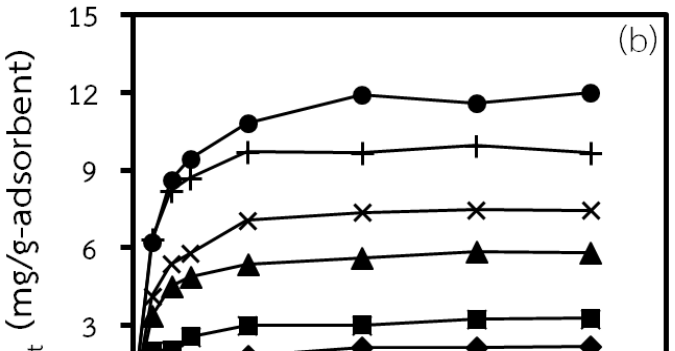

Figure 3.1 Plots of stigmasterol adsorption capacities of (a) SA-R, (b) SB-R, and (c) WB-R versus adsorption time, at 303 K and 5 wt% of adsorbent loading for various initial stigmasterol concentrations: (♦) 0.3, (■) 0.6, (▲) 0.9, (×) 1.2, (+) 1.5, (●) 1.8 mg/g-solution

In the case of SB-R (Figure 3.1 (b)), q_e increased from 2.15 to 11.83 mg/g-adsorbent, while in the case of WB-R (Figure 3.1 (c)), q_e increased from 2.73 to 13.30 mg/g-adsorbent. The adsorption capacity at equilibrium of WB-R was approximately 1.5 and 1.1 times higher than those of SA-R and SB-R, respectively.

3.3.1.2 Adsorption kinetics

Experimental kinetic data were comparatively analyzed based on pseudo-first-order and pseudo-second-order kinetic models which are expressed as Equations 2.6 and 2.8 in chapter 2, respectively.

Linear plots corresponding to the pseudo-first-order and pseudo-second-order models for SA-R, SB-R, and WB-R are shown in Figure 3.2 and 3.3, respectively. The kinetic parameters, k and q_e of each model were calculated from the slope and y-intercept of the corresponding linear plot and summarized in Table 3.2. The R^2 of the pseudo-second-order model for SA-R, SB-R, and WB-R were higher than those of the pseudo-first-order model, for all stigmasterol concentrations tested. The lowest value of R^2 obtained from the pseudo-second-order model was 0.9987 while the highest value of R^2 obtained from the pseudo-first-order model was 0.9943. Furthermore, the $q_{e,exp}$ agreed well with the $q_{e,cal}$ from the pseudo-second-order model (Δq_e < 8.2 %), while it did not agree well with $q_{e,cal}$ from the pseudo-first-order model. Based on these values of correlation coefficients and Δq_e, the pseudo-second-order model was considered to better describe the kinetics of stigmasterol adsorption on three resins. In addition, Figure 3.2 show plots of the linear form of the pseudo-first-order model that was found to be able to predict the adsorption rate sufficiently accurately for only the initial 15 to 30 min of contact times while the linear form of the pseudo-second-order model (Figure 3.3) was able to predict the adsorption rate accurately for all contact times up to 120 min. All of these results suggest that the pseudo-second-order model was more suitable for predicting the adsorption rate of stigmasterol. Therefore, the pseudo-second-order model was considered as the better model for describing the kinetics of phytosterol adsorption on all ion-exchange resins. For all cases, k_2 depended on the C_0. When C_0 was increased from 0.3 to 1.8 mg/g-solution, $k_{2,SA-R}$ decreased from 0.6018 to 0.0266, $k_{2,SB-R}$ decreased from 0.0585 to 0.0179, and $k_{2,WB-R}$ decreased from 0.0731 to 0.0345 g-adsorbent/(mg·min), indicating that the rates of adsorption on all ion-exchange resins decreased with increasing initial concentration of stigmasterol. It is possibly due to lower collisions between stigmasterol molecules when the concentration is low. Therefore, the faster stigmasterol molecules could be bonded to the active sites on the surface of the adsorbent. In addition, the dependence of k_2 on initial concentration was previously reported in several studies of many adsorption systems [50-53]. A theoretical analysis by Azizian [44] clearly shows that k_2 is not an intrinsic rate

constant of adsorption but it is a complex function of adsorption rate constant, desorption rate constant and initial concentration of adsorbate.

This information of kinetics adsorption data *can* be useful to calculate the adsorption capacity of the adsorbent at different times to find the sufficient time for adsorption equilibrium. It can be used to design the size and the operating time of an adsorption unit.

Table 3.2 Kinetic parameters of stigmasterol adsorption on SA-R, SB-R, and WB-R at 303 K and different initial concentrations of stigmaterol

Resin	C_0	$q_{e,exp}$	Pseudo-first-order				Pseudo-second-order			
			k_1	$q_{e,cal}$	Δq_e (%)	R^2 (-)	k_2	$q_{e,cal}$	Δq_e (%)	R^2 (-)
SA-R	0.3	2.44	0.3911	3.93	61.3	0.8525	0.6018	2.45	0.4	0.9994
	0.6	3.99	0.0745	2.59	35.2	0.8054	0.0668	4.14	3.7	0.9995
	0.9	4.86	0.1161	2.78	42.8	0.8327	0.1300	4.93	1.4	0.9997
	1.2	5.90	0.1409	5.54	6.1	0.9943	0.0636	6.06	2.8	0.9993
	1.5	8.11	0.0872	7.13	12.1	0.9834	0.0188	8.73	7.7	0.9989
	1.8	9.17	0.1095	8.51	7.2	0.9877	0.0266	9.57	4.4	0.9990
SB-R	0.3	2.15	0.0605	1.73	19.6	0.9475	0.0585	2.33	8.1	0.9997
	0.6	3.17	0.0911	2.52	20.5	0.9628	0.0588	3.39	6.9	0.9988
	0.9	5.75	0.0832	3.92	31.8	0.9121	0.0446	6.02	4.6	0.9998
	1.2	7.43	0.0943	6.17	16.9	0.9804	0.0312	7.76	4.5	0.9996
	1.5	9.76	0.1637	9.09	6.8	0.9899	0.0531	9.95	1.9	0.9993
	1.8	11.8	0.0772	8.84	25.3	0.9413	0.0179	12.4	4.9	0.9994
WB-R	0.3	2.73	0.1187	2.77	1.4	0.9518	0.0731	2.89	5.6	0.9987
	0.6	4.24	0.155	3.34	21.2	0.9894	0.1544	4.30	1.4	0.9990
	0.9	7.09	0.0757	4.89	31.1	0.9071	0.0392	7.31	3.1	0.9992
	1.2	8.92	0.0837	6.35	28.7	0.9394	0.0314	9.23	3.5	0.9997
	1.5	10.2	0.0812	6.99	31.5	0.9194	0.0296	10.5	3.0	0.9995
	1.8	13.3	0.0924	7.43	44.1	0.7996	0.0345	13.6	2.3	0.9998

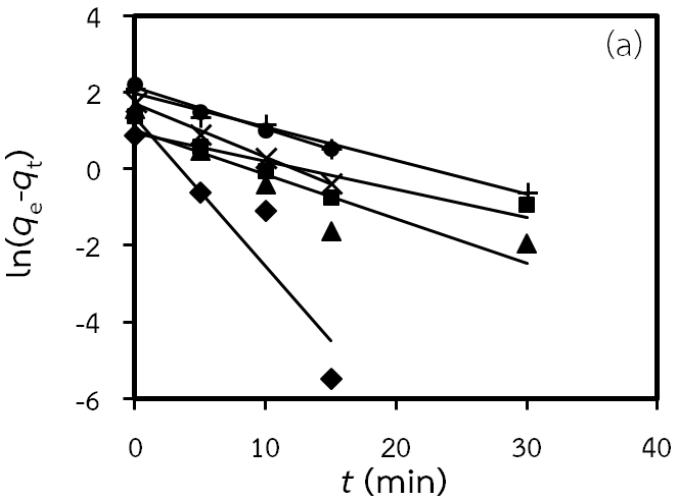
(a)
4
2
0
-2
-4
-6
0
10
20
30
40
t (min)
ln(qe-qt)

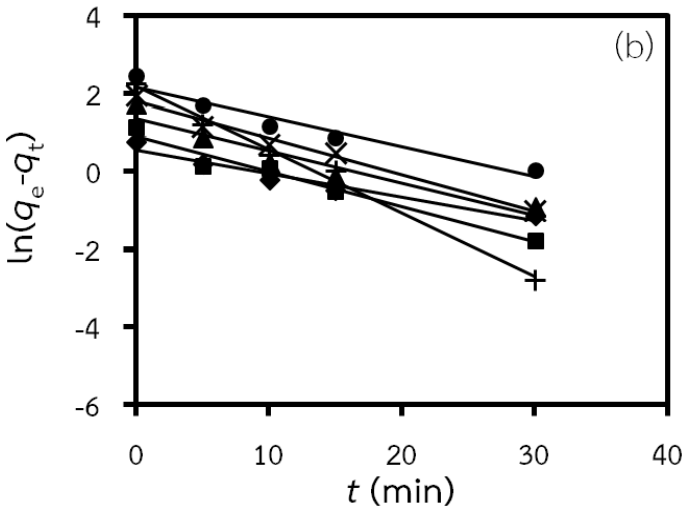
(b)
4
2
0
-2
-4
-6
0
10
20
30
40
t (min)
ln(qe-qt)

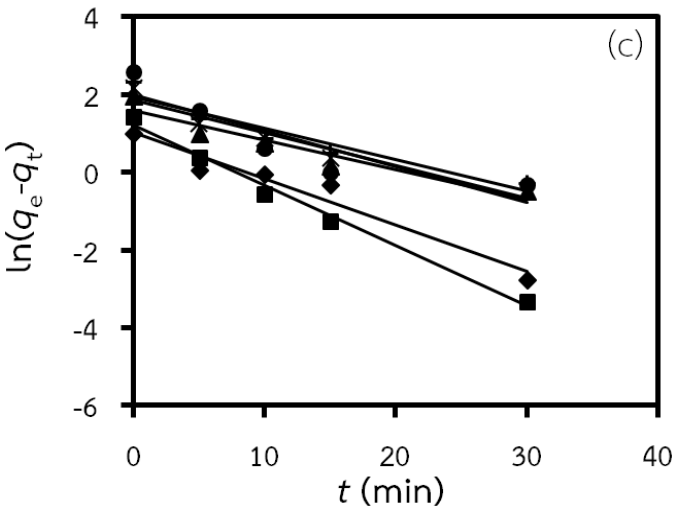
(c)
4
2
0
-2
-4
-6
0
10
20
30
40
t (min)
ln(qe-qt)

Figure 3.2 Linear plots of adsorption rate versus adsorption time of the pseudo-first-order model for (a) SA-R, (b) SB-R, and (c) WB-R at 303 K and 5 wt% of adsorbent loading for various initial stigmasterol concentrations: (♦) 0.3, (■) 0.6, (▲) 0.9, (×) 1.2, (+) 1.5, (●) 1.8 mg/g-solution

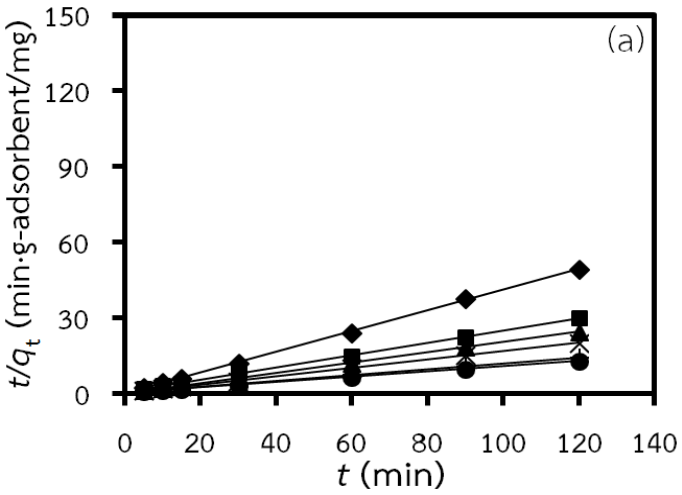

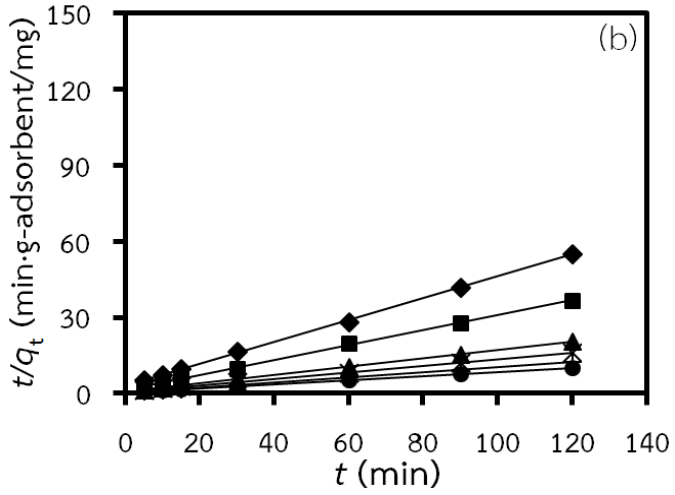

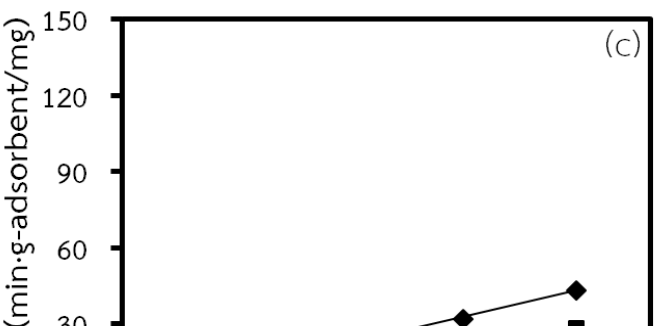

Figure 3.3 Linear plots of adsorption rate versus adsorption time of the pseudo-second-order model for (a) SA-R, (b) SB-R, and (c) WB-R at 303 K and 5 wt% of adsorbent loading for various initial stigmasterol concentrations: (♦) 0.3, (■) 0.6, (▲) 0.9, (×) 1.2, (+) 1.5, (●) 1.8 mg/g-solution

3.3.1.3 Adsorption isotherm

Adsorption isotherm was investigated at 298, 303, 308, and 313 K and discussed based on the data taken at 60 min after the start of the adsorption procedure. These conditions assure that the adsorption of stigmaterol has already come into equilibrium according to the results shown in the section of adsorption capacity. Figure 3.4 shows the dependence of adsorption capacity at equilibrium (q_e) on concentration of stigmasterol and 303 K. For SA-R, SB-R, and WB-R in the tested range of C_e, q_e increased with C_e and saturation of adsorption was not observed. Figure 3.5 shows the effect of temperature on q_e for various initial stigmasterol concentrations. For all cases, q_e decreased when temperature was increased. This result indicates that stigmasterol adsorption is an exothermic process. It should be noted that this dependence was clear in the case of high initial concentration but became less clear when the initial concentration was low. Equilibrium adsorption data were analyzed based on Langmuir, Freundlich, and linear isotherm models, using the corresponding linearized form of each model listed in Table 3.3. The Langmuir model was considered as an inappropriate model for prediction of isotherm of stigmasterol adsorption for SA-R, SB-R and WB-R because its value of R^2 was very low, and in some cases, q_m and K_{La} were negative, which signify no physical meaning for an adsorption process. Since the R^2 for the Freundlich model was larger than the R^2

for the linear model under all conditions, except the case of SA-R at 298 K and WB-R at 303 K, the Freundlich model was considered as the most suitable model for predicting the performance of adsorption at the equilibrium for all of the adsorbents. The values of K_F of WB-R were higher than those of SA-R and SB-R, indicating that the adsorption capacity of stigmasterol onto WB-R is higher than those of SA-R and SB-R. The calculated values of 1/*n* were nearly equal to 1.0 and several cases were more than 1.0, indicating that the adsorption of stigmasterol on SA-R, SB-R, and WB-R was surface energy heterogeneous. The values of 1/*n* more than 1.0 may be due to the increase of the interaction between stigmasterol and adsorbent that causes with favorable stigmasterol and stigmasterol interactions on the adsorbent surface. This showed that the adsorption of stigmasterol on SA-R, SB-R, and WB-R was multi-layer adsorption. In addition, for all cases, the calculated K_F decreased when the temperature of adsorption was increased. It indicates that all adsorbents have a much higher adsorption capacity at a low temperature than a high temperature. Regarding comparative energy consumption against those of other recovery methods, vacuum distillation operates at 413 to 623 K [11, 15-17, 19] and crystallization is used to separate phytosterol at a very low temperature in the range of 253 to 288 K [12-18, 20-22]. Therefore, adsorption is a promising method for reduction of energy consumption in the recovery of phytosterol in a large scale.

Table 3.3 Parameters and correlation coefficients for Langmuir, Freundlich, and linear models for isotherms of stigmasterol adsorption on SA-R, SB-R, and WB-R

Model		Langmuir: $q_e = \frac{q_m K_{La} C_e}{1 + K_{La} C_e}$			Freundlich: $q_e = K_F C_e^{1/n}$			Linear: $q_e = K_{Li} C_e$	
Linearized Equation		$\frac{C_e}{q_e} = \frac{1}{K_{La} q_m} + \frac{1}{q_m} C_e$			$\log q_e = \log K_F + \frac{1}{n} \log C_e$			$q_e = K_{Li} C_e$	
Resin	*T* (K)	K_{La}	q_m	R^2 (-)	K_F	1/*n* (-)	R^2 (-)	K_{Li}	R^2 (-)
SA-R	298	-0.198	-34.01	0.4696	8.590	1.180	0.9893	8.501	0.9900
	303	0.491	20.88	0.6389	6.734	0.722	0.9686	6.734	0.9328
	308	0.211	32.26	0.5156	5.519	0.841	0.9830	5.432	0.9797
	313	-0.137	-23.58	0.4030	3.816	1.122	0.9825	3.953	0.9491

SB-R	298	-0.096	-109.89	0.3446	11.564	1.053	0.9956	11.45	0.9900
	303	-0.164	-45.66	0.4745	8.993	1.120	0.9885	8.996	0.9874
	308	-0.012	-666.67	0.0062	8.341	1.017	0.9924	8.273	0.9862
	313	0.302	27.17	0.3625	6.180	0.749	0.9956	6.187	0.9306
WB-R	298	0.174	81.97	0.5951	12.154	0.904	0.9949	12.33	0.9848
	303	-0.070	-140.85	0.0852	10.558	1.025	0.9806	10.67	0.9827
	308	-0.241	-31.75	0.5670	10.177	1.203	0.9908	9.954	0.9863
	313	0.036	277.78	0.1017	9.627	0.983	0.9955	9.613	0.9942

Figure 3.4 shows good resemblances of the calculated curves and the experimental data for both Freundlich and linear models. Similar plots (in appendix A) were obtained at other temperatures (298, 308, and 313 K) and show good resemblances of the calculated curves and the experimental data as well. In the case of SA-R, nonlinear regression analysis was performed for both models and achieved high R^2 of 0.9775 and 0.9643 for the Freundlich model and linear model, respectively. In the case of SB-R and WB-R, similar results were obtained. Both models show good resemblances of the calculated curves and the experimental data. The results of a regression analysis reveal that the Freundlich model was slightly better than the linear model (the results are shown in appendix B). Therefore, the Freundlich model was considered the better model for prediction of the effect of C_e on q_e in stigmasterol adsorption on polymeric resins.

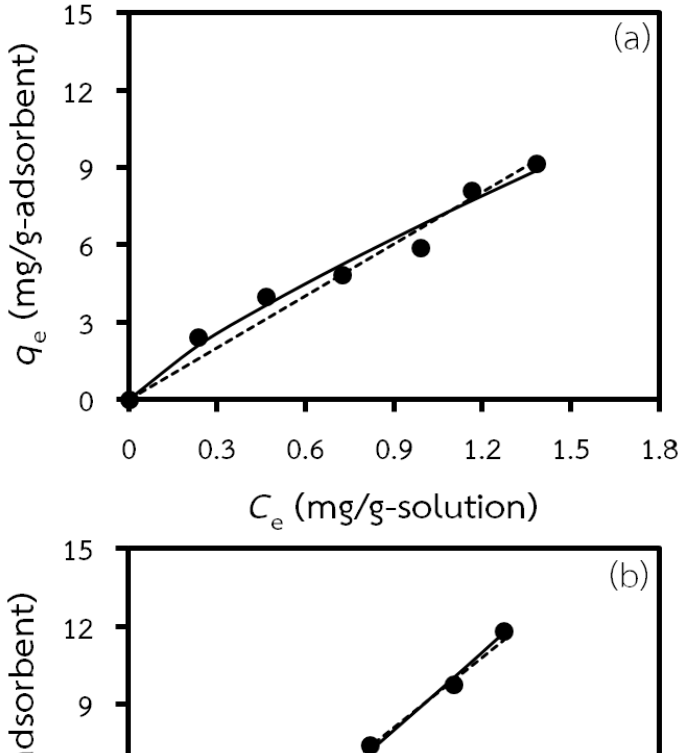

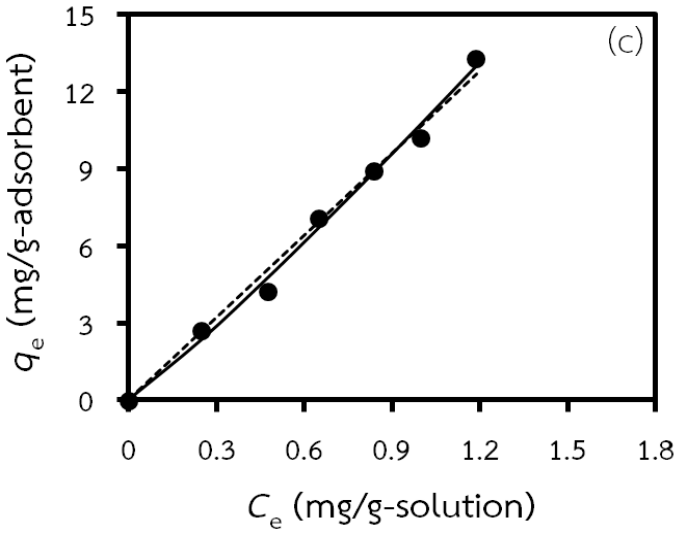

Figure 3.4 Dependences of (●) q_e on C_e calculated using (solid line) Freundlich and (dash line) linear model comparing with the experimental data for stigmasterol adsorption of (a) SA-R, (b) SB-R, and (c) WB-R, (T = 303 K, adsorbent loading = 5 wt%)

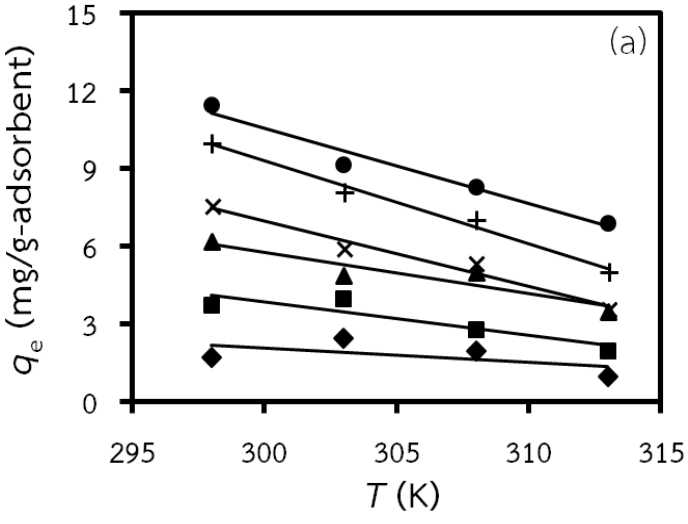

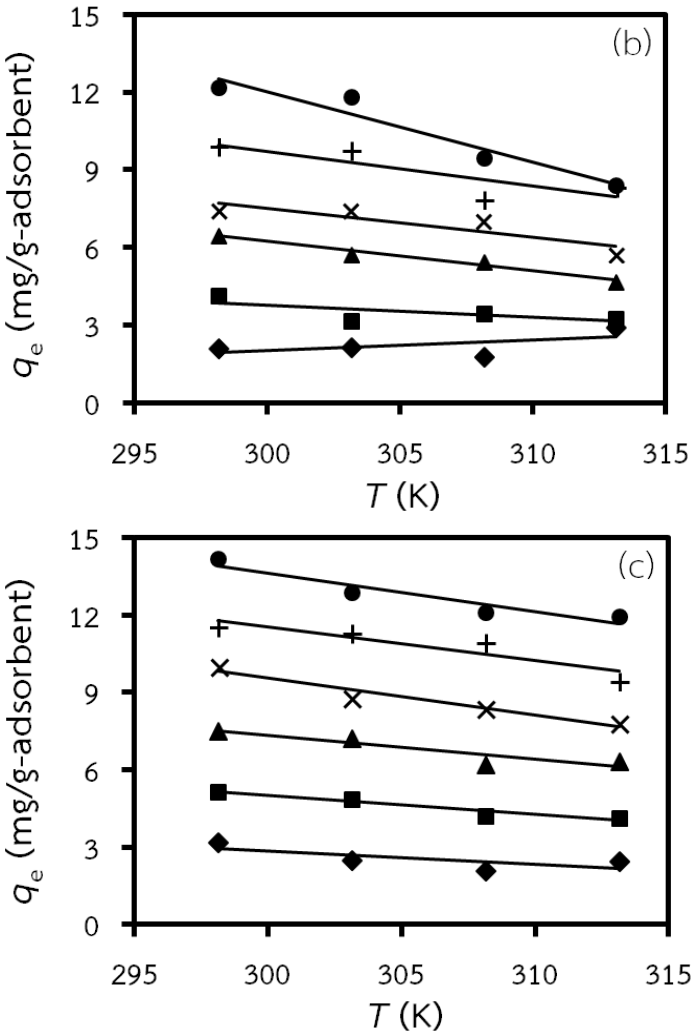

Figure 3.5 Effect of temperature on q_e of (a) SA-R, (b) SB-R, and (c) WB-R at equilibrium for various initial stigmasterol concentrations: (♦) 0.3, (■) 0.6, (▲) 0.9, (×) 1.2, (+) 1.5, (●) 1.8 mg/g-solution (T = 298 to 313 K, adsorbent loading = 5 wt%)

3.3.1.4 Adsorption thermodynamics

In order to obtain useful information for the design of the adsorption process, thermodynamics parameters of adsorption (ΔG, ΔH, and ΔS) were evaluated for all cases. Based on the discussion in the section of adsorption isotherm, adsorption equilibrium constants at various temperatures were calculated

by using Freundlich model, ΔG and ΔS were calculated by Equations 3.5 and 3.6, respectively.

$$\Delta G = -RT \ln K_F , \tag{3.5}$$

$$\ln K_F = \frac{\Delta S}{R} - \frac{\Delta H}{RT} . \tag{3.6}$$

By performing linear regression analysis of the plot between $\ln K_F$ and $1/T$, as shown in Figure 3.6, ΔH and ΔS were calculated from the slope and y-intercept of the obtained regression straight line.

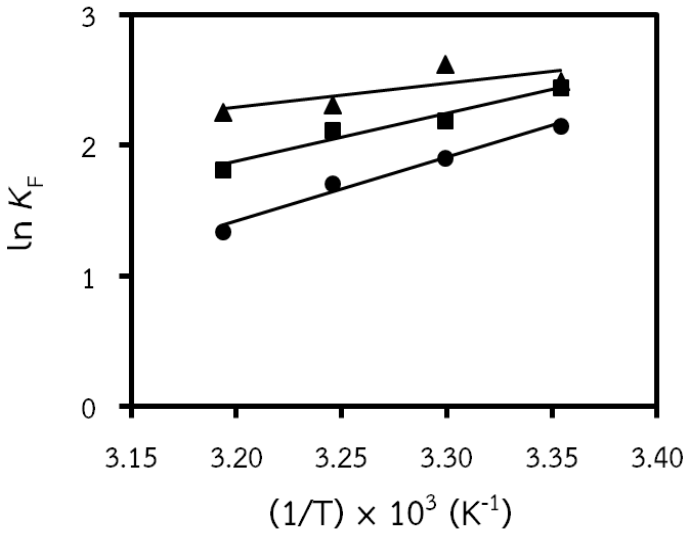

Figure 3.6 Plot of $\ln K_F$ versus $1/T$ for (●) SA-R, (■) SB-R, and (▲) WB-R

As summarized in Table 3.4, for the three adsorbents, the adsorption process produced negative values of ΔG, ΔH, and ΔS. The negative values of ΔG indicate that the adsorption is spontaneous and feasible. The increase of ΔG with respect to temperature indicates that the adsorption is more favorable at lower temperatures [53]. Since the calculated values of ΔG for all adsorbents were in the range of -20 to 0 kJ/mol, the stigmasterol adsorption on these three adsorbents can be considered as a physical adsorption process [54]. The negative values of ΔH indicate that the adsorption is exothermic and agreed well with the effect of

temperature on adsorption capacity at equilibrium discussed in the section of adsorption isotherm. A comparison of $\Delta H_{SA\text{-}R}$ (-40.81 kJ/mol), $\Delta H_{SB\text{-}R}$ (-30.32 kJ/mol), and $\Delta H_{WB\text{-}R}$ (-15.55 kJ/mol) indicates that the interaction between stigmasterol and SA-R is stronger than those for SB-R and WB-R. The negative value of ΔS indicates that the associative adsorption and decrease of the disorder of molecule between the solid/liquid interface due to the molecules adsorbed on solid surface are less free to move [55, 56].

Table 3.4 Thermodynamics parameters of stigmasterol adsorption on SA-R, SB-R, and WB-R

Resin	*T* (K)	ΔG (kJ/mol)	ΔH (kJ/mol)	ΔS (kJ/(mol·K))
SA-R	298	-5.33	-40.81	-0.12
	303	-4.81		
	308	-4.38		
	313	-3.49		
SB-R	298	-6.07	-30.32	-0.08
	303	-5.54		
	308	-5.43		
	313	-4.74		
WB-R	298	-6.19	-15.55	-0.03
	303	-6.63		
	308	-5.94		
	313	-5.90		

3.3.2 Recovery of phytosterol by using ion-exchange resins

The results from adsorption capacity at equilibrium showed that the adsorption capacity of SB-R and WB-R were higher than that of SA-R. This suggested that the amine group on the surface of SB-R and WB-R was capable to react with phytosterol than with the sulfonic group on the surface of SA-R. In addition, the result in the adsorption thermodynamics study showed that the enthalpy change of SA-R was more negative. It indicated that the phytosterol was adsorbed onto the SA-R surface at its high-energy adsorption sites which was difficult to desorb phytosterol from SA-R. Therefore, SB-R and WB-R were selected as the two most promising adsorbents to be used in the recovery process of phytosterol.

For both SB-R and WB-R, an adsorption experiment was carried out in n-heptane solution as a model solution containing stigmasterol at a concentration of 4.0 mg/g-solution. In each run, 2.5 g of model solution was mixed with 0.133 g of adsorbent (SB-R or WB-R), and then the mixture was shaken at 200 rpm and 303 K for 120 min. Figure 3.7 showed that the adsorption capacity of stigmasterol on WB-R was 43.75 mg/g-solution which was 1.1 times of that achieved by SB-R.

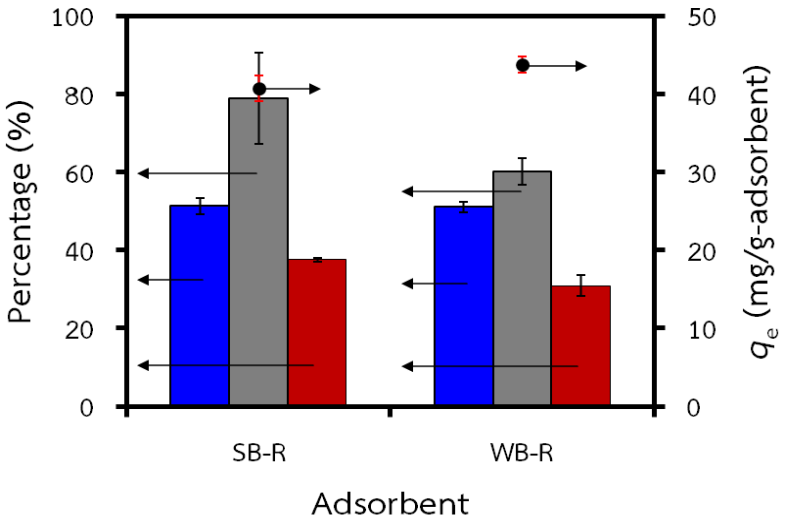

Figure 3.7 A comparison of (●) q_e, (blue bar) adsorption percentages, (gray bar) desorption percentages, and (red bar) recovery percentages from SB-R and WB-R

Regarding the desorption percentage of stigmasterol, the results showed that the desorption percentage of SB-R was higher than that of WB-R. The results suggest that SB-R was more capable of reacting with ethanol than with WB-R due to SB-R has a quaternary amine group as fixed positive charge, which is capable to react with the hydroxyl group on ethanol molecule than with the tertiary amine group on the surface of WB-R. However, the recovery percentage of both SB-R and WB-R were relatively low (30-37%). Therefore, it is interesting to find other absorbent materials with a high performance to used in phytosterol recovery.

Chapter 4
Recovery of Phytosterol by Using Silica-Based Adsorbent

4.1 Description

Molecular imprinting technique has been widely used for molecular recognition of adsorbent for separation of target molecules present in a liquid solution. This technique utilizes the interaction between the functional monomer and template molecule employed in polymerization, followed by template removal from the obtained polymer matrix to create recognition cavities. Regarding the development of a molecular imprinted material that uses phytosterol as a template molecule, several polymeric materials have been investigated in recent years.

Zhang et al. [57] synthesized a beta-sitosterol magnetic molecular-imprinted polymer (beta-sitosterol mag-MIP) by using a suspension polymerization method through microwave heating. This method has many advantages, especially the shorter polymerization time as compared with conventional methods. The results show that the obtained beta-sitosterol mag-MIP*s* had a higher adsorption capacity and selectivity for beta-sitosterol than those of magnetic non-imprinted polymers (mag-NIPs).

Hashim et al. [58] reported a comparison between non-covalent and covalent imprinting methods for synthesis of stigmasterol imprinted polymer. The results reveal that the polymer synthesized by the non-covalent imprinting method had a low stigmasterol affinity and selectivity. In contrast, the polymer synthesized by the covalent imprinting method demonstrated a much higher stigmasterol selectivity and binding recognition. These results suggest that the covalent imprinting method has a good potential for increasing the stability of the interaction between the template and functional monomer during the formation of binding site cavities.

Although molecular imprinted polymers may demonstrate a high affinity and selectivity for the target molecule, polymeric materials still have a disadvantage of instability caused by a high solution pH. Turner et al. [59] reported that variation of pH of organic solvent had an effect on the swelling or shrinking of polymers. This

effect is significant to the recognition property of polymers. For this reason, a molecular imprinting technique based on silica is an interesting choice due to silica-based materials having several advantages over polymer–based materials such as chemical inertness, negligible swelling in organic solvents, and high phytochemical and thermal stability [60].

A sol-gel process is a common method for synthesis of molecular imprinted silica (MIS). In this process, the template molecule interacts with an alkoxysilane precursor in the presence of an acid or basic catalyst, and the template molecule is encapsulated in a silica matrix. Specific adsorptive sites are created after the removal of the template molecule of the obtained silica matrix. There have been many studies that reported the use of a sol-gel process for producing molecular imprinted silica for selective recognition of steroid hormones.

Fujiwara et al. [61] reported a synthesis of molecular imprinted silica by a sol-gel method that used acetic anhydride as an alternative to water. The result reveals that progesterone and other analogous compounds were well adsorbed by several kinds of silica synthesized in the presence of cholesterol in organic solution. In addition, complicated processes have been used to prepare molecular imprinted silica for uses as chemical sensors, biosensors, and tailor-made purification materials.

Hsu and Yang [62] reported a synthesis of cholesterol MIP from a hydrophobic monomer by using a covalent method. The monomer, (cholesteryl propylcarbamate) triethoxysilane (Cho-TEICPS), was prepared by a reaction of cholesterol with triethoxy(3-isocyanato-propyl)silane to provide a hydrophobic interaction of cholesterol binding. Cho-TEICPS was polymerized with tetraethyl orthosilicate (TEOS) in the presence of cholesterol with an HCl or NH_4OH catalyst. The results demonstrate that the largest imprinting-induced promotion of binding value was obtained when the cholesterol MIP was synthesized with HCl = 0.01 M in a sol-gel solution. In addition, the cholesterol MIP showed a higher selectivity towards cholesterol in comparison with other steroid compounds.

Gupta and Kumar [63] fabricated an MIP for cholesterol (cholesterol MIP) using both non-hydrolytic and hydrolytic methods for cholesterol recognition. The results show that the percentage of adsorption was found to be higher for the cholesterol MIP synthesized by the hydrolytic method that used an HCl catalyst with phenyltriethoxysilane (PhTEOS) as the functional monomer. Several studies in

literature indicate that an acid-catalyzed sol-gel gelation method is an effective way that is able to produce a material with a higher surface area. According to previous reports, this method was satisfactory in a synthesis of pharmaceutical imprinted silica [64, 65].

This study reports the results of an application of an acid-catalyzed sol-gel gelation method to a synthesis of molecular imprinted silica (MIS) with phytosterol as the template molecule. The effects of synthesis factors including pH of the sol-gel solution, temperature, and the molar ratio (S/TEOS) of the phytosterol mixture to the alkoxysilane precursor (tetraethyl orthosilicate) on the adsorption and desorption capacities of the MIS were studied simultaneously in order to obtain optimal conditions for the synthesis of a high adsorption-capacity MIS for phytosterol from the model solution by using a central composite design.

4.2 Materials and methods

4.2.1 Materials

A phytosterol mixture was supplied from Acinopeptide Co., Ltd., (Chengdu, China). A composition analysis by using gas chromatography with flame ionized detector (GC-FID) revealed that the phytosterol mixture consisted of campesterol (24%), stigmasterol (31%), and beta-sitosterol (45%). Tetraethyl orthosilicate (TEOS) and cholesterol were supplied from Sigma-Aldrich chemical Co., Ltd., (Milwaukee, USA). Hydrochloric acid 37% was supplied from Merck Ltd., (Darmstadt, Germany). Methanol, acetonitrile and water were supplied from RCI Labscan Ltd., (Bangkok, Thailand). Acetic acid supplied from Merck Ltd., (Darmstadt, Germany) was HPLC grade and used without purification. Ethanol (AR grade) was supplied from RCI Labscan Ltd., (Bangkok, Thailand). N-heptane (AR grade) was supplied from Apex Chemicals Co., Ltd., (Bangkok, Thailand).

4.2.2 Methods

4.2.2.1 Preliminary molecular imprinted silica synthesis

In this study, a molecular imprinted silica (MIS) synthesis method was adapted from the work reported by Morais et al. [64]. In order to investigate the feasibility of synthesis of MIS by using phytosterol as a template molecule, a preliminary MIS was prepared by an acid-catalyzed sol-gel gelation

method and employed in a phytosterol recovery process in comparison with a non-imprinted silica (NIS). Following the procedure for MIS synthesis reported by Morais et al., solution A was prepared by adding 0.14 mmol phytosterol mixture into 10 ml TEOS in a 25 ml Erlenmeyer flask. The (S/TEOS) molar ratio was 3.24×10^{-3}. The mixture was stirred vigorously to completely dissolve the phytosterol mixture and form a homogeneous solution. Solution B was prepared by adding 37 % hydrochloric acid into deionized water to obtain an HCl concentration of 0.2 mol/L in the solution. Solution B (10 ml) was added to solution A and mixed into a sol-gel solution at ambient temperature and stirred for 96 h. The pH of the sol-gel solution was calculated according to Equation 4.1.

$$\mathrm{pH} = -\log(C_{\mathrm{HCl}}), \tag{4.1}$$

After being stirred for 96 h, the silica xerogel was dried at ambient temperature for 48 h, and the obtained silica xerogel was ground in a ceramic mortar. The template molecule was removed by a two-step solvent extraction procedure. In the first step of this procedure, 1 g of the silica powder embedded with the template molecule was shaken in 10 g of n-heptane at ambient temperature for 20 min. Then, the mixture was centrifuged at 4,000 rpm for 10 min in order to remove n-heptane. This first step was repeated 4 times, each time fresh n-heptane was used for shaking with the silica powder and then removed. In the second step, the same procedure was performed on the silica sample obtained from the first step, but ethanol was used to extract the template molecule instead of n-heptane, i.e., 1 g of the silica sample was extracted with 10 g of ethanol. To ensure that the template molecule was completely removed, the fourth extracting n-heptane and ethanol portions that were used to extract it were taken for analysis of the phytosterol in them by high performance liquid chromatography. If some phytosterol was found, the silica sample would be further extracted with fresh solvents. Non-imprinted silica (NIS) was prepared similarly to the preparation of MIS without an addition of the template molecule.

4.2.2.2 The design of experiment for the synthesis of molecular imprinted silica

A central composite design (CCD) was used to design the experiment, and a response surface methodology (RSM) was used to optimize the independent factors of MIS synthesis conditions with respect to the adsorption capacity of phytosterol. These independent factors were pH (*A*), temperature (*B*), and S/TEOS molar ratio (*C*) as shown in Table 4.1. The CCD used an alpha value of 2.0. The factorial, axial, and center points for each independent factors are shown in Table 4.2. The adsorption capacity of the adsorbent was selected as the response factor, and the relationship between the response factor and the independent factors were approximated by a quadratic model equation. The quality of the fitting quadratic model was expressed by the coefficient of determination (R^2), and the terms of the model were selected based on the *p*-value of each term at a 95% confidence level. The statistics of the fitting quadratic model was analyzed by analysis of variance (ANOVA). Finally, a comparison between the performances of MIS and NIS was done with the NIS synthesized by the same process as the synthesis of MIS, at a pH of 1.30 and a temperature of 310.5 K but without an addition of the template molecule.

Table 4.1 Factor levels in the central composite design

Factors	Name	Low	High
A	pH	0.6	2.0
B	Temperature (K)	298	323
C	S/TEOS molar ratio	2.23×10^{-4}	6.25×10^{-3}

Table 4.2 The experimental conditions from the central composite design (alpha value = 2.0)

Order	pH	*T* (K)	S/TEOS
1	0.95	304.25	1.73×10^{-3}
2	1.65	304.25	1.73×10^{-3}
3	0.95	316.75	1.73×10^{-3}
4	1.65	316.75	1.73×10^{-3}
5	0.95	304.25	4.74×10^{-3}
6	1.65	304.25	4.74×10^{-3}
7	0.95	316.75	4.74×10^{-3}
8	1.65	316.75	4.74×10^{-3}

9	0.60	310.5	3.24×10^{-3}
10	2.00	310.5	3.24×10^{-3}
11	1.30	298.0	3.24×10^{-3}
12	1.30	323.0	3.24×10^{-3}
13	1.30	310.5	2.23×10^{-4}
14	1.30	310.5	6.25×10^{-3}
15	1.30	310.5	3.24×10^{-3}
16	1.30	310.5	3.24×10^{-3}
17	1.30	310.5	3.24×10^{-3}

4.2.2.3 Silica characterization

The morphologies of MIS and NIS were investigated by transmission electron microscopy (TEM) with a high-resolution instrument (JEOL model JEM-2100) operating at 200 kV. Samples for TEM analyses were ultrasonically dispersed in ethanol, dropped onto a copper grid coated with carbon film, and then dried in vacuum. Functional groups of MIS and NIS were investigated by Fourier transform infrared (FT-IR) spectroscopy with IRPrestige-21 (Shimadzu, Japan) equipped with MIRacle ATR (PIKE Technologies, Inc.) with a resolution of 4 cm^{-1}. Specific surface area, total pore volume, and mean pore diameter were measured by Nitrogen adsorption isotherm at 77 K with BELSORP-max (BEL Japan. Inc.) equipped with BELPREP-vac II. Before analysis, samples were pretreated at vacuum drying at 383 K for 3 h. The specific surface area was calculated by using the Brunauer-Emmett-Teller (BET) and the pore size distribution was calculated by the Barret, Joyner, and Halenda (BJH) method.

4.2.2.4 Adsorption and desorption experiments

The adsorption experiment was carried out by using an n-heptane model solution containing the phytosterol mixture at a concentration of 4.0 mg/g-solution. In all tests, 2.5 g of the model solution was mixed with 0.133 g of adsorbent (MIS or NIS), and the mixture was then shaken at 200 rpm and 303 K for 10 h. At the end of adsorption process, the adsorbent was separated from the solution by filtration, and the concentration of phytosterol in the liquid phase was analyzed by HPLC. The adsorbent separated from the solution was left to dry at room temperature.

In the desorption experiment, the dried adsorbent was mixed with ethanol at a ratio of 10 g-ethanol/g-adsorbent. The mixture was then shaken in an orbital shaker at 200 rpm and 333 K for 2 h. After 2 h of desorption, the ethanol sample was taken to be heated at 333 K for 3 h in order to completely evaporate the ethanol. The residue obtained after ethanol evaporation was analyzed for phytosterol.

4.2.2.5 Phytosterol analytical method

The concentration of the phytosterol mixture was measured with a high performance liquid chromatograph (HPLC) system equipped with a UV detector. An injection valve with a 20-µl sample loop was used to introduce the sample into the HPLC system. Peak separation was achieved by using a reverse-phase column (Inertsil C8-3; 5 µm particle diameter, 250 mm length, 4.6 mm i.d., GL Sciences Inc, Japan). The measurement condition and mobile phase were adapted from the work reported by Chang et al. [49]. This condition was absorbance at 210 nm, while the mobile phase was a mixture of acetonitrile (85%), methanol (5%), and water containing 1% of acetic acid (10%). The flow rate of the mobile phase was 1.3 ml/min. Cholesterol in methanol (4.0 mg/g-solution) was used as the internal standard (ISTD) for quantification of the phytosterol in the mixture. In the quantification of phytosterol in the mixture from both the adsorbed and desorbed samples, n-heptane or ethanol was evaporated from 100 µl of the sample in the first step and methanol (800 µl) was added into the vial as a solvent. The sample was shaken at 200 rpm for 1 h, and then 200 µl of ISTD was added. Then, 100 µl of the prepared solution was injected into the HPLC system through the injection valve.

4.2.2.6 Evaluation of adsorption and desorption properties of the adsorbents

The adsorption performances of the adsorbents were evaluated in terms of the adsorption capacity at equilibrium calculated by Equation 4.2, and the adsorption percentage of phytosterol was calculated according to Equation 4.3,

$$q_e = \frac{(C_0 - C_e)W_{Sol}}{W_{Ads}}, \tag{4.2}$$

$$\%\mathrm{Ad} = \left(\frac{C_0 - C_e}{C_0} \right) \times 100, \tag{4.3}$$

The desorption performances of the adsorbents were evaluated from the desorption percentage of phytosterol calculated by Equation 4.4. The recovery percentage of phytosterol was quantified according to the following Equation 4.5,

$$\%\mathrm{De} = \left(\frac{W_{\mathrm{St,De}}}{W_{\mathrm{St,Ad}}} \right) \times 100, \tag{4.4}$$

$$\%\mathrm{Re} = \left(\frac{W_{\mathrm{St,De}}}{W_{\mathrm{T}}} \right) \times 100. \tag{4.5}$$

4.3 Results and discussion

4.3.1 Silica characterization

4.3.1.1 The morphology of molecular imprinted silica

The morphology and network structure of the molecular imprinted silica (MIS) and Non-imprinted silica (NIS) can be directly observed by a transmission electron microscope (TEM). Figure 4.1 shows TEM images of NIS ((a) and (b)) and MIS ((c) and (d)) in two-time magnification. NIS (Figure 4.1(a)) has a higher density in silica network than that of MIS (Figure 4.1(c)). Comparing NIS and MIS at a magnification of 150,000x, it can be seen that the particles of NIS were smaller than 25 nm while the particles of MIS were about 25-50 nm. This was probably due to the phytosterol molecules were embedded in silica matrix.

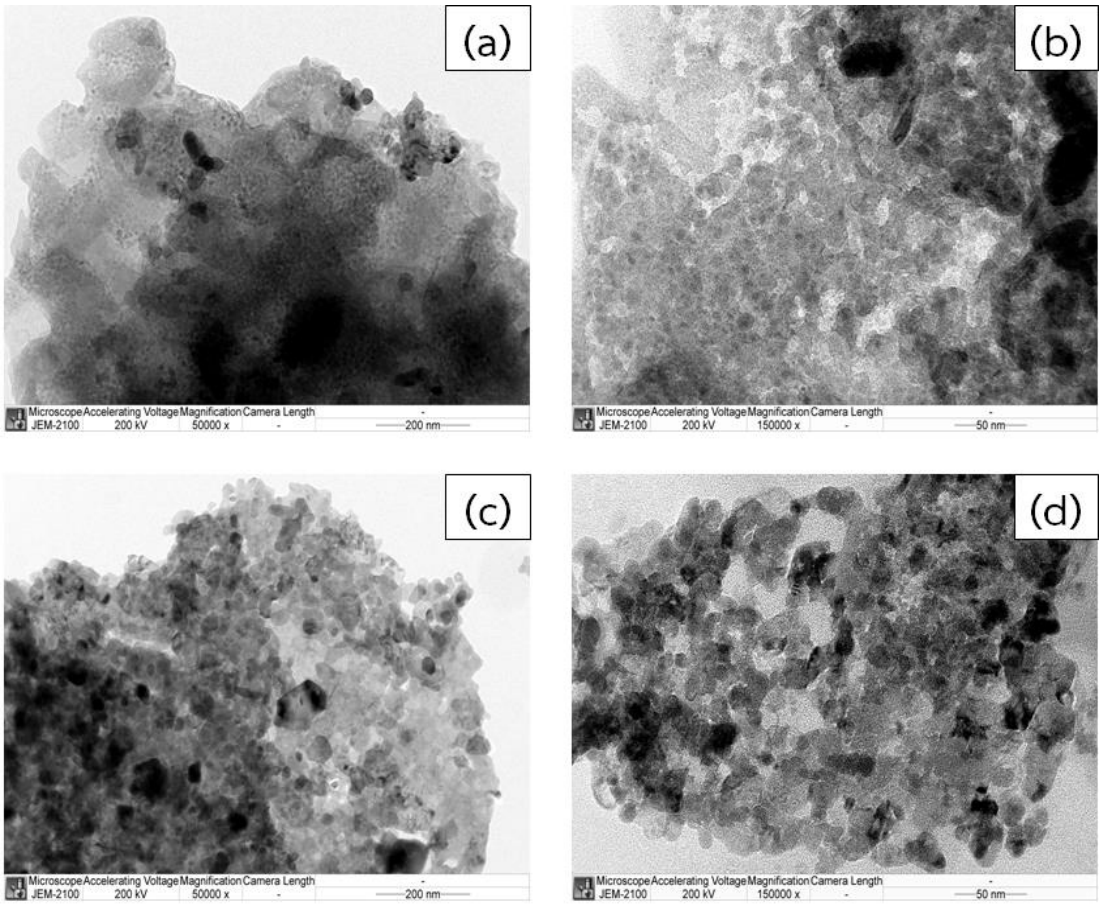

Figure 4.1 TEM images of ((a) and (b)) NIS and ((c) and (d)) MIS at two-time magnification

4.3.1.2 Functional groups of the molecular imprinted silica

The functional groups on MIS and NIS were identified by FT-IR spectra as shown in Figure 4.2. The general feature of the spectra of silica xerogels is the appearance of peaks at 690 to 3600 cm^{-1} associated with Si-OH stretching in the lower range of the wave numbers, while the peaks at the higher range of the wave numbers appeared due to hydroxyl (–OH) stretching of water molecule. The peak at 1100 cm^{-1} is associated with asymmetric stretching vibration of siloxane bond (Si–O–Si), and the peak at 800 cm^{-1} is associated with symmetric stretching vibration of Si–O–Si bond [66]. Figure 4.2 showed that large absorption peaks of –OH stretching of NIS and MIS appeared at 3348.42 and 3244.27 cm^{-1}, respectively. Large sharp peaks of Si–O–Si vibration appeared at 1049.28 and 1045.42 cm^{-1} for NIS and MIS, respectively as well as peaks of Si–O–Si appeared in the range of 700 to 1000 cm^{-1}. However, a comparison between NIS and MIS spectra indicated that the intensity of every peak in the NIS spectra was lower than the intensity of every peak in MIS spectra, especially those in the range of 700 to 1400 cm^{-1}. Phytosterol also gave an intense band at 1063.34 cm^{-1} that corresponds to the C-O group; an OH group band also appeared at 3549.99 cm^{-1} [67]. It was possible that there were still some traces of phytosterol left in the MIS.

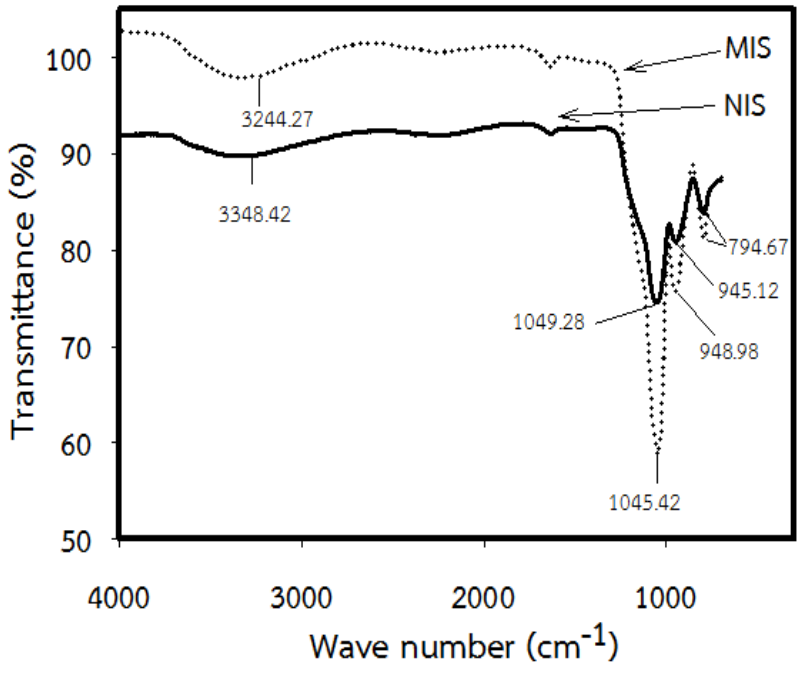

Figure 4.2 FTIR spectra of (solid line) NIS and (dash line) MIS

4.3.1.3 The surface analysis of MIS

Table 4.3 shows that the BET surface area, total pore volume, and mean pore diameter of MIS were higher than that of NIS. These results indicated a significant influence of the imprinting technique. The larger surface area and pore volume of MIS were obtained with the imprinting of phytosterol created additional pores in silica matrix. Considering the mean pore diameter of MIS, it possible that the pores in MIS were created by the imprinting of single phytosterol. This notion was based on the observation that the pore diameter of MIS was close to the sized of phytosterol molecule (1.91 nm in length, 0.58 nm in height, and 0.77 nm in wide) [68]

Table 4.3 The textural properties of the synthesized NIS and MIS

Sample	BET surface area (m^2/g)	Total pore volume (cm^3/g)	Mean pore diameter (nm)
NIS	617.38	0.2736	1.7726
MIS	767.06	0.3542	1.8472

4.3.2 Recovery of phytosterol by using the molecular imprinted silica

Phytosterol consists of a steroid part and an alkyl chain part. The steroid part is expected to be imprinted in the silica matrix during the sol-gel process. After the removal of phytosterol (template molecule) by solvent extraction, template-shaped pores in silica matrix will be created. Before the design of experiment for optimization of silica synthesis was attempted, a preliminary synthesis of molecular imprinted silica was performed to examine the feasibility of MIS synthesis by using phytosterol as a template molecule. The adsorption capacities of the synthesized MIS and NIS are shown in Figure 4.3. The recovery results show that

the adsorption capacity of MIS was higher than that of NIS. In addition, the recovery results show that the adsorption percentage of MIS was higher than that of NIS. These results suggest that the imprinting by phytosterol created additional pores in the silica matrix. Regarding the desorption percentage of phytosterol, the synthesized MIS and NIS gave the desorption percentages of phytosterol at 73.27 and 52.77 %, respectively. The results also show that the recovery percentage of phytosterol from MIS was 2.0 times higher than that from NIS. Comparison of the efficiencies of MIS and anion-exchange resins indicated that MIS showed a 1.7 and 1.6 times higher adsorption capacity than those achieved by SB-R and WB-R, respectively. In addition, the results also show that the recovery percentage of MIS of phytosterol from MIS was 1.6 and 2.0 times higher than that from SB-R and WB-R, respectively. The results show that molecular imprinted silica is a good alternative adsorbent for phytosterol recovery process.

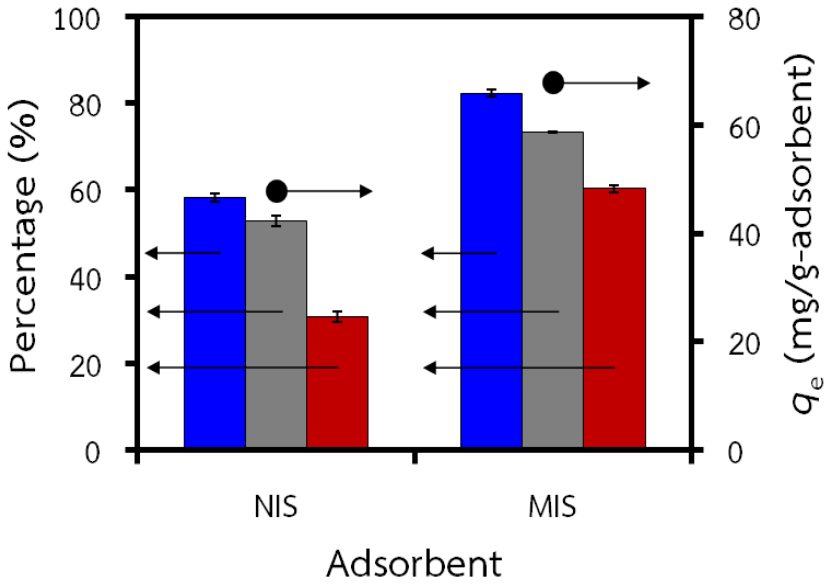

Figure 4.3 A comparison of (●) q_e, (blue bar) adsorption percentages, (gray bar) desorption percentages, and (red bar) recovery percentages from NIS and MIS

4.3.3 Effects of synthesis factors on the performance of the molecular imprinted silica

The preliminary experiment showed the full feasibility of the synthesis of MIS by using phytosterol as a template molecule and an acid-catalyzed sol-gel gelation method. In this part, the effects of synthesis factors including pH of sol-gel solution, temperature, and the S/TEOS molar ratio were investigated simultaneously to reveal the impact on the performance of the synthesized MIS when these factors were changed. Figure 4.4 shows comparisons of adsorption percentages and desorption percentages of phytosterol by the synthesized MIS under different combinations of the three factors. The effect of pH of sol-gel solution were investigated by focusing on the combinations number 9, 10, 15, 16, and 17 of which the other 2 factors: temperature (310.5 K) and S/TEOS (3.24×10^{-3}) were fixed. Combination number 9 at pH 0.6 showed the highest adsorption percentage of phytosterol and the highest adsorption capacity at 72.23 mg/g-adsorbent, which was 1.7 times higher than that of NIS as shown in Figure 4.5. On the other hand, combination number 10 at pH 2.0 showed the lowest adsorption percentage of phytosterol, and no phytosterol desorption.

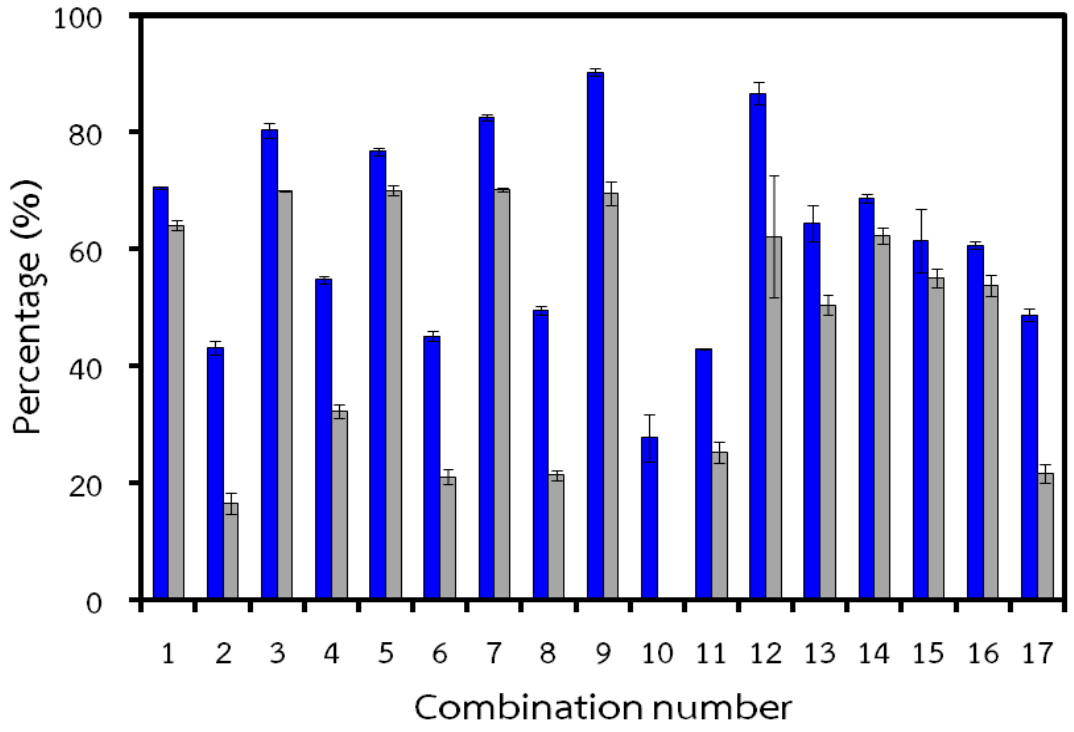

Figure 4.4 Comparisons of (blue bar) the adsorption percentages and (gray bar) desorption percentages of phytosterol by MIS synthesized under various combinations of factors

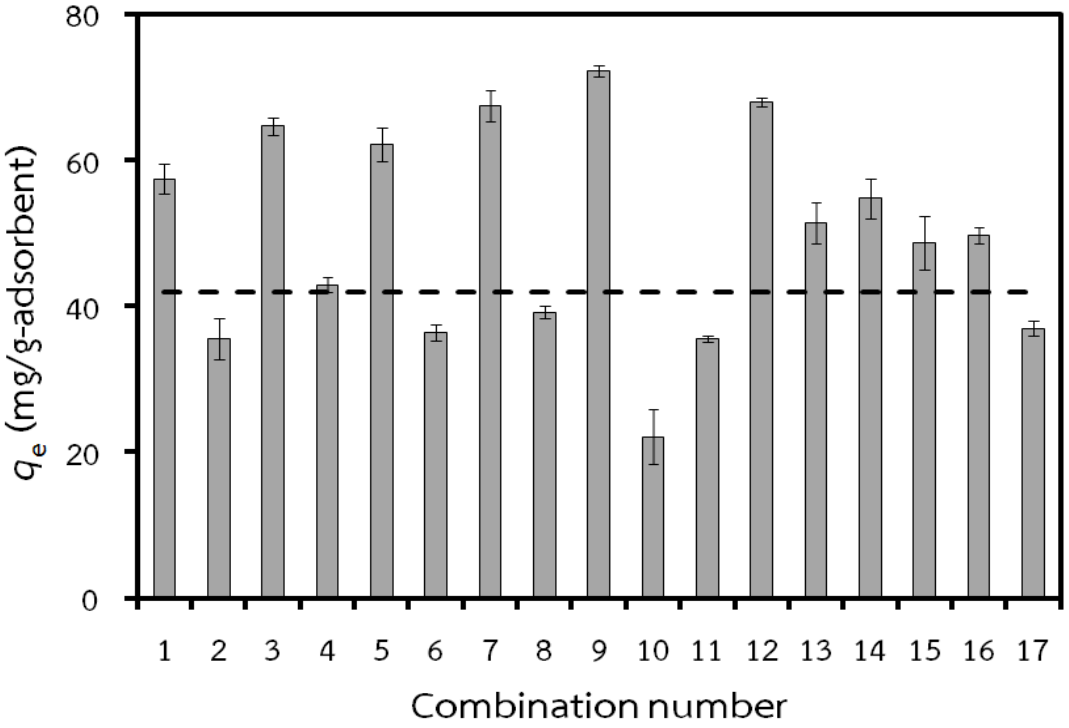

Figure 4.5 Adsorption capacities of (gray bar) different MIS synthesized under various combinations of factors compared to that of (dash line) NIS

To investigate the effect of temperature, combinations number of 11, 12, 15, 16, and 17 with a fixed pH at 1.3 and a fixed S/TEOS molar ratio at 3.24×10^{-3} were used. The results showed that combination number 12 at 323 K showed the highest adsorption percentage (adsorption capacity = 67.94 mg/g-adsorbent) and the highest desorption percentage, while combination number 11 at temperature 298 K showed the lowest adsorption percentage and the lowest desorption percentage. To investigate the effect of S/TEOS molar ratio, combinations number of 13, 14, 15, 16, and 17 with a fixed pH (1.3) and a fixed temperature (310.5 K) were used. The results showed that the combination number 14 at a S/TEOS molar ratio of 6.25×10^{-3} showed the highest adsorption percentage. This result indicated that more template

molecules gave a higher chance to create a lot of additional pores in the silica matrix. In addition, it gave the highest desorption percentage of phytosterol.

4.3.4 Statistical analysis

The results of the surface analysis and the adsorption capacity of phytosterol according to the central composite design (CCD) were statistically analyzed in order to identify the significant factors on the BET surface area and the adsorption capacity of phytosterol by the synthesized MIS.

4.3.4.1 BET surface area

Table 4.4 shows the results of an analysis of variance of BET surface area of the synthesized MIS under different combinations of the three factors. The *p*-values show that only the linear term of pH (*A*) was significant (*p*-value < 0.05). It seems that the rest terms had no effect on the BET surface area of MIS. However, a regression model was performed in order to obtain a suitable prediction model for the BET surface area of MIS, and the relationship between the BET surface area and the independent factors was shown in Equation (4.6).

Table 4.4 The results of an analysis of variance of the BET surface area of MIS

Term	Coefficient	S.E. coefficient	*p*-value
Constant	39,551.4	39.08	0
pH (*A*)	994.35	17.71	0.002
Temperature (*B*)	-259.97	17.71	0.355
S/TEOS (*C*)	308,992	17.71	0.908
A × *A*	208.04	16.1	0.157
B × *B*	0.44	16.1	0.321
C × *C*	2,913,861	16.1	0.693
A × *B*	-5.50	25.05	0.646
A × *C*	-22,418.2	25.05	0.651
B × *C*	-966.58	25.05	0.727

$$a_{s,BET} = 39,551.4 + 994.35A - 259.97B + 308,992C + 208.04A^2 + 0.44B^2 + 2,913,861C^2 - 5.5AB - 22,418.2AC - 966.58BC \quad (4.6)$$

where *A*, *B*, and *C* are pH, temperature, and S/TEOS molar ratio, respectively. The quadratic model fitted the experimental results well with R^2 of 79.74 %, indicating

that the regression model was able to predict the BET surface area of the synthesized MIS under different combinations of the three factors satisfactorily. Figure 4.6 (a) illustrates the effect of temperature and S/TEOS molar ratio on the BET surface area of the synthesized MIS, with a fixed pH at 1.3. Figure 4.6 (b) illustrates the effect of pH and S/TEOS molar ratio on the BET surface area of the synthesized MIS, with a fixed temperature at 310.5 K, and Figure 4.6 (c) illustrates the effect of pH and temperature on the BET surface area of the synthesized MIS, with a fixed S/TEOS molar ratio at 3.24×10^{-3}. The results indicate that the pH of the sol-gel solution played an important role in the synthesized MIS. Figure 4.6 (b) and 4.6 (c) show the low BET surface area at pH in the ranges of 1.5 – 2.0, while the BET surface area of the synthesized MIS increased rapidly when pH was lower than 1.5. The effect of pH could be explained by the rate of polymerization of silica. In general, the silica synthesized at pH very close to the point of zero charge of polymeric silica (the pH range of 1.5-2.0) [69], the solution has only neutral SiOH group, which is not easily to condense and results in a long gelation time in the sol-gel process [70]. Therefore, the network structure of silica is high density, and small pores are formed results in low surface area as showed in the Table C.14 (Appendix C). At the pH lower than that of the point of zero charge of polymeric silica, the protonated silanols ($SiOH_2^+$) are produced in the solution. They can rapidly eliminate of water, and encourage more the rate of condensation [70]. This results in decreasing gelation time and lead to the network structure of silica is low density. Therefore, the silica has larger pores and higher surface area. The results of an analysis of variance show the effect of temperature on the BET surface area was not significant. However, the results from the experiments and the prediction show that the BET surface area increased with increasing temperature as shown in Figure 4.6 (a) and 4.6 (c). The effect of temperature could be explained by a higher temperature encourages more hydrolysis reaction, and results in a shorter gelation time in the sol-gel process [71]. Therefore, the network structure of silica is less dense, and larger pores are formed results in high surface area. The effect of S/TEOS molar ratio on the BET surface area was slight effect as shown in Figure 4.6 (a) and 4.6 (b). The BET surface area increased with increasing S/TEOS molar ratio. This result indicated that the imprinting of phytosterol created additional pores in silica matrix. However, this result was clear in the case of low temperature in Figure 4.6 (a).

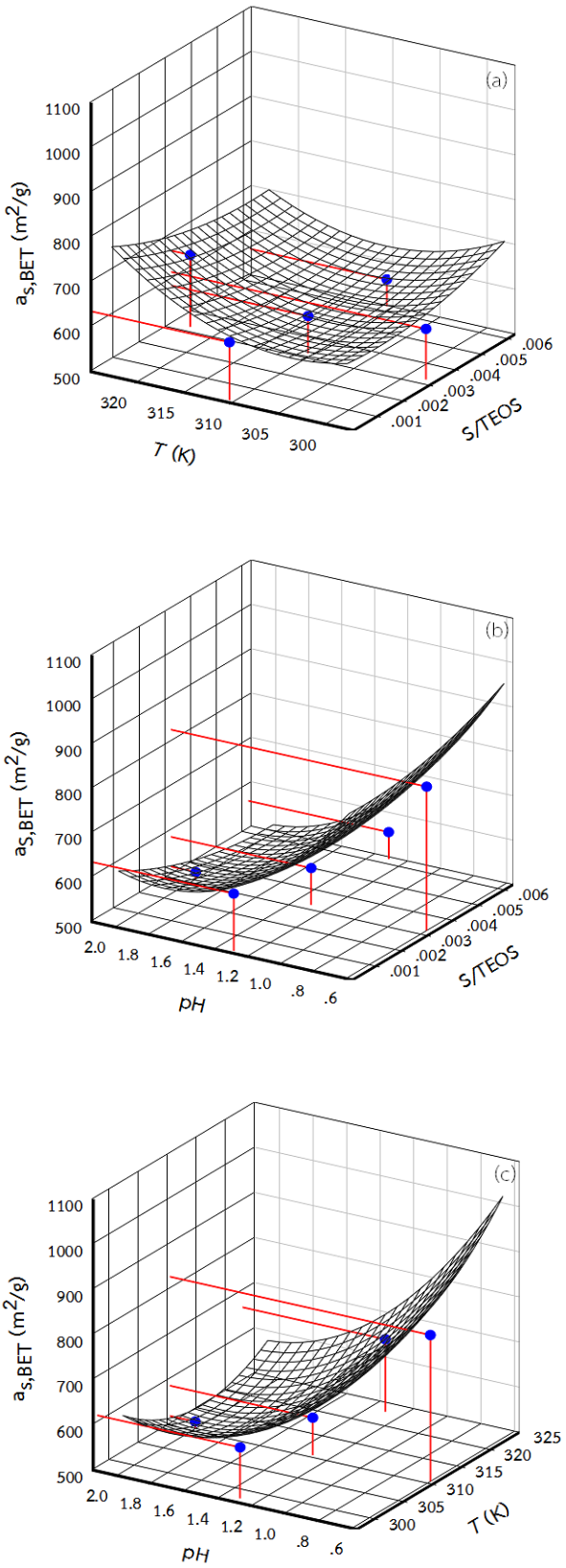

Figure 4.6 A three-dimensional response surface plot of the BET surface area of the synthesized MIS; (a) effect of temperature and S/TEOS molar ratio on the

BET surface area, with a fixed pH at 1.3, (b) effect of pH and S/TEOS molar ratio on the BET surface area, with a fixed temperature at 310.5 K, and (c) effect of pH and temperature on the BET surface area, with a fixed S/TEOS molar ratio at 3.24×10^{-3}

4.3.4.2 Adsorption capacity

The results of an analysis of variance of adsorption capacity of phytosterol to MIS is shown in Table 4.5.

Table 4.5 The results of an analysis of variance of the adsorption capacity of phytosterol to MIS

Term	Coefficient	S.E. coefficient	*p*-value
Constant	3,956.73	3.098	0.000
pH (*A*)	2.03	1.404	0.000
Temperature (*B*)	-26.19	1.404	0.006
S/TEOS (*C*)	24,501.60	1.404	0.630
$A \times A$	4.78	1.276	0.660
$B \times B$	0.04	1.276	0.217
$C \times C$	908,209.00	1.276	0.150
$A \times B$	-0.13	1.986	0.886
$A \times C$	-2,474.21	1.986	0.532
$B \times C$	-85.97	1.986	0.696

The regression coefficient, standard error, and *p*-value associated with Equation 4.7 are shown in Table 4.5. The statistical testing of the regression model was by an analysis of variance (ANOVA). The *p*-values show that the linear term of pH (*A*) and temperature (*B*) were significant (*p*-value < 0.05). Nevertheless, the linear term of S/TEOS molar ratio, the quadratic terms, and the interaction terms were insignificant (*p*-value > 0.05). However, the full regression model that did not leave out these insignificant terms was used to obtain a suitable prediction model for adsorption capacity of phytosterol because they might affect

the accuracy of the predictions. The relationships between the adsorption capacity and the independent factors are expressed by Equation 4.7 below,

$$q_e = 3,956.73 + 2.03A - 26.19B + 24,501.6C + 4.78A^2 + 0.04B^2 , \\ + 908,209C^2 - 0.13AB - 2,474.21AC - 85.97BC \quad (4.7)$$

where *A*, *B*, and *C* are pH, temperature, and S/TEOS molar ratio, respectively. It was found that the quadratic model fitted the experimental results well with R^2 of 93.27 %, indicating that the regression model was able to predict the adsorption capacity of phytosterol satisfactorily. In addition, the R^2 (adj) value was 84.62 %, indicating that the three factors were able to explain 84.62 % of the variation in the adsorption capacity of phytosterol. Figure 4.7 (a) illustrates the effect of temperature and S/TEOS molar ratio on the adsorption capacity of phytosterol, with a fixed pH at 1.3. Figure 4.7 (b) illustrates the effect of pH and S/TEOS molar ratio on the adsorption capacity of phytosterol, with a fixed temperature at 310.5 K, and Figure 4.7 (c) illustrates the effect of pH and temperature on the adsorption capacity of phytosterol, with a fixed S/TEOS molar ratio at 3.24×10^{-3}. These results indicate that the prediction results of the adsorption capacity of phytosterol were in good agreement with the experimental values. The adsorption capacity of phytosterol decreased with increasing solution pH as shown in Figure 4.7 (b) and 4.7 (c). This result indicates that the pH of the sol-gel solution played an important role in the synthesis of a high-performance MIS, as there has been a report that different amounts of cholesterol were adsorbed by cholesterol-imprinted microporous silica synthesized under different catalytic conditions [62]. The MIS synthesized at low pH showed higher adsorption capacity of phytosterol due to large surface area. In addition, temperature also played an important role in the impact on the adsorption capacity of phytosterol. The results show that the adsorption capacity increased with increasing temperature as shown in Figure 4.7(a) and 4.7(c). The effect of S/TEOS molar ratio on the adsorption capacity of phytosterol was slight effect as shown in Figure 4.7 (a) and 4.7 (b). The adsorption capacity increased with increasing S/TEOS molar ratio. The optimal values of three synthesis factors were determined. According to the obtained results, the optimum conditions for MIS synthesis was a pH of sol-gel solution at 0.6, a temperature at 323 K, and an S/TEOS molar ratio at

$6.25x10^{-3}$. Under these optimal conditions, the synthesized MIS showed the highest adsorption capacity of 103.34 mg/g-solution which was 2.5 times higher than that achieved by NIS.

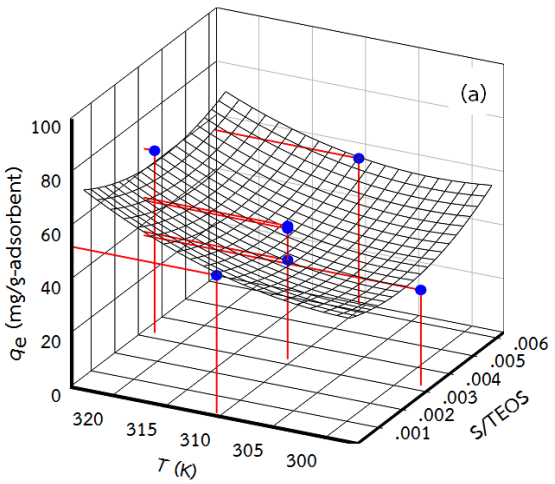

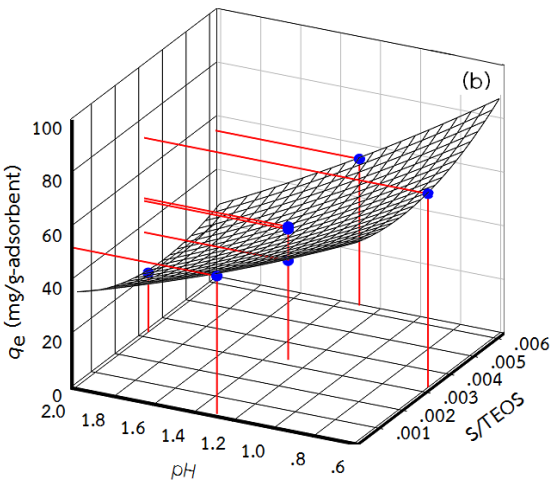

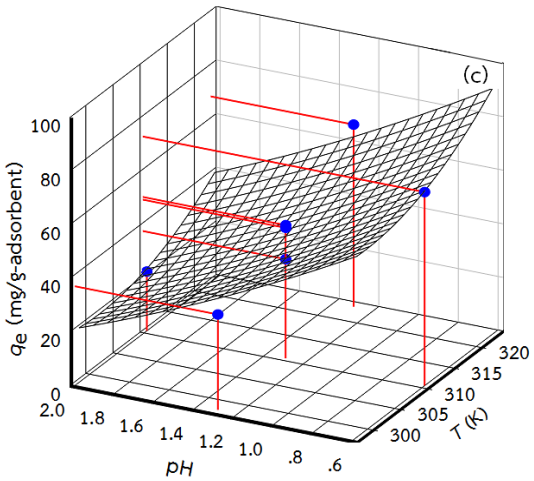

Figure 4.7 A three-dimensional response surface plot of the adsorption capacity of phytosterol to MIS; (a) effect of temperature and S/TEOS molar ratio on the adsorption capacity of phytosterol, with a fixed pH at 1.3, (b) effect of pH and S/TEOS molar ratio on the adsorption capacity of phytosterol, with a fixed temperature at 310.5 K, and (c) effect of pH and temperature on the adsorption capacity of phytosterol, with a fixed S/TEOS molar ratio at 3.24×10^{-3}

Chapter 5
Conclusion

This study focused on the selection of adsorption and desorption processes under mild condition for phytosterol recovery. The proposed process consisted of adsorption of phytosterol at 303 K and desorption of phytosterol in non-toxic ethanol at 343 K. Three types of commercial grade styrene-divinylbenzene copolymer ion-exchange resins (strong acid resin: SA-R, strong base resin: SB-R and weak base resin: WB-R) were considered as attractive adsorbents in this study. The study of behavior of phytosterol adsorption on three resins showed that the adsorption rate of phytosterol on SA-R, SB-R, and WB-R could be well described by pseudo-second-order kinetics model. The equilibrium adsorption data fitted better with a Freundlich isotherm model than Langmuir and linear isotherm models. Freundlich adsorption isotherm constant indicated that the adsorption of phytosterol on three resins favoured low temperature, and it showed multi-layer adsorption. The thermodynamic parameters showed that the adsorption was an exothermic process, spontaneous and more favorable at a lower temperature. To investigate the potential of the proposed two-step process, adsorption of phytosterol in model solution and desorption of phytosterol in ethanol were performed by using a batch system. SB-R and WB-R were selected as the promising adsorbents to be used in the proposed process due to they showed a higher adsorption capacity than that of SA-R. In the adsorption step, the adsorption capacity of phytosterol on WB-R was 43.75 mg/g-adsorbent which was 1.1 times of that achieved by SB-R. In the desorption step, the desorption percentage of SB-R was 78.94 % which was 1.3 times of that achieved by WB-R, and the recovery percentage of both SB-R and WB-R were in the range of 30-37 %.

In addition, molecular imprinted silica (MIS) was also use as an alternative adsorbent for phytosterol recovery. The results of silica characterization showed that the BET surface area, total pore volume, and mean pore diameter of MIS were higher than that of NIS. This significantly influenced the quantity of adsorption and desorption of phytosterol. Regarding the recovery of phytosterol, the adsorption capacity of MIS was 68.01 mg/g-adsorbent which was 1.4 times of that achieved by non imprinted

silica (NIS). MIS and NIS gave the desorption percentages of phytosterol at 73.27 and 52.77 %, respectively. The results also show that the recovery percentage of phytosterol from MIS was 2.0 times higher than that from NIS. In addition, comparison of the efficiencies of MIS and anion-exchange resins indicated that MIS showed a 1.7 and 1.6 times higher adsorption capacity than those achieved by SB-R and WB-R, respectively. The results also show that the recovery percentage of MIS of phytosterol from MIS was 1.6 and 2.0 times higher than that from SB-R and WB-R, respectively. The effects of synthesis factors on the BET surface area and the adsorption capacity of MIS were studied. An analysis of response surface showed that the pH of solution was found to have the largest effect on the BET surface area and the adsorption capacity of MIS. The optimum conditions for MIS synthesis was a pH of sol-gel solution of 0.6, a temperature of 323 K, and an S/TEOS molar ratio of 6.25×10^{-3}. The results showed that the synthesized MIS gave the highest adsorption capacity of 103.34 mg/g-solution which was 2.5 times of that achieved by NIS.

The results of this study demonstrate that the proposed process for phytosterol recovery consisted of adsorption and desorption can be operated under mild condition. This is a promising method for reduction of energy consumption in the phytosterol recovery in a large scale. In addition, this study also demonstrate the feasibility of synthesis of molecular imprinted silica (MIS) by using phytosterol as a template molecule. The results indicated that the synthesized MIS had a high efficiency on adsorption and desorption of phytosterol which is a good alternative adsorbent for phytosterol recovery process.

References

[1] Verleyen T., Verhe R., Garcia L., Dewettinck K., Huyghebaert A. and Greyt W.D. "Gas Chromatographic Characterization of Vegetable Oil Deodorization Distillate." **J. Chromatogr. A,** vol. 921, no. 2, Jul. 2001. pp. 277-285

[2] Gunawan S., Ju Y.H. "Vegetable Oil Deodorizer Distillate: Characterization, Utilization and Analysis." **Sep. Purif. Rev.,** vol. 38, no. 3, Apr. 2009. pp. 207-241

[3] Wright T., Wiyono E. **"Indonesia Oilseed and Products Update July 2014."** [Online].Available: http://www.thefarmsite.com/reports/contents/IndonesiaOilseeds31July2014.pdf. 2014.

[4] Abdi A., Wright T. and Rahmanulloh A.**"Oilseeds and Products Annual Report 2017."**[Online].Available:https://gain.fas.usda.gov/Recent%20GAIN%20Publications/Oilseeds%20and%20Products%20Annual_Jakarta_Indonesia_3-15-2017.pdf. 2017.

[5] Malaysian Palm Oil Board. **"Overview of the Malaysian Oil Palm Industry 2016."**[Online].Available: http://palmoilis.mpob.gov.my/index.php/overview-of-industry/510-overview-of-industry-2016. 2016.

[6] Malaysian Palm Oil Board. **"Overview of the Malaysian Oil Palm Industry 2017."**[Online].Available: http://palmoilis.mpob.gov.my/index.php/overview-of-industry/593-overview-of-industry-2017. 2017.

[7] Richey B., Preechajarn S. **"Thailand Palm Oil Production Supply Demand Update."** [Online]. Available: https://gain.fas.usda.gov/Recent%20GAIN%20Publications/Palm%20Oil%20ProductionSupplyDemand%20Update_Bank_Thailand_6-12-2-15.pdf. 2015.

[8] Santella R., Preechajarn S. **"Thailand Oilseed and Product Annual 2016."** [Online]. Available:https://gain.fas.usda.gov/Recent%20GAIN%20Publications/Oilseeds%20and%20Products%20Annual_Bangkok_Thailand_5-2-2016.pdf. 2016.

[9] Echim C., Verhé R., Greyt W.D. and Stevens C. "Production of Biodiesel from Side - Stream Refining Products." **Energy Environ. Sci.,** vol. 2, no. 11, Sep. 2009. pp. 1131-1141

[10] Fernandes P., Cabral J.M.S. "Phytosterols: Applications and Recovery Methods." **Biores. Technol.,** vol. 98, no. 12, Sep. 2007. pp. 2335-2350

[11] Rohr R. **"Process for Separating Unsaponifiable Valuable Products from Raw Materials."** U.S. Patent no. US2003/0120095 A1, January 2003

References (cont.)

[12] Yang H., Yan F., Wu D., Huo M., Li J., Cao Y. and Jiang Y. "Recovery of Phytosterols from Waste Residue of Soybean Oil Deodorizer Distillate." **Bioresour. Technol.,** vol. 101, no. 5, Mar. 2010. pp. 1471-1476

[13] Khatoon S., Rajan R.G.R. and Krishna A.G.G. "Physicochemical Characteristics and Composition of Indian Soybean Oil Deodorizer Distillate and the Recovery of Phytosterols." **J. Am. Oil Chem. Soc.,** vol. 87, no. 3, Mar. 2010. pp. 321-326

[14] Brown W., Smith F.E. **"Process for Separating Tocopherols and Sterols from Deodorizer Sludge and the Like."** U.S. Patent no. 3153055, October 1964

[15] Fizet C. **"Process for Tocopherols and Sterols from Natural Sources."** U.S. Patent no. 5487817, January 1996

[16] Moreira E.A., Baltanás M.A. "Recovery of Phytosterols from Sunflower Oil Deodorizer Distillates." **J. Am. Oil. Chem. Soc.,** vol. 81, no. 2, Feb. 2004. pp. 161-167

[17] Wollmann G., Schwarzer J. and Gutsche B. **"Processes for Producing Sterols from Fatty Acid Production Residues."** U.S. Patent no. 6956125 B2, October 2005

[18] Carmona M.A., Jiménez C., Sanchidrián C.J., Peña F. and Ruiz J.R. "Isolation of Sterols from Sunflower Oil Deodorizer Distillate." **J. Food Eng.,** vol. 101, no. 2, Nov. 2010. pp. 210-213

[19] Ghosh S., Bhattacharyya D.K. "Isolation of Tocopherol and Sterol Concentrate from Sunflower Oil Deodorizer Distillate." **J. Am. Oil. Chem. Soc.,** vol. 73, no. 10, Oct. 1996. pp. 1271-1274

[20] Smith F.E. **"Separation of Tocopherols and Sterols from Deodorizer Sludge and the Like."** U.S. Patent no. 3335154, August 1967

[21] Yan F., Yang H., Li J. and Wang H. "Optimization of Phytosterols Recovery from Soybean Oil Deodorizer Distillate." **J. Am. Oil. Chem. Soc.,** vol. 89, no. 7, Jul. 2012. pp. 1363-1370

[22] Savinova T.S., Diep N.T., Voishvillo N.E., Andryushina V.A., Karpova N.V., Beletskaya I.P. and Huy L.D. "Extraction of a Mixture of Phytosterols from Soybean Processing By-Product and Its Use in the Manufacture of 9α-Hydroxyandrost-4-En-3, 17-Dione." **Pharm. Chem. J.,** vol. 46, no. 3, Mar. 2012. pp. 40-43

[23] Barder T.J. **"Purification of Sterols with Activated Carbon as Adsorbent and Chlorobenzene as Desorbent."** U.S. Patent no. 4882065, November 1989

[24] Barder T.J., Johnson P. **"Adsorption Separation of Sterols from Tall Oil Pitch Carbon Adsorbent."** U.S. Patent no. 4849112, July 1989

References (cont.)

[25] Barder T.J., Bedwell W.B. and Johnson S.P. **"Separation of Sterols from Low-Acid Feeds with Magnesium Silicate and Methyl-Tert-Butyl Ether Desorbent."** U.S. Patent no. 4977243, December 1990

[26] Mukawa T., Goto T. and Takeuchi T. "Post-Oxidative Conversion of Thiol Residue to Sulfonic Acid in the Binding Sites of Molecularly Imprinted Polymers: Disulfide Based Covalent Molecular Imprinting for Basic Compounds." **Analyst,** vol. 127, no. 11, Sep. 2002. pp. 1407-1409

[27] Anasthas H.M., Gaikar V.G. "Adsorptive Separations of Alkylphenols Using Ion-Exchange Resins." **React. Funct. Polym**., vol. **39**, no. 3, Mar. 1999. pp. 227-237

[28] Moreau R. A., Whitaker B. D. and Hicks K.B. "Phytosterols, Phytostanols, and Their Conjugates in Foods: Structural Diversity, Quantitative Analysis, and Health-Promoting Uses." **Prog. Lipid Res.,** vol. 41, no. 6, Nov. 2002. pp. 457-500

[29] Phillips K.M., Ruggio D.M., Toivo J.I., Swank M.A. and Simpkins A.H. "Free and Esterified Sterol Composition of Edible Oils and Fats." **J. Food Comp. Anal.,** vol. 15, no. 2, Apr. 2002. pp. 123-142

[30] Rochfort S., Panozzo J. “Phytochemicals for Health, the Role of Pulses.” **J. Agric. Food Chem.,** vol. 55, no. 20, Sep. 2007. pp. 7981-7994

[31] Bouic P.J.D. “Sterols and Sterolins: New Drugs for the Immune System ?” Drug Discovery Today, vol. 7, no. 14, Jul. 2002 pp. 775-778

[32] Verleyen T., Forcades M., Verhe R., Dewettinck K., Huyghebaert A. and Greyt W.D. “Analysis of Free and Esterified Sterols in Vegetable Oils.” **J. Am. Oil Chem. Soc.,** vol. 79, no. 2, Feb. 2002. pp. 117–122

[33] Wong A., Norman H.S.O. and MacMillan A.K. **“Method for the Preparation of Phytosterols from Tall Oil Pitch.**” U.S. patent no. 8338564 B2, December 2012

[34] Gunawan S., Kasim N.S. and Ju Y.H. **“**Separation and Purification of Squalene from Soybean Oil Deodorizer Distillate.” **Sep. Purif. Technol.,** vol. 60, no. 2, Apr. 2008. pp. 128-135

[35] Hirota Y., Nagao T., Watanabe Y., Suenaga M., Nakai S., Kitano M., Sugihara A. and Shimada A. “Purification of Steryl Esters from Soybean Oil Deodorizer Distillate.” **J. Am. Oil. Chem. Soc.,** vol. 80, no. 4, Apr. 2003. pp. 341-346

[36] Jacobs L. **“Process for the Production of Tocotrienols**” U.S. patent no. 6838104 B2, January 2005

References (cont.)

[37] Posada L.R., Shi J., Kakuda Y. and Xue S.J. “Extraction of Tocotrienols from Palm Fatty Acid Distillates Using Molecular Distillation.” **Sep. Purif. Technol.,** vol. 57, no. 2, Oct. 2007. pp. 220-229

[38] Top A.G.M. “Production and Utilization of Palm Fatty Acid Distillate (PFAD).” **Lipid Technol.,** vol. 22, no. 1, Jan. 2010. pp. 11-13

[39] Bondioli P., Mariani C., Lanzani A., Fedeli E. and Muller A. “Squalene Recovery from Olive Oil Deodorizer Distillates.” **J. Am. Oil Chem. Soc.,** vol. 70, no. 8, Aug. 1993. pp. 763-766

[40] Liu Y. “Some Consideration on the Langmuir Isotherm Equation.” **Colloid Surf. A.: Physicochem. Eng. Aspects,** vol. 274, no. 1-3, Feb. 2006. pp. 34-36

[41] Reed B.E., Matsumoto M.R. "Modeling Cadmium Adsorption by Activated Carbon Using the Langmuir and Freundlich Isotherm Expressions." **Sep. Sci. Technol.**, vol. 28, no. 13-14, 1993. pp. 2179-2195

[42] Lin J., Wang L. "Comparison Between Linear and Non-Linear forms of Pseudo-First-Order and Pseudo-Second-Order Adsorption Kinetic Models for the Removal of Methylene Blue by Activated Carbon." **Front. Environ. Sci. Engin. China,** vol. 3, no. 3, Sep. 2009. pp. 320-324

[43] Ho Y.S., Mckay G. "Pseudo–Second Order Model for Sorption Processes." **Process Biochem.,** vol. 34, no. 5, Jul. 1999. pp. 451-465

[44] Azizian S. "Kinetic Models of Sorption: a Theoretical Analysis." **J. Colloid Interf. Sci.,** vol. 276, no. 1, Aug. 2004. pp. 47-52

[45] Brinker, C.J. and Scherer, G.W. 1990. **Sol-Gel Science: The Physics and Chemistry of Sol-Gel Processing.** San Diego : Academic Press, Inc.

[46] García M.E.D., Laíño R.B. "Molecular Imprinting in Sol-Gel Materials: Recent Developments and Applications." **Microchim. Acta,** vol. 149, no. 1-2, Feb. 2005. pp. 19-36

[47] Novak B.M. "Hybrid Nanocomposite Materials-Between Inorganic Glasses and Organic Polymers." **Adv. Muter.,** vol. 5, no. 6, Jun. 1993. pp. 422-433

[48] Trinh T.K., Kang L.S. "Application of Response Surface Method as an Experimental Design to Optimize Coagulation Tests." **Environ. Eng. Res.**, vol. 15, no. 2, Jun. 2010. pp. 63-70

[49] Chang C.J., Chang Y.F., Lee H.Z., Lin J.Q. and Yang P.W. "Supercritical Carbon Dioxide Extraction of High–Value Substances from Soybean Oil Deodorizer Distillate." **Ind. Eng. Chem. Res.,** vol. 39, no. 12, Oct. 2000. pp. 4521-4525

References (cont.)

[50] Ho Y.S., Mckay G. "Batch Lead (II) Removal from Aqueous Solution by Peat: Equilibrium and Kinetics." **Trans. IChemE.,** vol. 77, no. 3, May 1999. pp. 165- 173

[51] Hameed B.H., Ahmad A.L. and Latiff K.N.A. "Adsorption of Basic Dye (Methylene Blue) onto Activated Carbon Prepared from Rattan Sawdust." **Dyes Pigm.,** vol. 75, no. 1, 2007. pp. 143-149 [52] Chen H., Zhao J. "Adsorption Study

for Removal of Congo Red Anionic Dye Using Organo–Attapulgite." **Adsorption,** vol. 15, no. 4, Aug. 2009. pp. 381-389

[53] Chu B.S., Baharin B.S., Man Y.B.C. and Quek S.Y. "Separation of Vitamin E from Palm Fatty Acid Distillate Using Silica: I Equilibrium of Batch Adsorption." **J. Food Eng.,** vol. 62, no. 1, Mar. 2004. pp. 97-103

[54] Yu Y., Zhuang Y.Y. and Wang Z.H. "Adsorption of Water–Soluble Dye onto Functionalized Resin." **J. Colloid Interf. Sci.,** vol. 242, no. 2, Oct. 2001. pp. 288-293

[55] Scheckel K.G., Sparks D.L. "Temperature Effects on Nickel Sorption Kinetics at the Mineral–Water Interface." **Soil Sci. Soc. Am. J.,** vol. 65, no. 3, May-Jun. 2001. pp. 719-728

[56] Rattanaphani S., Chairat M., Bremner J.B. and Rattanaphani V. "An Adsorption and Thermodynamic Study of Lac Dyeing on Cotton Pretreated with Chitosan." **Dyes Pigm.,** vol. 72, no. 1, 2007. pp. 88-96

[57] Zhang Z., Tan W., Hu Y. and Li G. "Simultaneous Determination of Trace Sterols in Complicated Biological Samples by Gas Chromatography–Mass Spectrometry Coupled with Extraction using β-Sitosterol Magnetic Molecularly Imprinted Polymer Beads." **J. Chromatogr. A,** vol. 1218, no. 28, Jul. 2011. pp. 4275-4283

[58] Hashim S.N.N.S., Boysen R.I., Schwarz L.J., Danylec B. and Hearn M.T.W. "A Comparison of Covalent and Non-Covalent Imprinting Strategies for the Synthesis of Stigmasterol Imprinted Polymers." **J. Chromatogr. A,** vol. 1359, no. 12, Sep. 2014. pp. 35-43

[59] Turner N.W., Piletska E.V., Karim K., Whitcombe M., Malecha M., Magan N., Baggiani C. and Piletsky S.A. "Effect of the Solvent on Recognition Properties of Molecularly Imprinted Polymer Specific for Ochratoxin A." **Biosens. Bioelectron,** vol. 20, no. 6, Dec. 2004. pp. 1060-1067

[60] Walcarius A., Collinson M.M. "Analytical Chemistry with Silica Sol-Gels: Traditional Routes to New Materials for Chemical Analysis." **Annu. Rev. Anal. Chem.,** vol. 2, Feb. 2009. pp. 121-143

References (cont.)

[61] Fujiwara M., Nishiyama M., Yamamura I., Ohtsuki S. and Nomura R. "A Sol-Gel Method Using Acetic Anhydride in the Presence of Cholesterol in Organic Solution Media: Preparation of Silicas that Recognize Steroid Hormones." **Anal. Chem.,** vol. 76, no. 8, Apr. 2004. pp. 2374-2381 [62] Hsu C.W., Yang M.C. "Enhancement of the Imprinting Effect in Cholesterol-Imprinted Microporous Silica." **J. Non Cryst. Solids,** vol. 354, no. 34, Sep. 2008. pp. 4037-4042

[63] Gupta R., Kumar A. "Synthesis and Characterization of Sol–Gel-Derived Molecular Imprinted Polymeric Materials for Cholesterol Recognition." **J. Sol-Gel Sci. Technol.,** vol. 58, no. 1, Apr. 2011. pp. 182-194

[64] Morais E.C., Correa G.G., Brambilla R., Dos Santos J.H.Z. and Fisch A.G. "Selective Silica-Based Sorbent Materials Synthesized by Molecular Imprinting for Adsorption of Pharmaceuticals in Aqueous Matrices." **J. Sep. Sci.,** vol. 36, Jan. 2013. pp. 636-643

[65] Morais E.C., Brambilla R., Correa G.G., Dalmoro V. and Dos Santos J.H.Z. "Imprinted Silicas for Paracetamol Preconcentration Prepared by the Sol–Gel Process." **J. Sol-Gel Sci. Technol.,** vol. 83, no. 1, Jul. 2017. pp. 90-99

[66] Ibrahem S., Ibrahem H. "Synthesis and Study the Effect of H_2O/TEOS Ratio of the Silica Xerogel by Sol-Gel Method." **Int. Arch. App. Sci. Technol.,** vol. 5, no. 1, Mar. 2014. pp. 1-5

[67] Patra A., Jha S., Murthy P.N., Manik and Sharone A. "Isolation and Characterization of Stigmast-5-en-3β-ol (β-sitosterol) from the Leaves of *Hygrophila spinosa* T. Anders." **Inter. J. Pharm. Sci. Res.,** vol. 1, no. 2, Mar. 2010. pp. 95-100

[68] Yanghong L. **"Stereochemical Studies on the Metabolism of Sterols by *Saccharomyces cerevisiae* Strain GL7."** M.S. Thesis of Texas Tech University. 1996

[69] Karmakar B., De G. and Ganguli D. "Dense Silica Microspheres from Organic and Inorganic Acid Hydrolysis of TEOS." **J. Non-Cryst. Solids**, vol. 272, no. 2-3, Aug. 2000. pp. 119-126

[70] Curran M.D., Stiegman A.E. "Morphology and Pore Structure of Silica Xerogels Made at low pH." **J. Non-Cryst. Solids**, vol. 249, no. 1, Jul. 1999. pp. 62-68

[71] Estella J., Echeverría J.C., Laguna M. and Garrido J.J. "Silica Xerogels of Tailored Porosity as Support Matrix for Optical Chemical Sensors. Simultaneous Effect

of pH, Ethanol:TEOS and Water:TEOS Molar Ratios, and Synthesis Temperature on Gelation Time, and Textural and Structural Properties." **J. Non-Cryst. Solids,** vol. 353, no. 3, Mar. 2007. pp. 286-294

Appendices

Appendix A

Figures

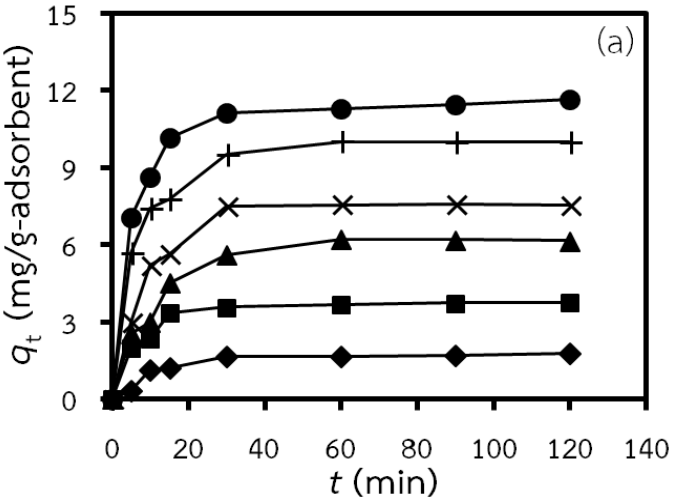
(a)
q_t (mg/g-adsorbent)
15
12
9
6
3
0
0 20 40 60 80 100 120 140
t (min)

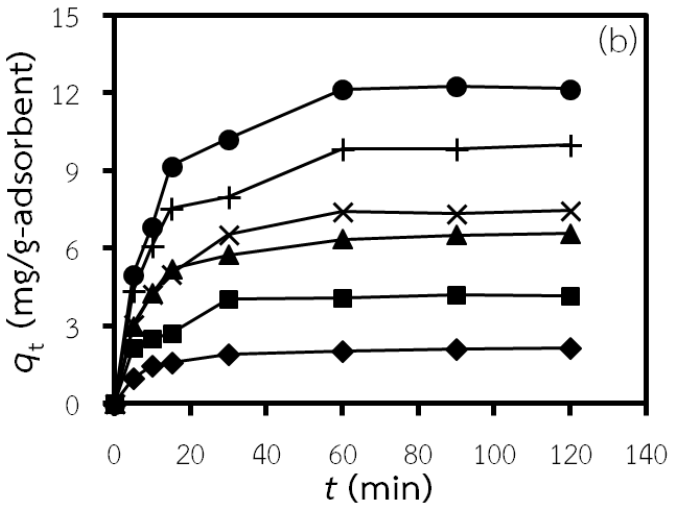
(b)
q_t (mg/g-adsorbent)
15
12
9
6
3
0
0 20 40 60 80 100 120 140
t (min)

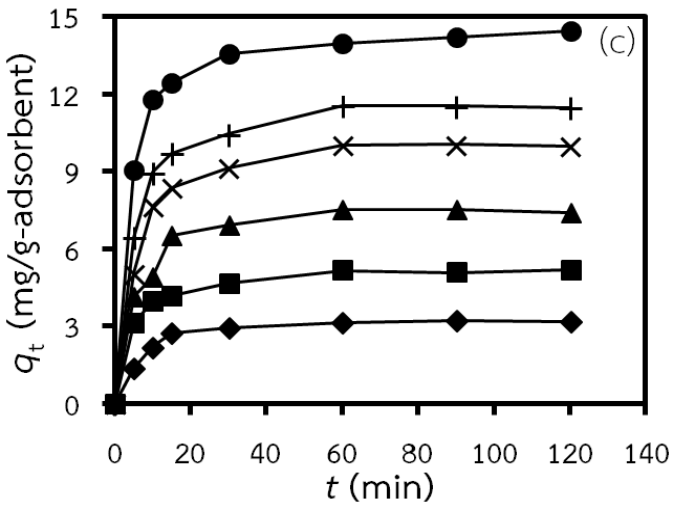
(c)
q_t (mg/g-adsorbent)
15
12
9
6
3
0
0 20 40 60 80 100 120 140
t (min)

Figure A.1 Plots of stigmasterol adsorption capacities of (a) SA-R, (b) SB-R, and (c) WB-R versus adsorption time, at 298 K and 5 wt% of adsorbent loading for various initial stigmasterol concentrations: (♦) 0.3, (■) 0.6, (▲) 0.9, (×) 1.2, (+) 1.5, (●) 1.8 mg/g-solution

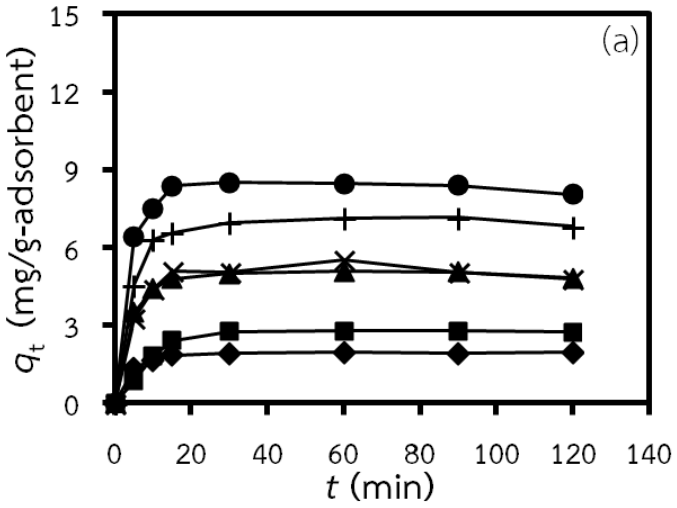

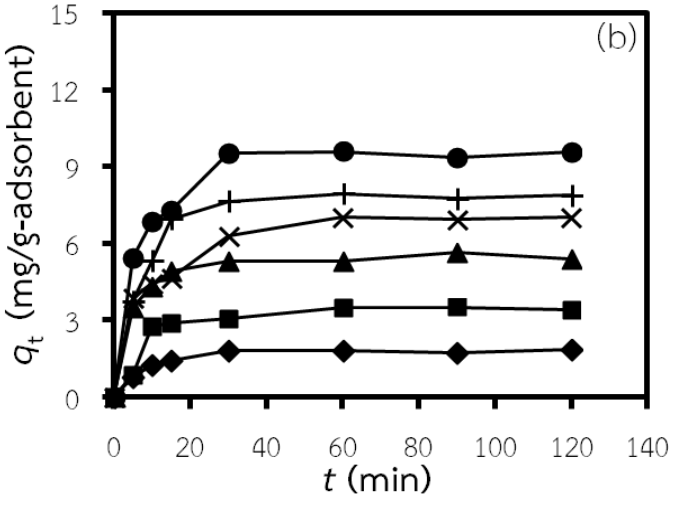

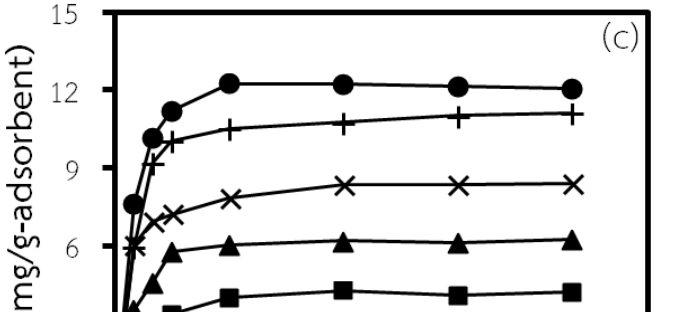

Figure A.2 Plots of stigmasterol adsorption capacities of (a) SA-R, (b) SB-R, and (c) WB-R versus adsorption time, at 308 K and 5 wt% of adsorbent loading for various initial stigmasterol concentrations: (♦) 0.3, (■) 0.6, (▲) 0.9, (×) 1.2, (+) 1.5, (●) 1.8 mg/g-solution

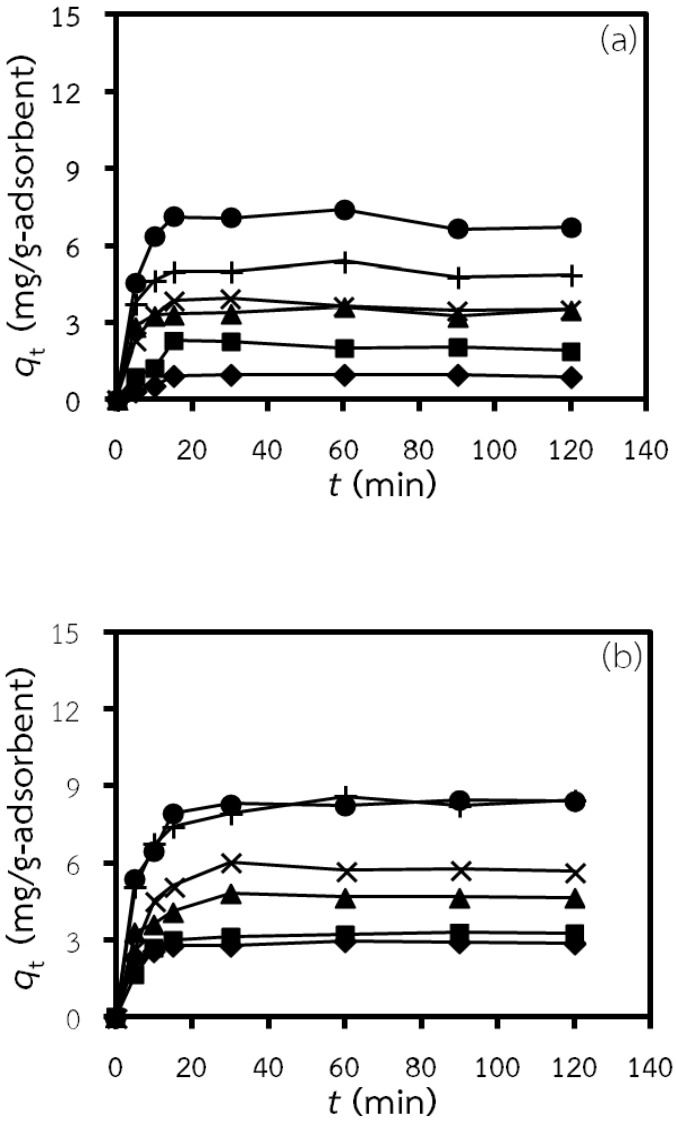

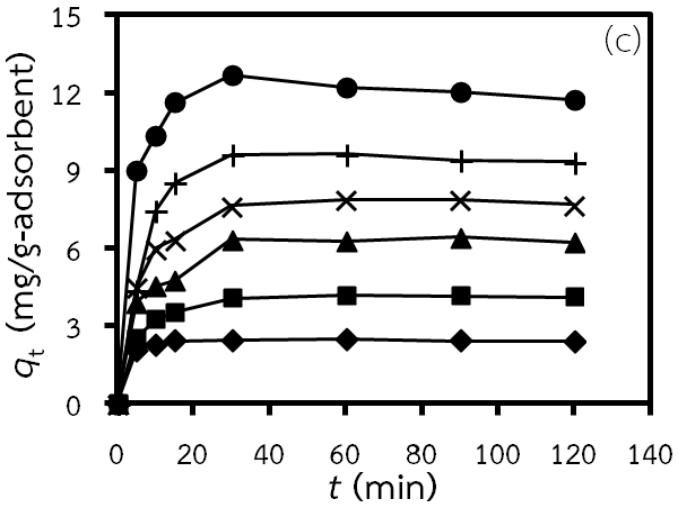

Figure A.3 Plots of stigmasterol adsorption capacities of (a) SA-R, (b) SB-R, and (c) WB-R versus adsorption time, at 313 K and 5 wt% of adsorbent loading for various initial stigmasterol concentrations: (♦) 0.3, (■) 0.6, (▲) 0.9, (×) 1.2, (+) 1.5, (●) 1.8 mg/g-solution

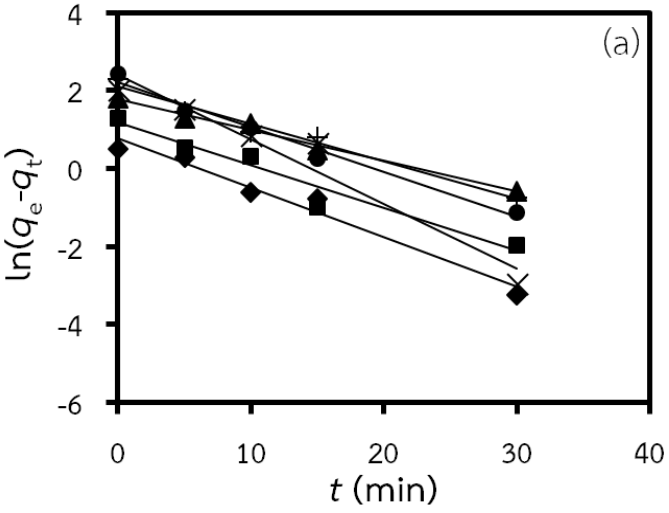

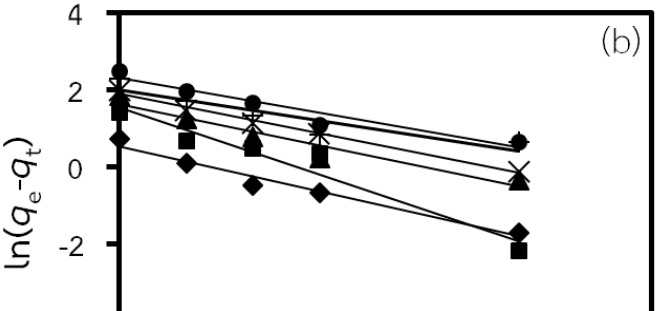

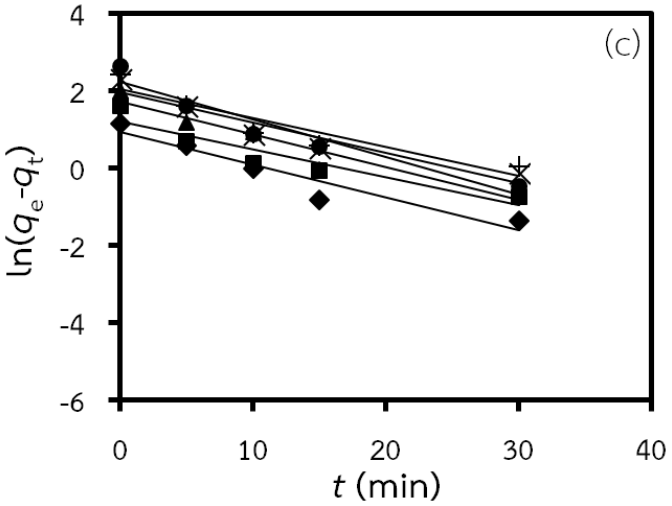

Figure A.4 Linear plots of adsorption rate versus adsorption time of the pseudo-first-order model for (a) SA-R, (b) SB-R, and (c) WB-R at 298 K and 5 wt% of adsorbent loading for various initial stigmasterol concentrations: (♦) 0.3, (■) 0.6, (▲) 0.9, (×) 1.2, (+) 1.5, (●) 1.8 mg/g-solution

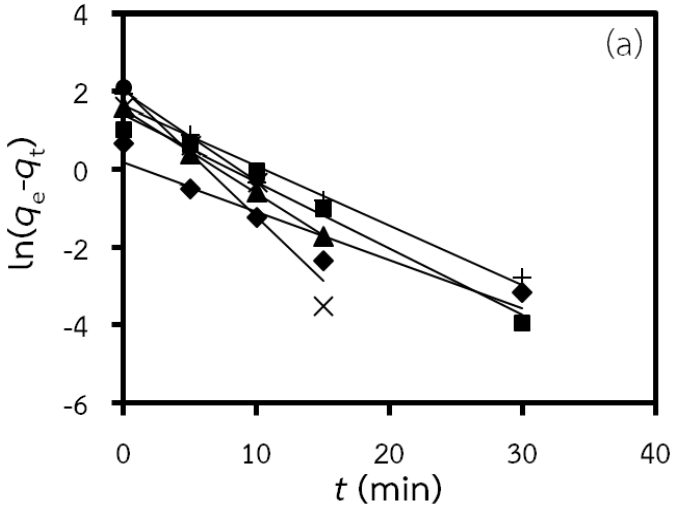

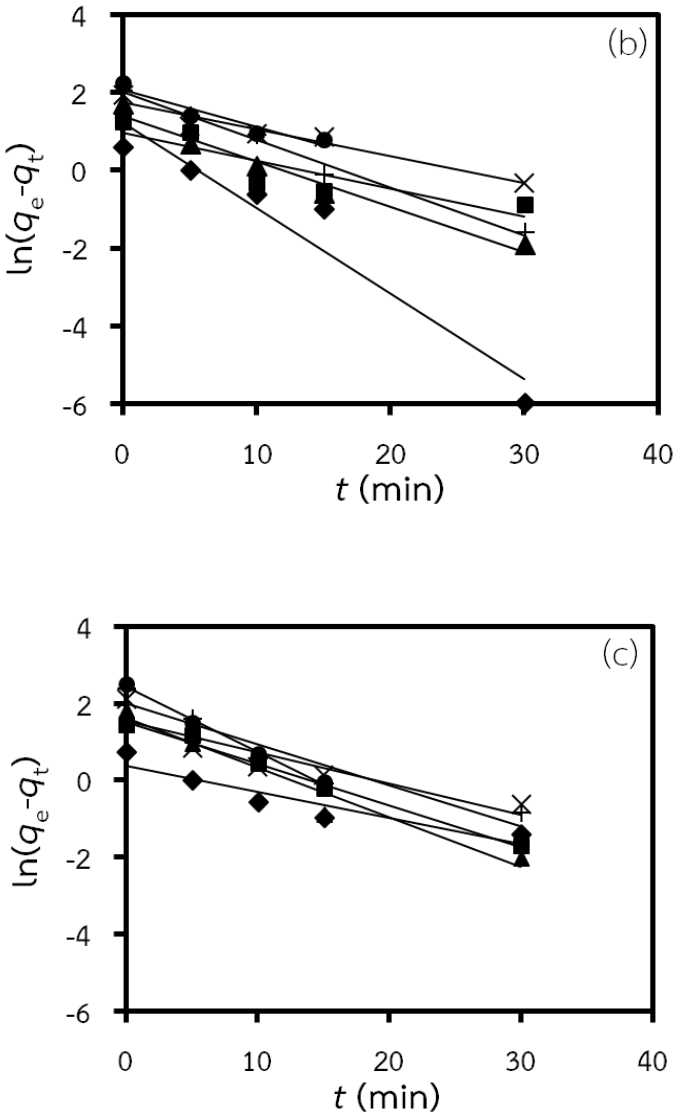

Figure A.5 Linear plots of adsorption rate versus adsorption time of the pseudo-first-order model for (a) SA-R, (b) SB-R, and (c) WB-R at 308 K and 5 wt% of adsorbent loading for various initial stigmasterol concentrations: (♦) 0.3, (■) 0.6, (▲) 0.9, (×) 1.2, (+) 1.5, (●) 1.8 mg/g-solution

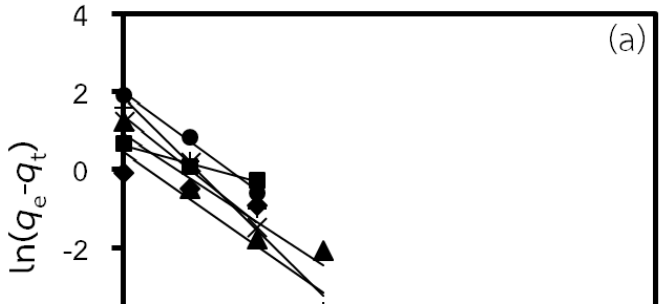

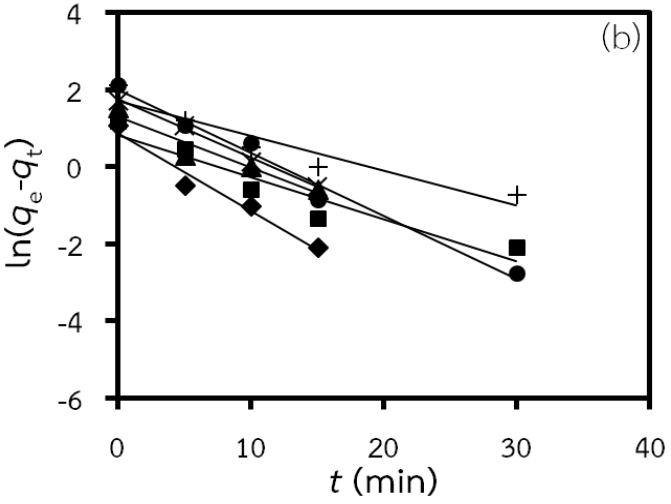
(b)
4
2
0
-2
-4
-6
0
10
20
30
40
ln(qe-qt)
t (min)

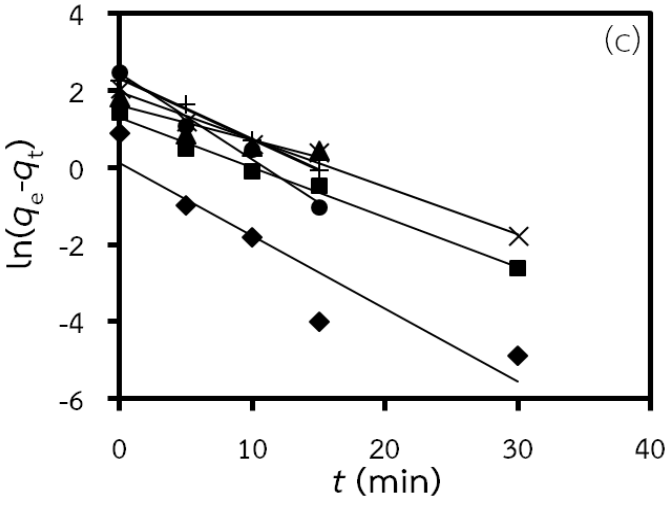
(c)
4
2
0
-2
-4
-6
0
10
20
30
40
ln(qe-qt)
t (min)

Figure A.6 Linear plots of adsorption rate versus adsorption time of the pseudo-first-order model for (a) SA-R, (b) SB-R, and (c) WB-R at 313 K and 5 wt% of adsorbent loading for various initial stigmasterol concentrations: (♦) 0.3, (■) 0.6, (▲) 0.9, (×) 1.2, (+) 1.5, (●) 1.8 mg/g-solution

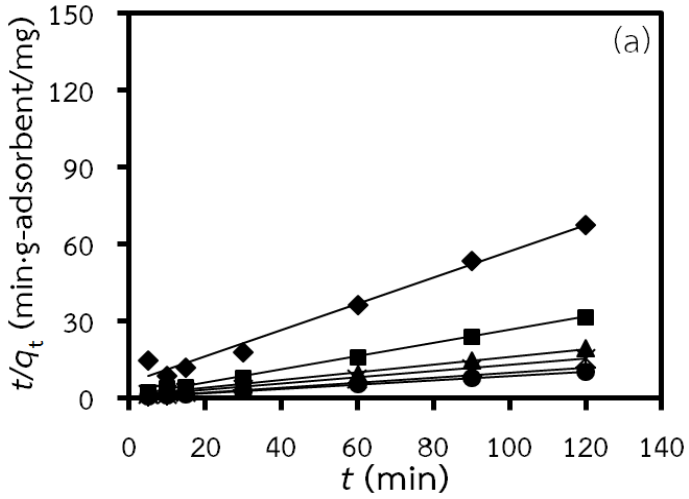

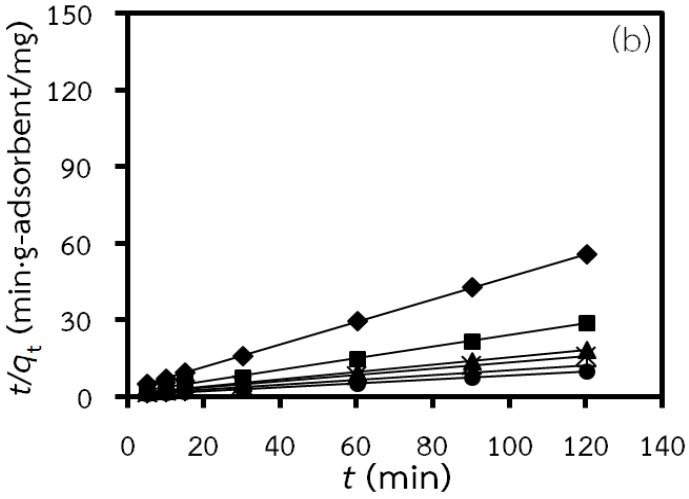

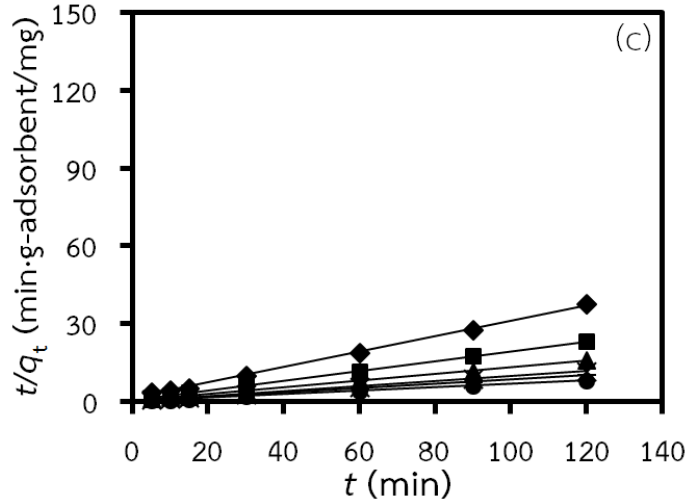

Figure A.7 Linear plots of adsorption rate versus adsorption time of the pseudo-second-order model for (a) SA-R, (b) SB-R, and (c) WB-R at 298 K and 5 wt% of adsorbent loading for various initial stigmasterol concentrations: (♦) 0.3, (■) 0.6, (▲) 0.9, (×) 1.2, (+) 1.5, (●) 1.8 mg/g- solution

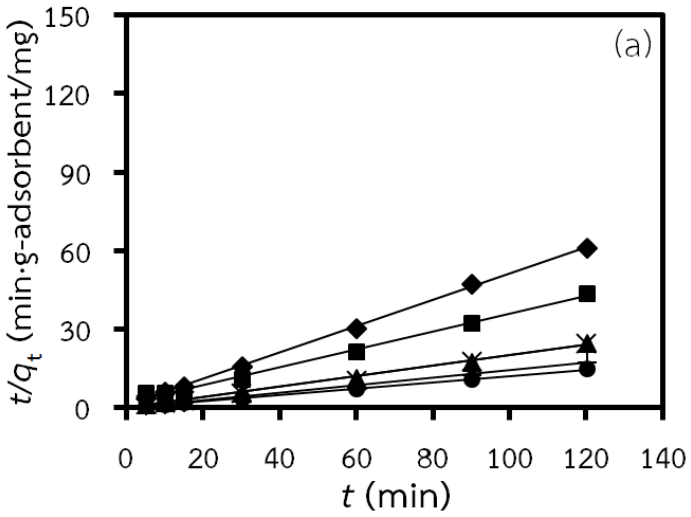

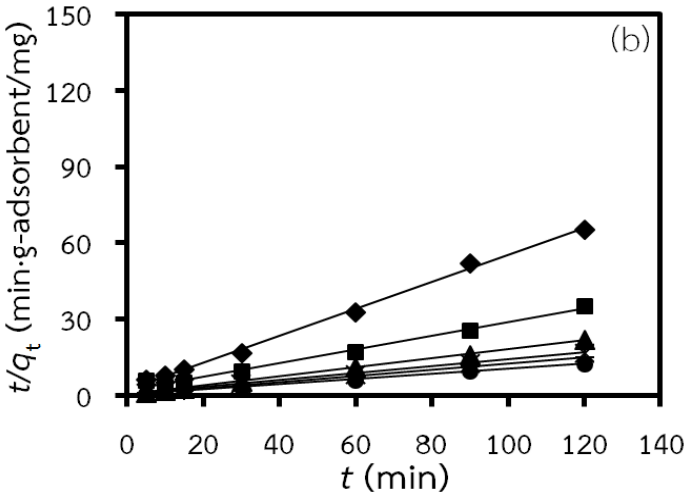

Figure A.8 Linear plots of adsorption rate versus adsorption time of the pseudo-second-order model for (a) SA-R, (b) SB-R, and (c) WB-R at 308 K and 5 wt% of adsorbent loading for various initial stigmasterol concentrations: (♦) 0.3, (■) 0.6, (▲) 0.9, (×) 1.2, (+) 1.5, (●) 1.8 mg/g- solution

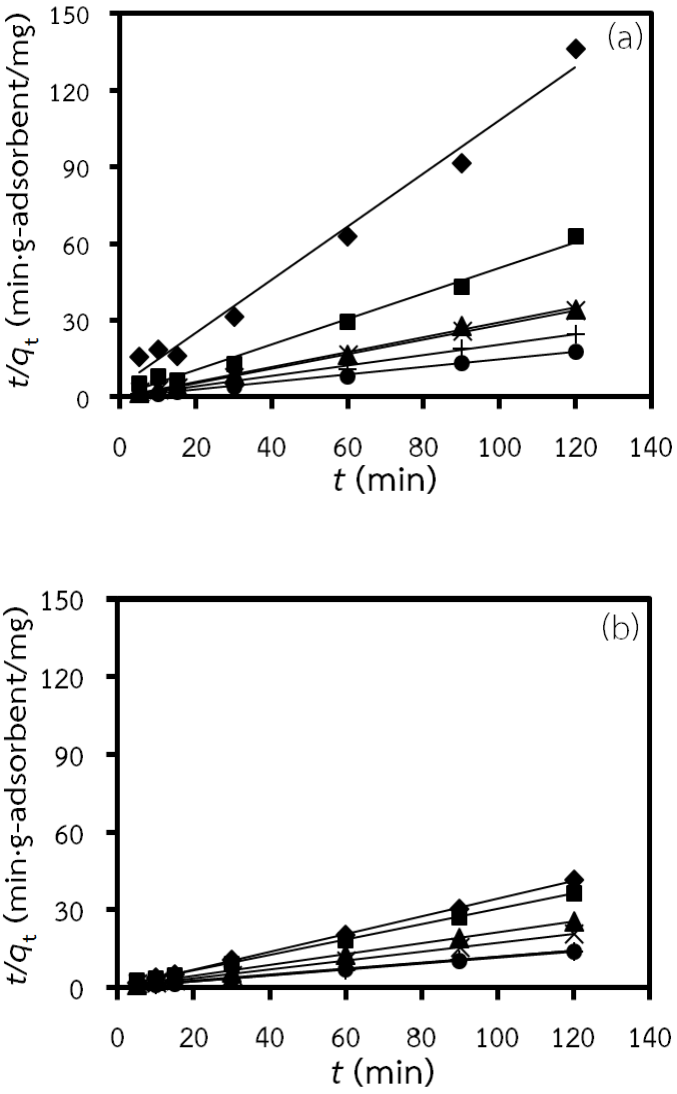

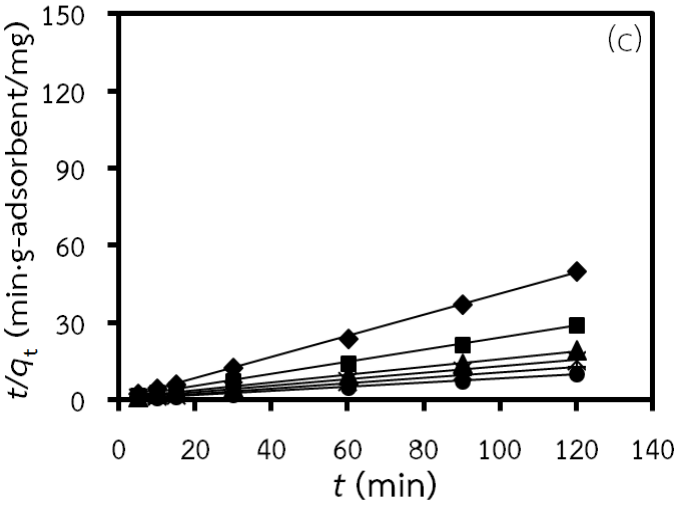

Figure A.9 Linear plots of adsorption rate versus adsorption time of the pseudo-second-order model for (a) SA-R, (b) SB-R, and (c) WB-R at 313 K and 5 wt% of adsorbent loading for various initial stigmasterol concentrations: (♦) 0.3, (■) 0.6, (▲) 0.9, (×) 1.2, (+) 1.5, (●) 1.8 mg/g-solution

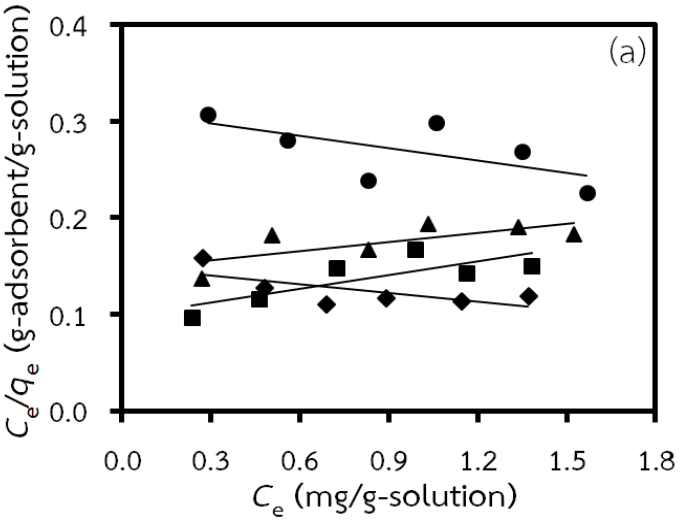

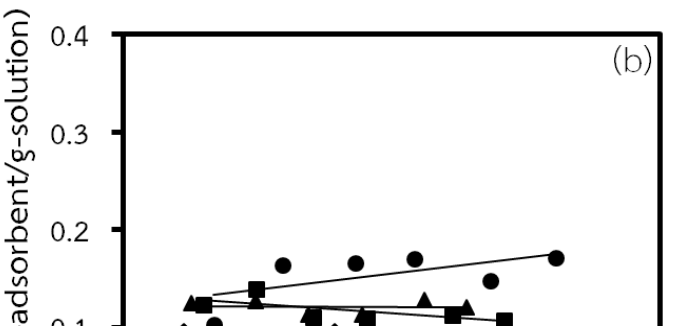

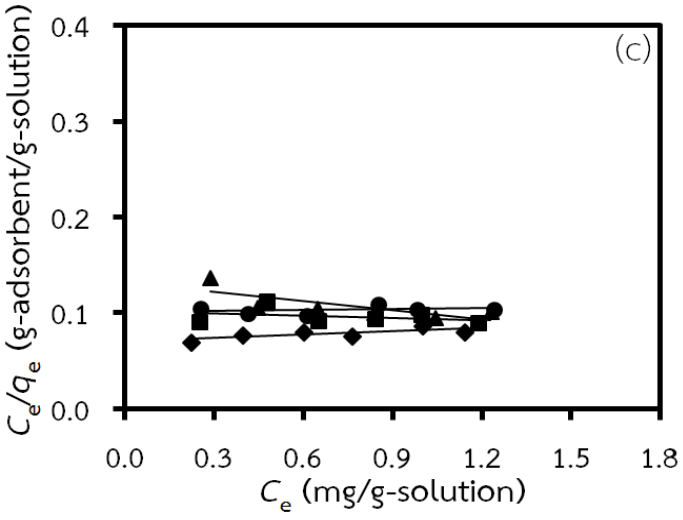

Figure A.10 Linear plots of Langmuir adsorption isotherm for stigmasterol on (a) SA-R, (b) SB-R, and (c) WB-R at (♦) 298 K, (■) 303 K, (▲) 308 K, and (●) 313 K

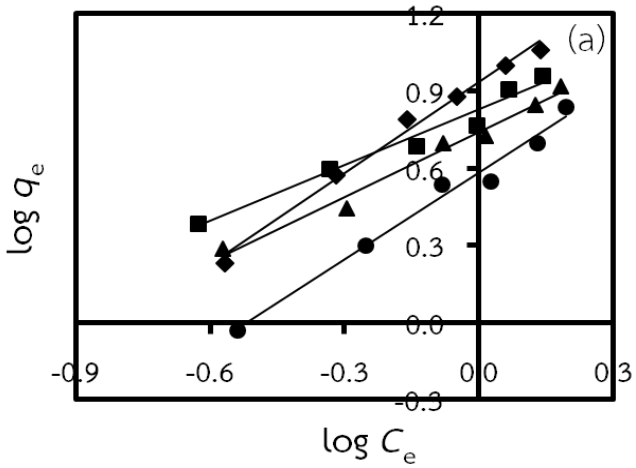

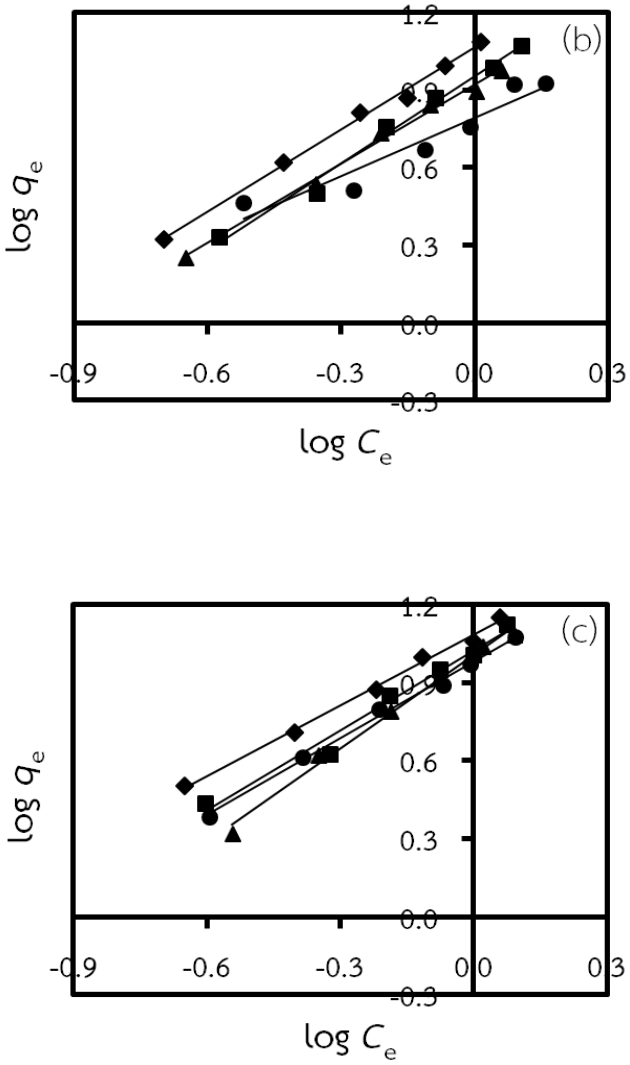

Figure A.11 Linear plots of Freundlich adsorption isotherm for stigmasterol on (a) SA-R, (b) SB-R, and (c) WB-R at (♦) 298 K, (■) 303 K, (▲) 308 K, and (●) 313 K

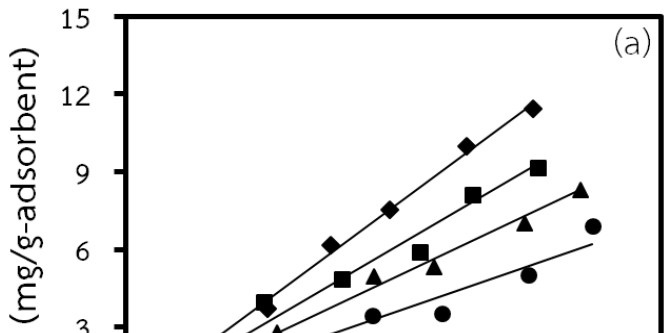

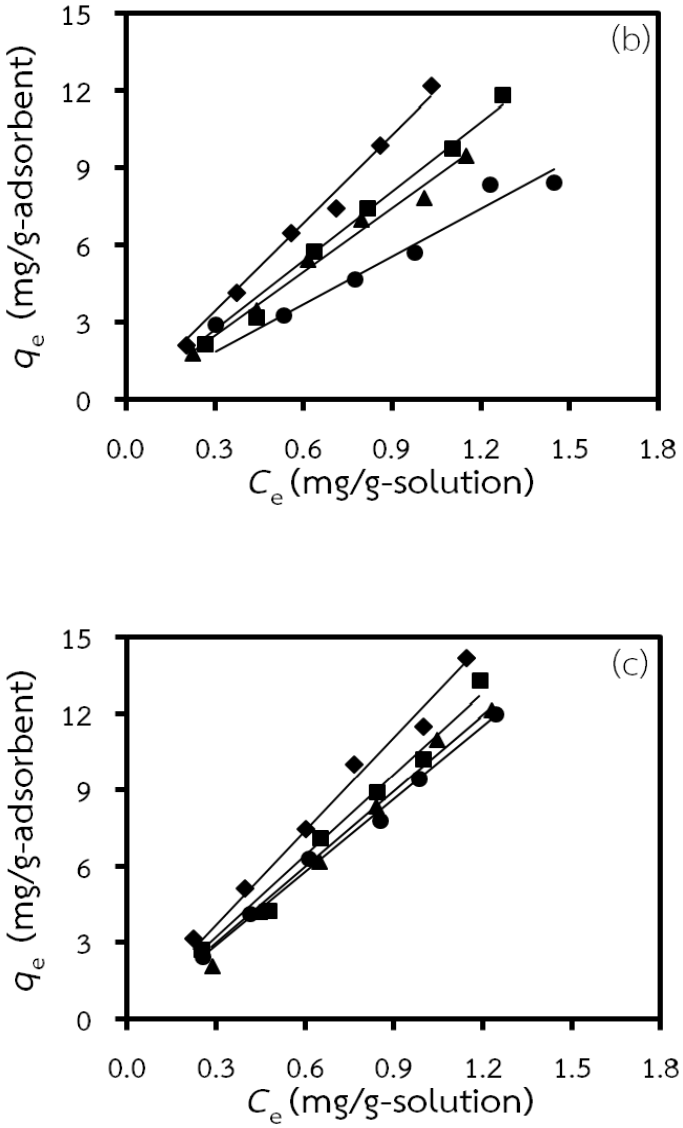

Figure A.12 Linear plots of linear adsorption isotherm for stigmasterol on (a) SA-R, (b) SB-R, and (c) WB-R at (♦) 298 K, (■) 303 K, (▲) 308 K, and (●) 313 K

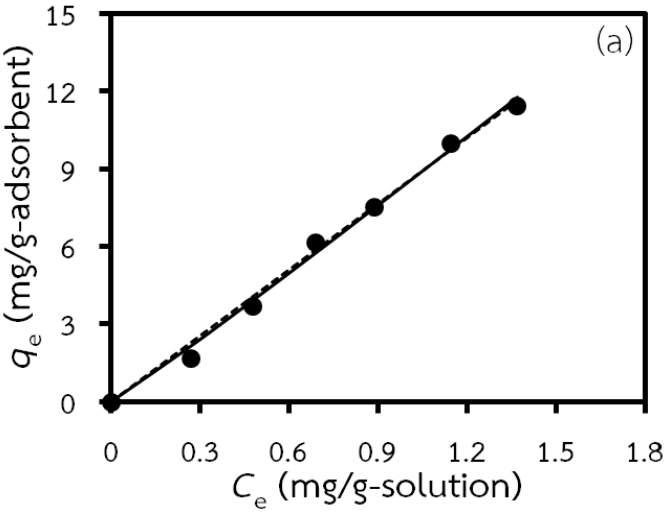
(a)
q_e (mg/g-adsorbent)
C_e (mg/g-solution)
0
3
6
9
12
15
0
0.3
0.6
0.9
1.2
1.5
1.8

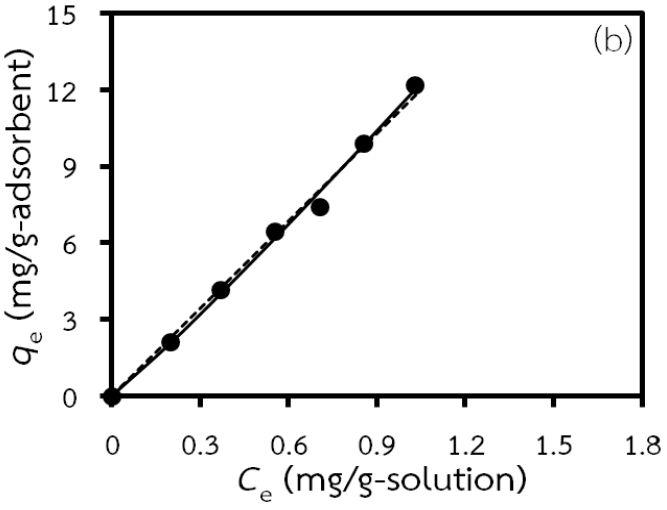
(b)
q_e (mg/g-adsorbent)
C_e (mg/g-solution)
0
3
6
9
12
15
0
0.3
0.6
0.9
1.2
1.5
1.8

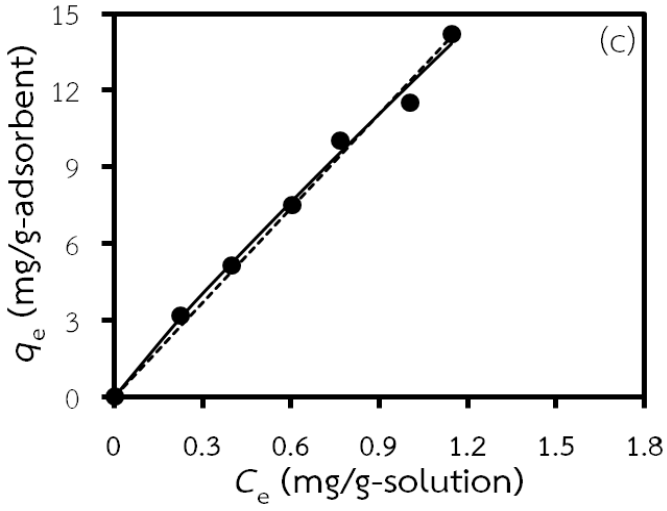
(c)
q_e (mg/g-adsorbent)
C_e (mg/g-solution)
0
3
6
9
12
15
0
0.3
0.6
0.9
1.2
1.5
1.8

Figure A.13 Dependences of (●) q_e on C_e calculated using (solid line) Freundlich and (dash line) linear model comparing with the experimental data for stigmasterol adsorption of (a) SA-R, (b) SB-R, and (c) WB-R, (T = 298 K, adsorbent loading = 5 wt%)

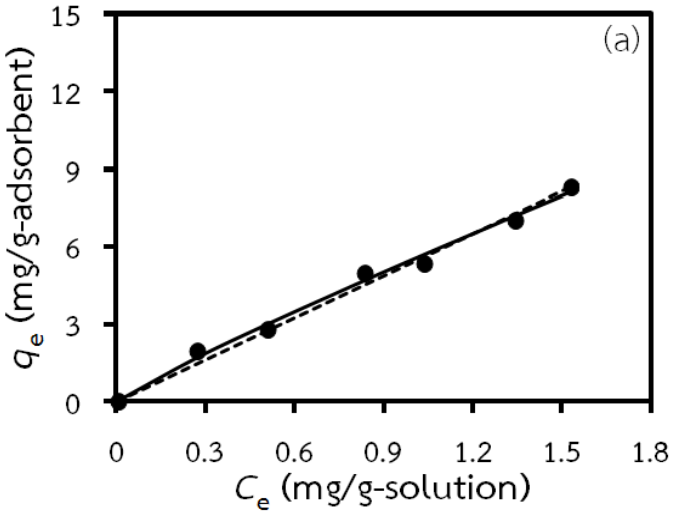

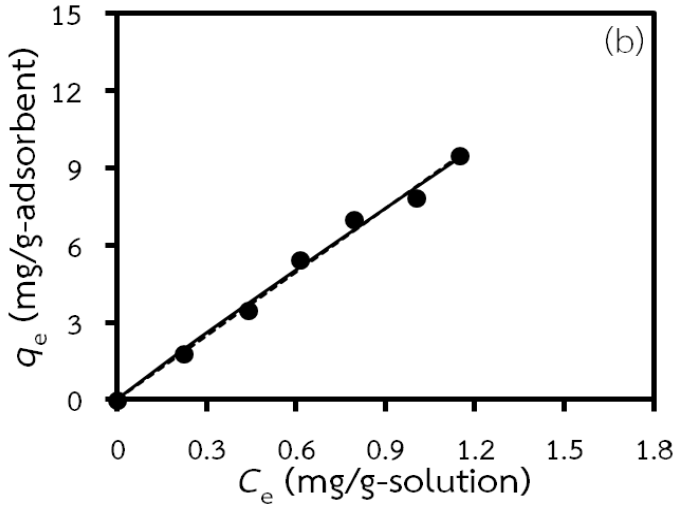

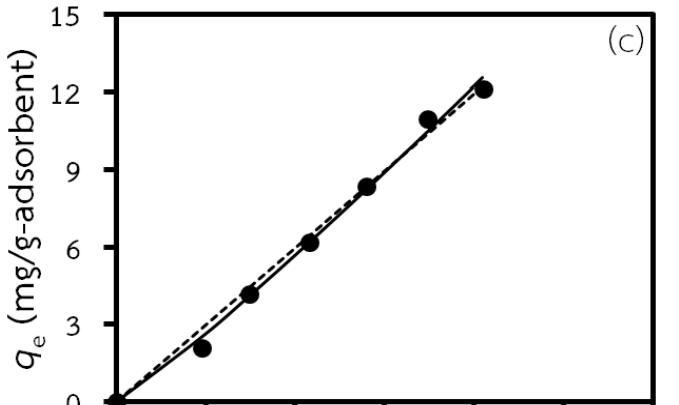

Figure A.14 Dependences of (●) q_e on C_e calculated using (solid line) Freundlich and (dash line) linear model comparing with the experimental data for stigmasterol adsorption of (a) SA-R, (b) SB-R, and (c) WB-R, (T = 308 K, adsorbent loading = 5 wt%)

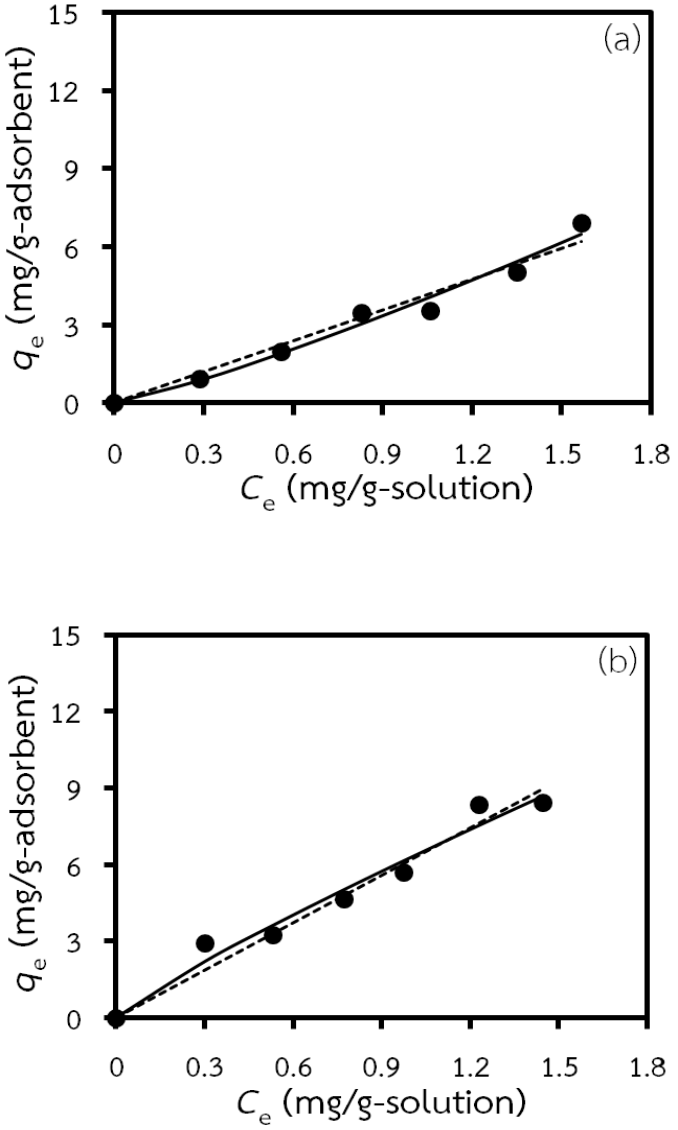

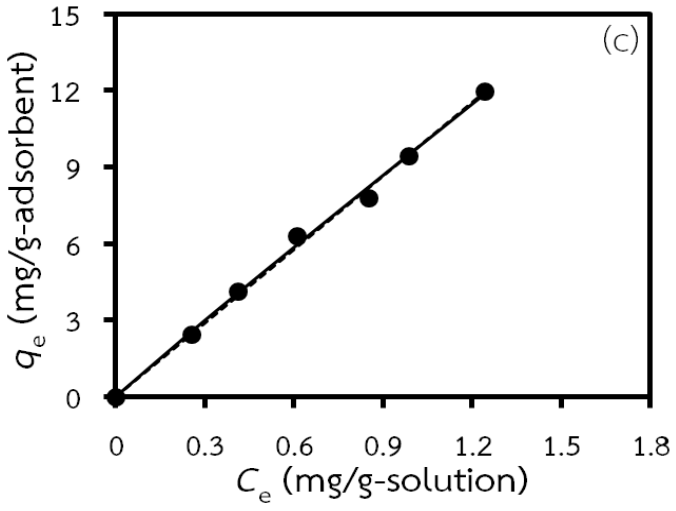

Figure A.15 Dependences of (●) q_e on C_e calculated using (solid line) Freundlich and (dash line) linear model comparing with the experimental data for stigmasterol adsorption of (a) SA-R, (b) SB-R, and (c) WB-R, (T = 313 K, adsorbent loading = 5 wt%)

Appendix B

Calculated parameters

Table B.1 Kinetic parameters of stigmasterol adsorption on SA-R, SB-R, and WB-R at 298 K and different initial concentrations of stigmaterol

Resin	C_0	$q_{e,exp}$	Pseudo-first-order				Pseudo-second-order			
			k_1	$q_{e,cal}$	Δq_e (%)	R^2 (-)	k_2	$q_{e,cal}$	Δq_e (%)	R^2 (-)
SA-R	0.3	1.70	0.1271	2.20	29.5	0.9690	0.0428	1.95	15.0	0.9807
	0.6	3.72	0.1095	3.22	13.5	0.9442	0.0597	3.92	5.1	0.9990
	0.9	6.19	0.0790	6.00	3.1	0.9859	0.0189	6.69	8.1	0.9964
	1.2	7.56	0.1660	11.15	47.5	0.9448	0.0231	8.00	5.8	0.9975
	1.5	10.01	0.0958	8.21	18.0	0.9760	0.0253	10.40	3.9	0.9995
	1.8	11.46	0.1149	9.05	21.0	0.9803	0.0267	11.92	4.0	0.9998
SB-R	0.3	2.10	0.0775	1.72	18.1	0.9681	0.0731	2.26	7.5	0.9998
	0.6	4.15	0.1151	4.67	12.5	0.9391	0.0361	4.43	6.9	0.9975
	0.9	6.47	0.0713	5.07	21.6	0.9291	0.0246	6.91	6.8	0.9998
	1.2	7.41	0.0683	6.67	10.1	0.9907	0.0156	8.05	8.5	0.9989
	1.5	9.89	0.0529	7.39	25.3	0.8404	0.0130	10.64	7.6	0.9988
	1.8	12.19	0.0599	10.02	17.9	0.9228	0.0100	13.14	7.8	0.9985
WB-R	0.3	3.19	0.0851	2.54	20.2	0.9124	0.0618	3.35	5.1	0.9986
	0.6	5.14	0.0719	3.36	34.7	0.8749	0.0510	5.34	3.8	0.9996
	0.9	7.50	0.0848	5.66	24.5	0.9084	0.0331	7.78	3.7	0.9989
	1.2	10.03	0.0785	7.17	28.5	0.9006	0.0246	10.42	3.9	0.9994
	1.5	11.53	0.0747	7.63	33.8	0.8653	0.0239	11.92	3.4	0.9996
	1.8	14.21	0.0973	9.26	34.8	0.9221	0.0236	14.75	3.8	0.9999

Table B.2 Kinetic parameters of stigmasterol adsorption on SA-R, SB-R, and WB-R at 308 K and different initial concentrations of stigmaterol

Resin	C_0	$q_{e,exp}$	Pseudo-first-order				Pseudo-second-order			
			k_1	$q_{e,cal}$	Δq_e (%)	R^2 (-)	k_2	$q_{e,cal}$	Δq_e (%)	R^2 (-)
SA-R	0.3	1.95	0.1245	1.20	38.5	0.9076	0.3077	1.98	1.8	0.9994
	0.6	2.78	0.1708	3.99	43.4	0.9819	0.0608	2.94	5.7	0.9940
	0.9	4.99	0.2180	4.80	3.7	0.9985	0.4543	4.95	0.8	0.9980
	1.2	5.33	0.3277	7.88	47.9	0.9033	1.4319	4.97	6.8	0.9946
	1.5	7.03	0.1534	5.14	26.9	0.9742	0.1579	7.02	0.1	0.9981
	1.8	8.31	0.2335	7.48	10.0	0.9760	1.4544	8.21	1.2	0.9985
SB-R	0.3	1.80	0.2195	3.43	90.7	0.9249	0.1139	1.90	5.2	0.9967
	0.6	3.47	0.0722	2.62	24.4	0.7739	0.0364	3.71	7.2	0.9875
	0.9	5.45	0.1160	3.99	26.8	0.9703	0.0751	5.60	2.7	0.9989
	1.2	7.00	0.069	5.67	19.0	0.9463	0.0220	7.44	6.3	0.9985
	1.5	7.85	0.1231	7.55	3.8	0.9867	0.0310	8.18	4.1	0.9985
	1.8	9.49	0.0961	7.96	16.1	0.9103	0.0276	9.86	3.9	0.9987
WB-R	0.3	2.09	0.0676	1.46	30.2	0.8667	0.0832	2.23	6.8	0.9984
	0.6	4.20	0.1087	4.60	9.5	0.9912	0.0253	4.58	9.1	0.9869
	0.9	6.18	0.1291	5.06	18.1	0.9529	0.0558	6.39	3.2	0.9993
	1.2	8.36	0.0808	4.66	44.3	0.8374	0.0489	8.57	2.5	0.9999
	1.5	10.96	0.1063	7.44	32.1	0.8982	0.0296	11.38	3.8	0.9996
	1.8	12.14	0.1697	11.34	6.5	0.9954	0.0499	12.32	1.5	0.9994

Table B.3 Kinetic parameters of stigmasterol adsorption on SA-R, SB-R, and WB-R at 313 K and different initial concentrations of stigmaterol

Resin	C_0	$q_{e,exp}$	Pseudo-first-order				Pseudo-second-order			
			k_1	$q_{e,cal}$	Δq_e (%)	R^2 (-)	k_2	$q_{e,cal}$	Δq_e (%)	R^2 (-)
SA-R	0.3	0.94	0.2408	1.59	69.0	0.7801	0.2481	0.96	2.6	0.9851
	0.6	1.99	0.0953	1.92	3.5	0.9838	0.3020	2.01	0.7	0.9889
	0.9	3.46	0.2245	2.49	28.0	0.9243	0.5085	3.46	0.2	0.9961
	1.2	3.55	0.2722	3.95	11.2	0.9821	0.2835	3.53	0.6	0.9980
	1.5	5.02	0.3375	6.32	26.0	0.9652	0.7988	4.89	2.5	0.9966
	1.8	6.92	0.2505	7.35	6.2	0.9931	0.6386	6.76	2.3	0.9966
SB-R	0.3	2.92	0.2019	2.41	17.5	0.9682	0.3443	2.93	0.5	0.9996
	0.6	3.25	0.1094	2.31	28.9	0.9044	0.0993	3.37	3.6	0.9993
	0.9	4.66	0.1336	3.75	19.6	0.9265	0.1179	4.75	1.9	0.9993
	1.2	5.71	0.1532	5.90	3.3	0.9939	0.0663	5.87	2.8	0.9977
	1.5	8.33	0.0904	5.55	33.4	0.9038	0.0436	8.62	3.5	0.9992
	1.8	8.43	0.1634	7.43	11.9	0.9810	0.0523	8.60	2.0	0.9996
WB-R	0.3	2.44	0.1884	1.12	54.1	0.8738	4.2322	2.42	0.8	0.9995
	0.6	4.14	0.1293	3.65	11.8	0.9902	0.0945	4.24	2.3	0.9994

	0.9	6.30	0.0896	4.97	21.1	0.8391	0.0460	6.51	3.3	0.9980
	1.2	7.80	0.1229	7.13	8.6	0.9848	0.1252	7.99	2.4	0.9988
	1.5	9.45	0.1576	10.04	6.2	0.9950	0.0394	9.66	2.3	0.9977
	1.8	11.97	0.2221	11.34	5.3	0.9768	0.3115	11.92	0.4	0.9988

Table B.4 Parameters and correlation coefficients of non linear regression for Freundlich and linear adsorption isotherms for stigmasterol on SA-R, SB-R, and WB-R

Models		Freundlich: $q_e = K_F C_e^{1/n}$			Linear: $q_e = K_{Li} C_e$	
Resin	T (K)	K_F (mg/(g-adsorbent(mg/g-solution)$^{1/n}$))	n (-)	R^2 (-)	K_{Li} (g-solution/g-adsorbent)	R^2 (-)
SA-R	298	8.483	0.958	0.9943	8.501	0.9936
	303	8.033	1.227	0.9775	6.734	0.9643
	308	5.529	1.111	0.9920	5.432	0.9884
	313	3.793	0.836	0.9758	3.953	0.9661
SB-R	298	11.638	0.933	0.9955	11.450	0.9938
	303	9.005	0.902	0.9958	8.996	0.9919
	308	8.240	1.040	0.9925	8.273	0.9920

	313	6.269	1.144	0.9698	6.187	0.9636
WB-R	298	12.217	1.088	0.9939	12.331	0.9913
	303	10.755	0.910	0.9926	10.671	0.9897
	308	10.003	0.907	0.9950	9.954	0.9915
	313	9.596	1.030	0.9969	9.613	0.9966

Appendix C

Experimental data

Table C.1 Stigmasterol adsorption capacities of SA-R, SB-R, and WB-R versus adsorption time, at 298 K and 5 wt% of adsorbent loading for various initial stigmasterol concentrations (data of Figure A.1)

SA-R						
C_0 (mg/g-solution)	0.3	0.6	0.9	1.2	1.5	1.8
t (min)	q_t (mg/g-adsorbent)					
0	0.00	0.00	0.00	0.00	0.00	0.00
5	0.33	2.00	2.55	2.97	5.68	7.05
10	1.13	2.34	3.00	5.20	7.40	8.63
15	1.22	3.35	4.53	5.64	7.79	10.16
30	1.66	3.58	5.62	7.51	9.53	11.13
60	1.64	3.67	6.22	7.55	10.02	11.29
90	1.68	3.73	6.19	7.59	10.00	11.44
120	1.77	3.77	6.15	7.54	9.99	11.66
SB-R						
C_0 (mg/g-solution)	0.3	0.6	0.9	1.2	1.5	1.8
t (min)	q_t (mg/g-adsorbent)					
0	0.00	0.00	0.00	0.00	0.00	0.00
5	0.98	2.14	2.97	3.06	4.37	5.00
10	1.47	2.50	4.25	4.25	6.10	6.85
15	1.58	2.73	5.19	5.00	7.54	9.18
30	1.92	4.03	5.74	6.53	7.99	10.23
60	2.04	4.09	6.35	7.42	9.83	12.14
90	2.11	4.20	6.50	7.35	9.85	12.27
120	2.16	4.16	6.56	7.48	9.99	12.16
WB-R						
C_0 (mg/g-solution)	0.3	0.6	0.9	1.2	1.5	1.8

t (min)	q_t (mg/g-adsorbent)					
0	0.00	0.00	0.00	0.00	0.00	0.00
5	1.36	3.11	4.15	5.05	6.46	9.07
10	2.20	3.97	4.90	7.65	8.97	11.78
15	2.75	4.19	6.52	8.38	9.70	12.44
30	2.93	4.66	6.93	9.16	10.46	13.57
60	3.16	5.17	7.53	10.04	11.55	13.96
90	3.23	5.08	7.54	10.05	11.55	14.20
120	3.17	5.18	7.43	9.98	11.48	14.46

Table C.2 Stigmasterol adsorption capacities of SA-R, SB-R, and WB-R versus adsorption time, at 303 K and 5 wt% of adsorbent loading for various initial stigmasterol concentrations (data of Figure 3.1)

SA-R						
C_0 (mg/g-solution)	0.3	0.6	0.9	1.2	1.5	1.8
t (min)	q_t (mg/g-adsorbent)					
0	0.00	0.00	0.00	0.00	0.00	0.00
5	1.89	2.17	3.22	3.41	4.19	4.69
10	2.10	3.03	4.18	4.54	4.84	6.42
15	2.43	3.51	4.66	5.21	6.40	7.43
30	2.46	3.59	4.72	5.93	7.56	9.15
60	2.48	3.98	4.91	5.92	7.74	9.16
90	2.39	4.01	4.83	5.86	8.33	9.14
120	2.43	3.99	4.86	5.91	8.27	9.21
SB-R						
C_0 (mg/g-solution)	0.3	0.6	0.9	1.2	1.5	1.8
t (min)	q_t (mg/g-adsorbent)					
0	0.00	0.00	0.00	0.00	0.00	0.00
5	0.95	2.01	3.35	4.13	6.35	6.21
10	1.35	2.05	4.49	5.37	8.21	8.62
15	1.54	2.56	4.86	5.77	8.71	9.43
30	1.83	3.00	5.34	7.05	9.70	10.80

60	2.12	3.01	5.59	7.36	9.67	11.89
90	2.15	3.24	5.85	7.48	9.94	11.60
120	2.18	3.27	5.81	7.44	9.67	11.99
WB-R						
C_0 (mg/g-solution)	0.3	0.6	0.9	1.2	1.5	1.8
t (min)	q_t (mg/g-adsorbent)					
0	0.00	0.00	0.00	0.00	0.00	0.00
5	1.65	2.77	4.37	5.40	6.13	8.44
10	1.78	3.66	4.99	6.50	7.76	11.45
15	2.00	3.95	5.91	7.45	8.52	12.29
30	2.67	4.20	6.47	8.30	9.45	12.57
60	2.67	4.20	7.16	8.96	10.22	13.32
90	2.78	4.34	7.10	8.87	10.25	13.27
120	2.75	4.18	7.02	8.92	10.12	13.32

Table C.3 Stigmasterol adsorption capacities of SA-R, SB-R, and WB-R versus adsorption time, at 308 K and 5 wt% of adsorbent loading for various initial stigmasterol concentrations (data of Figure A.2)

SA-R						
C_0 (mg/g-solution)	0.3	0.6	0.9	1.2	1.5	1.8
t (min)	q_t (mg/g-adsorbent)					
0	0.00	0.00	0.00	0.00	0.00	0.00
5	1.35	0.88	3.49	3.26	4.56	6.43
10	1.65	1.83	4.42	4.41	6.30	7.51
15	1.85	2.42	4.80	5.11	6.58	8.38
30	1.90	2.76	4.99	5.07	6.97	8.53
60	1.97	2.80	5.09	5.53	7.13	8.48
90	1.90	2.80	5.06	5.06	7.16	8.40
120	1.97	2.75	4.81	4.81	6.81	8.05
SB-R						
C_0 (mg/g-solution)	0.3	0.6	0.9	1.2	1.5	1.8
t (min)	q_t (mg/g-adsorbent)					

0	0.00	0.00	0.00	0.00	0.00	0.00
5	0.79	0.85	3.51	3.90	3.73	5.41
10	1.27	2.74	4.33	4.43	5.31	6.85
15	1.43	2.88	4.90	4.66	6.95	7.28
30	1.79	3.05	5.30	6.28	7.64	9.52
60	1.83	3.50	5.32	7.01	7.93	9.57
90	1.72	3.51	5.63	6.96	7.74	9.35
120	1.84	3.40	5.40	7.03	7.88	9.55
WB-R						
C_0 (mg/g-solution)	0.3	0.6	0.9	1.2	1.5	1.8
t (min)	q_t (mg/g-adsorbent)					
0	0.00	0.00	0.00	0.00	0.00	0.00
5	1.07	0.98	3.56	6.04	5.96	7.63
10	1.52	2.67	4.58	6.93	9.19	10.17
15	1.71	3.39	5.77	7.22	10.04	11.19
30	1.84	4.02	6.05	7.82	10.52	12.24
60	2.06	4.29	6.20	8.35	10.75	12.23
90	2.03	4.09	6.11	8.35	11.01	12.13
120	2.17	4.22	6.24	8.38	11.11	12.05

Table C.4 Stigmasterol adsorption capacities of SA-R, SB-R, and WB-R versus adsorption time, at 313 K and 5 wt% of adsorbent loading for various initial stigmasterol concentrations (data of Figure A.3)

SA-R						
C_0 (mg/g-solution)	0.3	0.6	0.9	1.2	1.5	1.8
t (min)	q_t (mg/g-adsorbent)					
0	0.00	0.00	0.00	0.00	0.00	0.00
5	0.32	0.88	2.85	2.30	3.76	4.55
10	0.53	1.22	3.29	3.32	4.64	6.35
15	0.92	2.29	3.34	3.85	4.99	7.11
30	0.95	2.28	3.37	3.95	4.98	7.07
60	0.95	2.02	3.64	3.64	5.41	7.41

90	0.98	2.07	3.25	3.48	4.78	6.65
120	0.88	1.90	3.50	3.52	4.86	6.69
SB-R						
C_0 (mg/g-solution)	0.3	0.6	0.9	1.2	1.5	1.8
t (min)	q_t (mg/g-adsorbent)					
0	0.00	0.00	0.00	0.00	0.00	0.00
5	2.29	1.66	3.30	2.70	5.08	5.41
10	2.56	2.69	3.64	4.54	6.74	6.49
15	2.80	2.99	4.11	5.10	7.41	7.94
30	2.80	3.13	4.81	6.05	7.93	8.30
60	2.94	3.20	4.67	5.71	8.58	8.23
90	2.93	3.29	4.67	5.75	8.21	8.45
120	2.88	3.27	4.65	5.67	8.45	8.41
WB-R						
C_0 (mg/g-solution)	0.3	0.6	0.9	1.2	1.5	1.8
t (min)	q_t (mg/g-adsorbent)					
0	0.00	0.00	0.00	0.00	0.00	0.00
5	2.06	2.53	3.90	4.49	4.38	8.98
10	2.27	3.24	4.54	5.98	7.43	10.34
15	2.42	3.51	4.73	6.33	8.52	11.61
30	2.43	4.07	6.32	7.63	9.60	12.68
60	2.50	4.18	6.26	7.87	9.64	12.19
90	2.42	4.14	6.42	7.86	9.39	12.01
120	2.40	4.11	6.21	7.67	9.32	11.71

Table C.5 Dependences of q_e on C_e calculated using Freundlich and linear model comparing with the experimental data for adsorption of stigmasterol on SA-R, SB-R, and WB-R at 298 K, adsorbent loading = 5 wt% (data of Figure A.13)

Resin	C_e (mg/g-solution)	$q_{e,\ Experiment}$ (mg/g-adsorbent)	$q_{e,\ Freundlich\ model}$ (mg/g-adsorbent)	$q_{e,\ Linear\ model}$ (mg/g-adsorbent)
SA-R	0.00	0.00	0.00	0.00

	0.27	1.70	2.16	2.29
	0.48	3.72	3.92	4.05
	0.69	6.19	5.74	5.85
	0.89	7.56	7.49	7.54
	1.14	10.01	9.77	9.73
	1.37	11.46	11.77	11.64
SB-R	0.00	0.00	0.00	0.00
	0.20	2.10	2.07	2.29
	0.37	4.15	4.01	4.24
	0.55	6.47	6.17	6.34
	0.71	7.41	8.02	8.09
	0.86	9.89	9.86	9.81
	1.03	12.19	12.02	11.80
WB-R	0.00	0.00	0.00	0.00
	0.22	3.19	3.08	2.75
	0.40	5.14	5.21	4.88
	0.60	7.50	7.67	7.43
	0.76	10.03	9.55	9.43
	1.00	11.53	12.23	12.34
	1.14	14.21	13.82	14.10

Table C.6 Dependences of q_e on C_e calculated using Freundlich and linear model comparing with the experimental data for adsorption of stigmasterol on

SA-R, SB-R, and WB-R at 303 K, adsorbent loading = 5 wt% (data of Figure 3.4)

Resin	C_e (mg/g-solution)	$q_{e,\ Experiment}$ (mg/g-adsorbent)	$q_{e,\ Freundlich\ model}$ (mg/g-adsorbent)	$q_{e,\ Linear\ model}$ (mg/g-adsorbent)
SA-R	0.00	0.00	0.00	0.00
	0.24	2.44	2.10	1.59
	0.46	3.99	3.64	3.11
	0.72	4.86	5.24	4.87
	0.99	5.90	6.75	6.65
	1.16	8.11	7.71	7.83
	1.38	9.17	8.88	9.31
SB-R	0.00	0.00	0.00	0.00
	0.27	2.15	2.08	2.40
	0.44	3.17	3.64	3.98
	0.63	5.75	5.43	5.70
	0.82	7.43	7.19	7.34
	1.10	9.76	10.02	9.91
	1.27	11.83	11.76	11.45
WB-R	0.00	0.00	0.00	0.00
	0.25	2.73	2.34	2.66
	0.48	4.24	4.75	5.07
	0.65	7.09	6.69	6.93
	0.84	8.92	8.88	8.96
	1.00	10.20	10.72	10.64
	1.19	13.30	12.99	12.67

Table C.7 Dependences of q_e on C_e calculated using Freundlich and linear model comparing with the experimental data for adsorption of stigmasterol on SA-R, SB-R, and WB-R at 308 K, adsorbent loading = 5 wt% (data of Figure A.14)

Resin	C_e (mg/g-solution)	$q_{e,\ Experiment}$ (mg/g-adsorbent)	$q_{e,\ Freundlich\ model}$ (mg/g-adsorbent)	$q_{e,\ Linear\ model}$ (mg/g-adsorbent)
SA-R	0.00	0.00	0.00	0.00
	0.27	1.95	1.69	1.45
	0.51	2.78	2.99	2.75
	0.83	4.99	4.68	4.51
	1.03	5.33	5.69	5.61
	1.34	7.03	7.18	7.26
	1.52	8.31	8.08	8.28
SB-R	0.00	0.00	0.00	0.00
	0.22	1.80	1.95	1.85
	0.44	3.47	3.73	3.63
	0.61	5.45	5.16	5.08
	0.79	7.00	6.61	6.57
	1.01	7.85	8.28	8.32
	1.15	9.49	9.41	9.50
WB-R	0.00	0.00	0.00	0.00
	0.29	2.09	2.52	2.85
	0.45	4.20	4.10	4.43
	0.65	6.19	6.20	6.45
	0.84	8.36	8.23	8.34
	1.04	10.96	10.48	10.39
	1.23	12.14	12.56	12.24

Table C.8 Dependences of q_e on C_e calculated using Freundlich and linear model comparing with the experimental data for adsorption of stigmasterol on SA-R, SB-R, and WB-R at 313 K, adsorbent loading = 5 wt% (data of Figure A.15)

Resin	C_e (mg/g-solution)	$q_{e,\ Experiment}$ (mg/g-adsorbent)	$q_{e,\ Freundlich\ model}$ (mg/g-adsorbent)	$q_{e,\ Linear\ model}$ (mg/g-adsorbent)
SA-R	0.00	0.00	0.00	0.00
	0.29	0.94	0.86	1.14
	0.56	1.99	1.89	2.21
	0.83	3.46	3.03	3.27
	1.06	3.55	4.06	4.19
	1.35	5.02	5.43	5.34
	1.57	6.92	6.49	6.20
SB-R	0.00	0.00	0.00	0.00
	0.30	2.92	2.20	1.87
	0.53	3.25	3.62	3.30
	0.77	4.66	5.01	4.79
	0.98	5.71	6.14	6.04
	1.23	8.33	7.51	7.61
	1.45	8.43	8.66	8.95
WB-R	0.00	0.00	0.00	0.00
	0.25	2.44	2.54	2.45
	0.41	4.14	4.07	3.97
	0.61	6.30	5.96	5.88
	0.85	7.80	8.22	8.19
	0.99	9.45	9.46	9.47

	1.24	11.97	11.85	11.94

Table C.9 Effect of temperature on the adsorption capacity of on SA-R, SB-R, and WB-R at various initial stigmasterol concentrations at temperature in the range of 298 to 313 K, adsorbent loading = 5 wt% (data of Figure 3.5)

SA-R						
C_0 (mg/g-solution)	0.3	0.6	0.9	1.2	1.5	1.8
T (K)	q_e (mg/g-adsorbent)					
298	1.70	3.72	6.19	7.56	10.01	11.46
303	2.44	3.99	4.86	5.90	8.11	9.17
308	1.95	2.78	4.99	5.33	7.03	8.31
313	0.94	1.99	3.46	3.55	5.02	6.92
SB-R						
C_0 (mg/g-solution)	0.3	0.6	0.9	1.2	1.5	1.8
T (K)	q_e (mg/g-adsorbent)					
298	2.10	4.15	6.47	7.41	9.89	12.19
303	2.15	3.17	5.75	7.43	9.76	11.83
308	1.80	3.47	5.45	7.00	7.85	9.49
313	2.92	3.25	4.66	5.71	8.33	8.43
WB-R						
C_0 (mg/g-solution)	0.3	0.6	0.9	1.2	1.5	1.8
T (K)	q_e (mg/g-adsorbent)					
298	3.19	5.14	7.50	10.03	11.53	14.21
303	2.51	4.86	7.23	8.80	11.30	12.89

308	2.09	4.20	6.18	8.36	10.96	12.14
313	2.44	4.14	6.30	7.80	9.45	11.97

Table C.10 q_e, %Ad, %De, and %Re from SB-R and WB-R (data of Figure 3.7)

Resin	q_e (mg/g-adsorbent)		%Ad		%De		%Re	
	Value	Standard error	Value	Standard error	Value	Standard error	Value	Standard error
SB-R	40.71	1.68	51.30	2.05	78.84	11.58	37.52	0.51
WB-R	43.75	1.05	51.00	1.26	60.13	3.49	30.90	2.69

Table C.11 q_e, %Ad, %De, and %Re from NIS and MIS (data of Figure 4.3)

Adsorbent	q_e (mg/g-adsorbent)		%Ad		%De		%Re	
	Value	Standard error	Value	Standard error	Value	Standard error	Value	Standard error
NIS	47.91	0.03	58.22	0.86	52.77	1.20	30.73	1.15
MIS	68.01	0.47	82.31	0.80	73.27	0.20	60.31	0.75

Table C.12 %Ad and %De of phytosterol by MIS synthesized under various combinations of factors (data of Figure 4.4)

Combination number	% Ad		% De	
	Value	Standard error	Value	Standard error
1	70.50	0.24	64.00	0.85
2	43.21	1.18	16.50	1.76
3	80.27	1.30	69.90	0.03
4	54.79	0.63	32.28	1.20
5	76.63	0.72	70.00	0.85
6	45.08	0.84	21.07	1.22
7	82.46	0.61	70.16	0.31
8	49.58	0.75	21.36	0.90
9	90.23	0.59	69.55	2.00

10	27.71	3.96	0.00	0.00
11	42.89	0.04	25.30	1.84
12	86.61	1.93	62.10	10.43
13	64.32	3.09	50.43	1.65
14	68.69	0.81	62.36	1.39
15	61.51	5.42	55.04	1.52
16	60.63	0.59	53.78	1.77
17	48.76	1.10	21.67	1.53

Table C.13 q_e of different MIS synthesized under various combinations of factors compared to that of NIS (data of Figure 4.5)

Order	Combination factor			q_e (mg/g-adsorbent)	
	pH	*T* (K)	S/TEOS	Value	Standard error
1	0.95	304.25	1.73×10^{-3}	57.44	2.10
2	1.65	304.25	1.73×10^{-3}	35.54	2.79
3	0.95	316.75	1.73×10^{-3}	64.65	1.23
4	1.65	316.75	1.73×10^{-3}	42.90	1.03
5	0.95	304.25	4.74×10^{-3}	62.18	2.29
6	1.65	304.25	4.74×10^{-3}	36.39	1.05
7	0.95	316.75	4.74×10^{-3}	67.48	2.17

8	1.65	316.75	4.74×10^{-3}	39.18	0.82
9	0.60	310.5	3.24×10^{-3}	72.23	0.80
10	2.00	310.5	3.24×10^{-3}	22.13	3.68
11	1.30	298.0	3.24×10^{-3}	35.57	0.43
12	1.30	323.0	3.24×10^{-3}	67.94	0.57
13	1.30	310.5	2.23×10^{-4}	51.43	2.82
14	1.30	310.5	6.25×10^{-3}	54.74	2.75
15	1.30	310.5	3.24×10^{-3}	48.66	3.66
16	1.30	310.5	3.24×10^{-3}	49.66	1.06
17	1.30	310.5	3.24×10^{-3}	36.94	1.00
NIS	1.30	310.5	-	41.87	-

Table C.14 The textural properties of different MIS synthesized under various combinations of factors

Order	Combination factor			The textural properties		
	pH	*T* (K)	S/TEOS	BET surface area (m^2/g)	Total pore volume (cm^3/g)	Mean pore diameter (nm)
1	0.95	304.25	1.73×10^{-3}	733.87	0.3408	1.8578
2	1.65	304.25	1.73×10^{-3}	587.01	0.249	1.6964
3	0.95	316.75	1.73×10^{-3}	813.92	0.3896	1.9149
4	1.65	316.75	1.73×10^{-3}	636.11	0.2676	1.683
5	0.95	304.25	4.74×10^{-3}	793	0.3639	1.8355

6	1.65	304.25	4.74×10^{-3}	615.97	0.2541	1.65
7	0.95	316.75	4.74×10^{-3}	853.76	0.4484	2.101
8	1.65	316.75	4.74×10^{-3}	611.54	0.2593	1.696
9	0.60	310.5	3.24×10^{-3}	824.42	0.4587	2.2257
10	2.00	310.5	3.24×10^{-3}	515.73	0.2175	1.6872
11	1.30	298.0	3.24×10^{-3}	613.09	0.2648	1.7275
12	1.30	323.0	3.24×10^{-3}	660.58	0.3171	1.9203
13	1.30	310.5	2.23×10^{-4}	628.96	0.2744	1.7449
14	1.30	310.5	6.25×10^{-3}	560.23	0.241	1.721
15	1.30	310.5	3.24×10^{-3}	582.84	0.2625	1.8018
16	1.30	310.5	3.24×10^{-3}	582.84	0.2625	1.8018
17	1.30	310.5	3.24×10^{-3}	582.84	0.2625	1.8018

Appendix D

Research outputs

CHEMICAL ENGINEERING TRANSACTIONS
VOL. 70, 2018
A publication of AIDIC
The Italian Association of Chemical Engineering
Online at www.aidic.it/cet
Guest Editors: Timothy G. Walmsley, Petar S. Varbanov, Rongxin Su, Jiří J. Klemeš

ISBN 978-88-95608-67-9; **ISSN** 2283-9216
DOI: 10.3303/CET1870080

Synthesis of Moleculary Imprinted Polymer Originated from TFMAA and TRIM for Sterol Separation

Chinakrit Ladadok, Sarawut Sinpichai, Nattawat Nonthanasin, Krittin Binabdullah, Duangkamol Na-Ranong*

Department of Chemical Engineering, Faculty of Engineering, King Mongkut's Institute of Technology Ladkrabang, 1, Chalongkrung 1, Ladkrabang, Bangkok 10520, Thailand
dnaranong@hotmail.com

Molecular imprinted polymer (MIP) was synthesized bulk polymerization using 2-(trifluoromethyl)acrylic acid (TFMAA) as a functional monomer, trimethylolpropane trimethacrylate (TRIM) as a cross-linker, benzoyl peroxide as an initiator, acetone as porogen solvent, and stigmasterol as template molecule to obtain adsorbent having high affinity and selectivity to stigmasterol for separation of stigmasterol or other sterols in liquid phase. Functional groups and the morphology of the obtained MIP were investigated by Fourier transform infrared (FT-IR) and scanning electron microscope (SEM), respectively. The performance in sterol adsorption of MIPs synthesized under various conditions was investigated using a model solution of sterol mixture in n-heptane with initial concentration of 1.40×10^{-4} kg/kg-solution comparing with non-imprinted polymer (NIP). Adsorbent (1 wt%) was added to model solution and shaken in an orbital shaker at 3.67 rps, 303 K for 2.16×10^{4} s. The analysis of variance (ANOVA) suggested that the cross-linker was more influential factor on the adsorption performance of MIP as compared to the template molecule and solvent. The optimization showed that MIP synthesized at 0.5×10^{-3} mol of cross-linker, 1.0×10^{-4} mol of template molecule, and 1.0×10^{-5} m^3 of solvent had highest percentage adsorption of 57.73 % which was 1.37 times of NIP.

1. Introduction

Sterols are generally found in small amounts naturally in many vegetable oils (Phillips et al., 2002) and deodorizer distillate (DD) by-product of deodorization (Gunawan and Ju, 2009). It was employed as starting material in food, cosmetics and pharmaceutical industries (Fernandes and Cabral, 2007). However, it is usually difficult to be separated from other compounds. In recent year, two main processes have been applied for the recovery of sterol from DD including chemical and physical treatments. In the first approach, FFA in DD was saponified and the resulted soap was removed from the obtained mixture by simple solid-liquid separation. In the last step, sterols were separated from the liquid mixture of unsaponifiable components by using either vacuum distillation (Rohr, 2003) or cold crystallization (Khatoon et al., 2010). In the second approach, FFA and glycerides were chemically transformed to fatty acid alkyl esters (FAAE) by esterification (Moreira and Baltanás, 2004) or esterification followed by transesterification (Wollmann et al., 2005). Then, vacuum distillation was applied to remove large fraction of FAAE. Similar to the former approach, cold crystallization was also applied as the last step of sterol isolation. However, the major problem of these processes was the high energy requirement. In general, vacuum distillation was operated at 100 to 133.32 Pa and 453 to 473 K to remove undesired compounds in the mixture from chemical treatment, and cold crystallization was used to separate sterol from the remaining mixture at low temperature between 253 to 288 K. Therefore, a method with high efficiency and more economical value should be developed to serve rapid growth of recent sterol demand.
Adsorption process with activated carbon (Barder, 1989) and magnesium silicate (Barder et al., 1990) were used to recover sterol from natural resources. However, these adsorbents have shown some significant disadvantages, which include high capital costs and low selectivity to sterol molecule. Therefore, it is necessary to develop the highly selective and economical adsorbent material for the recovery of sterol. Polymeric materials have been used in many applications in the field of chemistry and engineering such as separation processes (Ahmad et al., 2015), catalyst based (Protsenko et al., 2016), and biosensor (González-Delgado et al., 2016).

Please cite this article as: Ladadok C., Sinpichai S., Nonthanasin N., Binabdullah K., Na-Ranong D., 2018, Synthesis of moleculary imprinted polymer originated from tfmaa and trim for sterol separation , Chemical Engineering Transactions, 70, 475-480 DOI:10.3303/CET1870080

Molecular imprinted polymer (MIP) is one alternative technique to prepare the adsorbent with selective molecular recognition ability. This technique requires the template molecule to create cavities in polymer matrix after removal of template molecule.

In this study, MIPs were synthesized using 2-(trifluoromethyl)acrylic acid as a functional monomer, trimethylolpropane trimethacrylate as a cross-linker, benzoyl peroxide as an initiator, acetone as a porogen solvent, and stigmasterol as a template molecule to obtain adsorbent having high selectivity to stigmasterol for separation of stigmasterol or other sterols in liquid phase. Analysis of variance (ANOVA) was used to determine the effect of three synthesis factors of MIP such as amount of cross-linker, template molecule, and solvent for percentage adsorption of sterol. Functional groups and the morphology of MIP were investigated by Fourier transform infrared (FT-IR) and scanning electron microscope (SEM), respectively. Batch adsorption was performed to evaluate the performance of the obtained MIPs in sterol adsorption using a model solution of sterol mixture in n-heptane comparing with non-imprinted polymer (NIP).

2. Materials and Methods

2.1 Materials

2-(trifluoromethyl)acrylic acid (Alfa Aesar) as a functional monomer, trimethylolpropane trimethacrylate (Sigma-Aldrich) as a cross-linker, benzoyl peroxide (Merck) as an initiator, stigmasterol (Tama Biochemical) as a template molecule, and acetone (Asian scientific) as a porogen solvent. Sterol mixture (Acinopeptide) consisted campesterol (23.6 wt %), stigmasterol (28.2 wt %), and β-sitosterol (48.2 wt %) was used as an adsorbate. N-heptane (Apex Chemicals) was used as a model solution.

2.2 Synthesis of molecular imprinted polymer

2-(trifluoromethyl)acrylic acid (TFMAA), trimethylolpropane trimethacrylate (TRIM), stigmasterol and acetone were mixed in 6.0×10^{-5} m^3 glass bottle. A nitrogen gas was flowed into the mixture for 600 s to remove oxygen. Then the mixture was shaken by an orbital shaker at 3.67 rps and room temperature to form a homogeneous solution. After that, the solution was polymerized at 333 K by shaking at 3.67 rps for 8.64×10^{4} s. After polymerization process, the obtained solid polymer was ground by ceramic mortar. The obtained polymer powder was washed several times with distilled water to remove all unreacted reagent. The distillated water was separated from the polymer powder by centrifugation at 66.67 rps for 1.8×10^{3} s and the water was taken to analyze UV-absorption of residual excess unreacted reagent using UV-spectrophotometer. The polymer powder was dried at 383 K for 8.64×10^{4} s. To remove the template molecule from polymer powder, soxhlet extraction was used at 393 K for 8.64×10^{4} s with solution consisting of acetonitrile (85 vol%), methanol (5 vol%), and water containing 1 vol% of acetic acid (10 vol%). Different MIPs were synthesized by varying three independent factors such as amount of cross-linker (A), template molecule (B), and solvent (C) in the range of 0.5×10^{-3} to 1.5×10^{-3} mol, 1.0×10^{-4} to 1.5×10^{-4} mol, and 1.0×10^{-5} to 2.0×10^{-5} m^3, respectively. Amount of functional monomer and initiator were fixed at 1.0×10^{-3} and 8.5×10^{-5} mol, respectively. Conditions for MIPs synthesis were determined using central composite design (CCD) as shown in Table 1. Non-imprinted polymer (NIP) was synthesized without a template molecule with the same synthesis procedures as MIP.

Table 1: Conditions for MIPs synthesis determined by central composite design (alpha value = 2.0)

No.	Cross-linker $\times10^{3}$ (mol)	Template molecule $\times10^{4}$ (mol)	Solvent $\times10^{5}$ (m^3)
1	0.75	1.125	1.25
2	1.25	1.125	1.25
3	0.75	1.375	1.25
4	1.25	1.375	1.25
5	0.75	1.125	1.75
6	1.25	1.125	1.75
7	0.75	1.375	1.75
8	1.25	1.375	1.75
9	0.50	1.250	1.50
10	1.50	1.250	1.50
11	1.00	1.000	1.50
12	1.00	1.500	1.50
13	1.00	1.250	1.00
14	1.00	1.250	2.00
STD	1.00	1.250	1.50

2.3 Characterization of molecular imprinted polymer

Morphology of MIP and NIP was investigated by Scanning electron microscope (SEM) using EVO®MA10 (ZEISS). Extra high-tension voltage level was 1.5×10^{4} V. Functional groups of MIP and NIP were investigated by Fourier transform infrared (FT-IR) using IRPrestige-21 (Shimadzu, Japan) equipped with MIRacle ATR (PIKE Technologies, Inc.) with a resolution of 4 cm^{-1}.

2.4 Adsorption performance test

The adsorption performance of MIPs synthesized under various conditions was investigated using a model solution of sterol mixture in n-heptane with initial concentration of 1.40×10^{-4} kg/kg-solution comparing with NIP. Adsorbent (1 wt%) was added to model solution and shaken in an orbital shaker at 3.67 rps, 303 K for 2.16×10^{4} s. Sample before and after adsorption were taken for quantitative analysis of campesterol, stigmasterol, and β-sitosterol. Analysis was performed using a gas chromatography connected with flame ionized detector (GC-2010plus; Shimadzu). Peak separation was achieved using a ZB-5HT capillary column (30 m in length, 3.2×10^{-4} m in internal diameter, 1.0×10^{-7} m in film thickness; Phenomenex). Tricaprin was used as an internal standard. Adsorption performance was evaluated by the percentage adsorption of sterol (% Ads), adsorption capacity (q), and selectivity base on stigmasterol (S_i) were calculated according to Eq(1), Eq(2), and Eq(3).

$$\%\,Ads = \frac{C_0 - C}{C_0} \times 100 \tag{1}$$

$$q = \frac{(C_0 - C)W_{sol}}{W_{ads}} \tag{2}$$

$$S_i = \left(\frac{W_{i,0} - W_i}{W_{i,0}}\right)\left(\frac{W_{stigma,0}}{W_{stigma,0} - W_{stigma}}\right) \tag{3}$$

Where C_0 and C are liquid-phase concentration of stigmasterol at initial and at time t, respectively. W_{sol} is the weight of the solution, and W_{ads} is the weight of adsorbent used. $W_{i,0}$ and W_i are the weight of species "i" at initial and at time t, respectively. $W_{stigma,0}$ and W_{stigma} are the weight of stigmasterol at initial and at time t, respectively.

2.5 Statistical analysis

The percentage adsorption of sterol was selected as the response factor, and the relationship between response factor and independent factors was approximated by quadratic model equation. The statistical of fitted quadratic model was analyzed by analysis of variance (ANOVA). The quality of fitted quadratic model was expressed by coefficient of determination (R^2), and the significant terms of model were evaluated based on the p-value with 95 % confidence.

3. Results and Discussion

3.1 Polymer characterization

The functional groups on both of polymers were explained by FT-IR spectra as shown in Figure 1. Both of NIP and MIP absorption peaks were similar and had small sharp peak of C-H vibration at 2,960 cm^{-1}, large sharp peak of C = O vibration at 1,710 cm^{-1} and the peak of C-F appeared over a very broad range of 1,000–1,400 cm^{-1}. These peaks were identified as the groups C - H, C = O, and C = F on TFMAA (Fauziah et al., 2015).

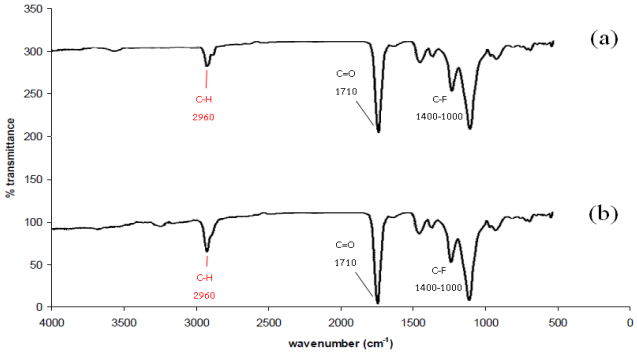

Figure 1: FT-IR spectra of (a) NIP and (b) MIP

However, absorption peak of O-H was not found on both FT-IR spectra. It is possible that O-H group undergo interaction with other functional groups. The comparison of spectra between NIP and MIP indicated that intensity of C-H peak on the NIP spectra was less than MIP spectra. It is possible that the residue of stigmasterol contained in MIP. The surface of MIP synthesized at condition number 9 (Figure 2(b)) was rougher than NIP, see Figure 2(a). Furthermore, the porous of MIP was larger than NIP. It suggested that the imprinted of stigmasterol created additional pores in polymer matrix.

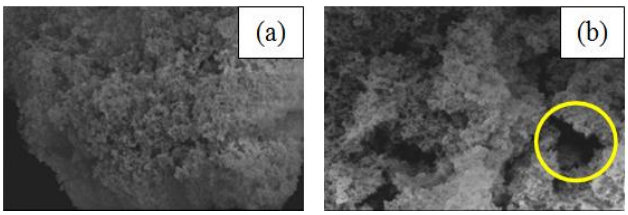

Figure 2: SEM images at a magnification of 20,000x of (a) NIP and (b) MIP

3.2 Adsorption performance

The adsorption performance of adsorbents was investigated using a model solution of sterol mixture (campesterol, stigmasterol, and β-sitosterol) in n-heptane. MIPs were synthesized under various conditions to use in the sterol adsorption comparing with NIP. Figure 3 showed the adsorption performance of MIPs comparing with NIP. MIP synthesized at condition number 9 (0.5×10^{-3} mol of cross-linker, 1.25×10^{-4} mol of template molecule, and 1.5×10^{-5} ml of solvent) adsorbed greater amount of sterol comparing with NIP. The adsorption capacities of MIP synthesized at condition number 9 and NIP were 5.93×10^{-3} and 5.85×10^{-3} kg/kg-adsorbent, respectively. However, the adsorption result revealed that all of MIPs synthesized adsorbed campesterol, stigmasterol, and β-sitosterol with the same percentage of initial amounts in model solution ($S_{campesterol} = S_{\beta\text{-}sitosterol} = 1.0$). No specific selectivity for stigmasterol adsorption should be result from very similar structure of these sterols. Based on the adsorption capacity, the result indicated that the maximum sterol adsorption capacity of MIPs (q = 5.93×10^{-3} kg/kg-adsorbent) was 5.3 times higher than the capacity of MIP synthesized using TFMAA as a functional monomer, TRIM as a cross linker and β-sitosterol as a template molecule of some reported (Fauziah et al., 2015). Therefore, it was thus a promising adsorbent and could be used for recovery of sterol by adsorption method.

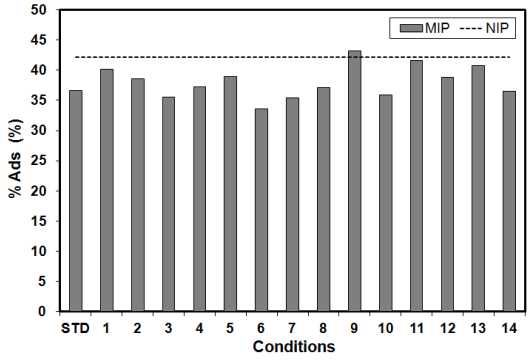

Figure 3: Adsorption performance of MIPs comparing with NIP at 303 K for 2.16×10^4 s

3.3 Statistical analysis

The results of the percentage adsorption of sterol by MIPs synthesized under various conditions were selected to analyze in order to identify significant effect of factors on the percentage adsorption of sterol by synthesized molecular imprinted polymer. The analysis of variance of percentage adsorption was summarized in Table 2. The p-value showed that the linear terms (A, B, and C), quadratic terms (A×A, B×B, and C×C) and interaction terms (A×B, A×C, and B×C) were insignificant (p-value > 0.05). It seems that all terms had no effect on the adsorption performance of MIP. However, a regression model was performed in order to obtain a suitable prediction model for percentage adsorption of sterol, and the relationship between the percentage adsorption and the independent factors was shown in Eq(4).

$$\%\,Ads = 2860 - 74.7A - 257.8B - 58.4C + 14.8A^2 + 70.3B^2 + 11.0C^2 + 41.3AB - 7.4AC + 23.2BC \quad (4)$$

Table 2: The analysis of variance of percentage adsorption of sterol by MIP

Terms	Coefficient	S.E. coefficient	p-value
Constant	286.04	1.765	0.000
Cross-linker (A)	-74.68	0.500	0.070
Template (B)	-257.78	0.500	0.210
Solvent (C)	-58.37	0.500	0.121
A × A	14.80	0.601	0.185
B × B	70.30	0.601	0.127
C × C	10.99	0.601	0.305
A × B	41.34	0.708	0.127
A × C	-7.46	0.708	0.539
B × C	23.28	0.708	0.351

The fit of model was checked by the coefficient of determination (R^2), which was calculated to be 79.39 % indicating that 79.39 % of the variability in the response could be explained by the model. Figure 4(a), 4(b), and 4(c) show the three-dimensional response surface which were shown the effect of MIP synthesis factors on the percentage adsorption of sterol. Figure 4(a) illustrated the effect of amount of template molecule and solvent on the percentage adsorption of sterol, with amount of cross-linker was fixed at 1.0×10^{-3} mol. Figure 4(b) illustrated the effect of amount of cross-linker and solvent on the percentage adsorption of sterol, with amount of template molecule was fixed at 1.25×10^{-4} mol, and Figure 4(c) illustrated the effect of amount of cross-linker and template molecule on the percentage adsorption of sterol, with amount of solvent was fixed at 1.5×10^{-5} m^3.

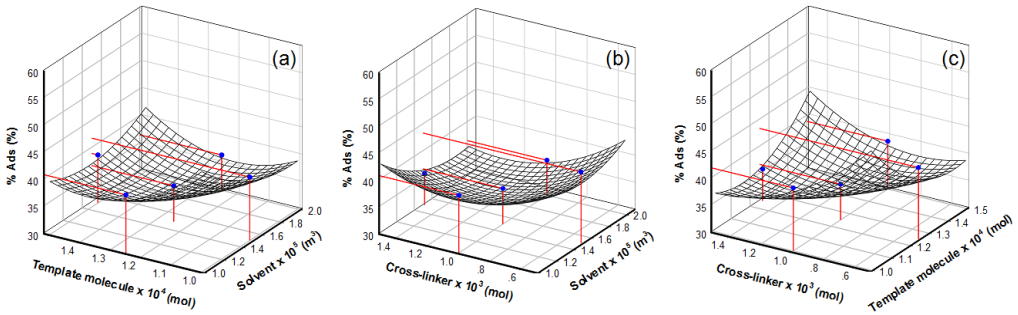

Figure 4: Three-dimensional response surface plot of the percentage adsorption of sterol by MIP; (a) effect of amount of template molecule and solvent, amount of cross-linker = 1.0×10^{-3} mol, (b) effect of amount of cross-linker and solvent, amount of template molecule = 1.25×10^{-4} mol, (c) effect of amount of cross-linker and template molecule, amount of solvent = 1.5×10^{-5} m^3 comparing with the experimental data (blue circle symbol)

The results indicated that the prediction result of the percentage adsorption of sterol was in good agreement with the experimental values. The percentage adsorption of sterol by MIP was found to decrease with increasing amount of cross-linker as shown in Figure 4(b) and 4(c). It can be seen that amount of cross-linker was more influential factor on the adsorption performance of MIP as compared to the other two factors. The high amount of cross-linker inhibited the diffusion of the template reducing the efficiency of the imprinting process (Rechichi et al., 2007). In addition, the amount of cross-linker can control the degree of MIP swelling. The rigidity of MIP is a consequence of the excess of cross-linking agents. The rigidity makes very difficult to remove template molecule from MIP, it results in the number of molecular recognition sites becomes less than the number of sites expected from the amount of template molecule used due to some template molecule are embed in the polymer matrix (Park et al., 2005). These results were presented by the case of the amount of template molecule in the range of 1.0×10^{-4} to 1.35×10^{-4} mol as shown in Figure 4(C), the MIP synthesized with 0.5×10^{-3} mol of cross-linker exhibited higher percentage adsorption than that 1.5×10^{-3} mol of cross-linker. However, MIPs synthesized with 0.5×10^{-3} mol of cross-linker exhibited low percentage adsorption when increasing amount of template molecule. It is possible that the excess amount of template molecule interacted with the functional monomer as well as with the cross-linker. This could reduce the number of interaction between the functional monomer and cross-linker which could generate fewer effective cavities in the polymer matrix and reduce the number of molecular recognition sites. According to the optimization, the result showed that MIP synthesized at 0.5×10^{-3} mol of cross-linker, 1.0×10^{-4} mol of template molecule, and 1.0×10^{-5} m^3 of solvent had highest percentage adsorption of 57.73 % which was 1.37 times of NIP.

4. Conclusions

Molecular imprinted polymers (MIPs) were synthesized by bulk polymerization using TFMAA as a functional monomer, TRIM as a cross-linker, benzoyl peroxide as an initiator, acetone as porogen solvent, and stigmasterol as a template. The analysis of variance (ANOVA) suggested that cross-linker was more influential factor on the adsorption performance of MIP compared to template molecule and solvent. The optimization showed that MIP synthesized at 0.5×10^{-3} mol of cross-linker, 1.0×10^{-4} mol of template molecule, 1.0×10^{-5} m^3 of solvent had the highest adsorption capacity of 57.73 % (1.37 times of NIP). Moreover, adsorption was successfully performed at 303 K. In considering energy requirement for adsorption compared with vacuum distillation at temperature of 453 to 473 K or cold crystallization at 253 to 288 K, adsorption is promising method for sterol recovery in large scale with fewer energy requirement.

Acknowledgments

Financial supports from Thailand Research Fund (TRF) and King Mongkut's Institute of Technology Ladkrabang (KMITL) under Royal Golden Jubilee Ph.D. program (PHD/0021/2555) are appreciatively acknowledged. This research was also funded by National Research Council of Thailand (NRCT).

References

Ahmad A.L., Lah N.F.C., Low S.C., 2015, Molecular imprinted polymer for atrazine detection sensor: preliminary study, Chemical Engineering Transactions, 45, 1483-1488.

Barder T.J., 1989, Purification of sterols with activated carbon as adsorbent and chlorobenzene as desorbent, US Patent, 4882065, USA.

Barder T.J., Bedwell W.B., Johnson S.P., 1990, Separation of sterols from low-acid feeds with magnesium silicate and methyl-tert-butyl ether desorbent, US Patent, 4977243, Washington DC, USA.

Fauziah St., Taba P., Amran Muh. B., Budi P., Hariani S N., 2015, Synthesis, characterization, and optimization of β-sitosterol imprinted polymers using TFMAA as functional monomer, International Journal of Applied Chemistry, 11, 487-495.

Fernandes P., Cabral J.M.S., 2007, Phytosterols: Applications and recovery methods, Bioresource Technology, 98, 2335–2350.

González-Delgado Á.D., Barajas-Solano A.F., Peralta-Ruiz Y.Y., 2016, Microalgae immobilization using hydrogels for environmental applications: study of transient photopolymerization, Chemical Engineering Transactions, 47, 457-462.

Gunawan S., Ju Y.H., 2009, Vegetable oil deodorizer distillate: characterization, utilization and analysis, Separation & Purification Reviews, 38, 207-241.

Khatoon S., Raja Rajan R.G., Gopala Krishna A.G., 2010, Physicochemical characteristics and composition of Indian soybean oil deodorizer distillate and the recovery of phytosterols, Journal of the American Oil Chemists' Society, 87, 321-326.

Moreira E.A., Baltanás M. A., 2004, Recovery of phytosterols from sunflower oil deodorizer distillates, Journal of the American Oil Chemists' Society, 81, 161-167.

Park H.R., Yoon S.D., Bang E.Y., Rogers K.R., Chough S.H., 2005, Molecular imprinting polymers for the separation of toluic acid isomers, Journal of Applied Polymer Science, 96, 650-654.

Phillips K.M., Ruggio D.M., Toivo J.I., Swank M.A., Simpkins A.H., 2002, Free and esterified sterol composition of edible oils and fats, Journal of Food Composition and Analysis, 15, 123-142.

Protsenko I.I., Nikoshvili L.Z., Matveeva V.G., Sulman E.M., Rebrov E., 2016, Selective hydrogenation of levulinic acid to gamma-valerolactone using polymer-based Ru-containing catalysts, Chemical Engineering Transactions, 52, 679-684.

Rechichi A., Cristallini C., Vitale U., Ciardelli G., Barbani N., Vozzi G., Giusti P., 2007, New biomedical devices with selective peptide recognition properties. Part 1: Characterization and cytotoxicity of molecularly imprinted polymers, Journal of Cellular and Molecular Medicine, 11, 1367-1376.

Rohr R., 2003, Process for separation unsaponifiable valuable products from raw materials, US Patent, 2003/0120095 A1, USA.

Wollmann G., Schwarzer J., Gutsche B., 2005, Processes for producing sterols from fatty acid production residues, US Patent, 6956125 B2, USA.

CHEMICAL ENGINEERING TRANSACTIONS
VOL. 70, 2018
A publication of AIDIC
The Italian Association of Chemical Engineering
Online at www.aidic.it/cet
Guest Editors: Timothy G. Walmsley, Petar S. Varbanov, Rongxin Su, Jiří J. Klemeš

ISBN 978-88-95608-67-9; **ISSN** 2283-9216
DOI: 10.3303/CET1870180

Kinetics, Isotherm, and Thermodynamics of Adsorption of Sterol on Strong Acid Ion Exchange Resin

Chinakrit Ladadok[a], Takehiro Yamaki[b], Keigo Matsuda[c], Hideyuki Matsumoto[d], Duangkamol Na-Ranong[a,*]

[a]Department of Chemical Engineering, Faculty of Engineering, King Mongkut's Institute of Technology Ladkrabang, 1 Chalongkrung 1, Ladkrabang, Bangkok 10520, Thailand
[b]National Institute of Advanced Industrial Science and Technology, Research Institute for Chemical Process Technology 1-1-1 Higashi, Tsukuba, Ibaraki, Japan
[c]Department of Chemistry and Chemical Engineering, Graduate School of Science and Engineering, Yamagata University 4-3-16, Jonan, Yonezawa-shi, Yamagata 992-8510, Japan
[d]Department of Chemical Science and Engineering, School of Materials and Chemical Technology, Tokyo Institute of Technology, 2-12-1 Ookayama, Meguro-ku, Tokyo 152-8552, Japan
dnaranong@hotmail.com

Kinetics, isotherm and thermodynamics of sterol adsorption on styrene-divinylbenzene based ion-exchange resin with strong acid was investigated at temperature in the range of 298 to 313 K using a model solution of stigmasterol in n-heptane with initial concentration in the range of 0.3×10^{-3} to 1.8×10^{-3} kg/kg-solution. Adsorbent (5 wt%) was added to the model solution and isothermal adsorption was performed at 3.33 rps for 7.2×10^{3} s. Kinetics of sterol adsorption was analysed based on pseudo-first-order and pseudo-second-order models. The results revealed that pseudo-second-order model agreed with the experimental data, much better than pseudo-first-order model. At the equilibrium of adsorption, adsorption capacity (q_e) decreased when the temperature was increased. This result indicated that sterol adsorption was exothermic. Analysis of adsorption isotherm data based on Langmuir, Freundlich and linear models showed that Freundlich was the best model that could predict the adsorption isotherm data. Adsorption equilibrium constants calculated based on Freundlich model at various temperatures were used to calculate Gibb's free energy change (ΔG), enthalpy change (ΔH), and entropy change (ΔS). The increase of ΔG with respect to temperature indicated that the adsorption was more favourable at lower temperatures. The negative value of ΔH indicated that the adsorption was exothermic and agreed well with the effect of temperature on adsorption capacity. The negative value of ΔS indicated associative adsorption and decrease of the randomness between the solid/liquid interfaces due to the adsorption.

1. Introduction

Sterols have several beneficial bioactivities such as anti-cancer and decrease the risk of coronary heart disease. They have been widely used as starting material in food, cosmetics and pharmaceutical industries (Fernandes and Cabral, 2007). Over the past several decades, deodorizer distillate (DD) which is a by-product in a vegetable refinery plant became one of the most important sources of natural sterols. DD contains free fatty acids (FFA), monoglycerides (MG), diglycerides (DG), triglycerides (TG) and small amount of some bioactive compounds (Verleyen et al., 2001). Sterols have been successfully recovered from DD by two main methods. These methods were designed to remove undesired compounds (FFA and glycerides) from DD, followed by sterols separation. In one method, FFA in DD was saponified and then the resulted soap was removed from the mixture by simple solid-liquid separation. After that, sterols were separated from the resulted concentrate mixture by crystallization (Khatoon et al., 2010) or vacuum distillation (Rohr, 2003). The another method, FFA and other glycerides were transformed to fatty acid alkyl ester (FAAE) by esterification (Moreira and Baltanás, 2004) or esterification followed by transesterification (Wollmann et al., 2005). In the sterols preconcentration step, FAAE fraction was removed by vacuum distillation to obtain high yield of sterols. Similar to the former method, crystallization was applied as the last step for sterols separation. Although these methods have been

Please cite this article as: Ladadok C., Yamaki T., Matsuda K., Matsumoto H., Na-Ranong D., 2018, Kinetics, isotherm, and thermodynamics of adsorption of sterol on strong acid ion exchange resin , Chemical Engineering Transactions, 70, 1075-1080 DOI:10.3303/CET1870180

successfully applied to recover sterols from DDs, they require large energy consumption. In general, vacuum distillation is operated at 100 to 133.32 Pa and 453 to 473 K to remove undesired compounds in the resulted mixture from chemical treatment, and cold crystallization was used to separate sterols from the remaining mixture at low temperature (253 to 288 K). A simple, efficient, and economical method should be developed to serve the growth of sterols demand. Adsorption is widely used in separation of minor components from liquid mixture under mild conditions. The use of adsorbent is the basis of all adsorption techniques. Polymeric resins have been widely used to remove pollutants such as phenol (Victor-Ortega et al., 2016) or polyphenols (Njimou et al., 2017) from aqueous solutions because of low cost and high abundance. Based on chemical resistance and simplicity of operation, styrene-divinylbenzene based ion-exchange resin with strong acid (SA-R) was considered as attractive adsorbent in the sterol recovery process. The objective of this study was to investigate behavior of sterol adsorption on SA-R. Isothermal batch adsorption was performed using a model solution of stigmasterol in n-heptane to evaluate adsorption capacity. Kinetics of sterol adsorption was evaluated based on pseudo-first-order and pseudo-second-order models. Adsorption data at equilibrium were analyzed based on Langmuir, Freundlich and linear isotherms and three important thermodynamics parameters (i.e. Gibb's free energy change: ΔG, enthalpy change: ΔH and entropy change: ΔS) were calculated and the adsorption behavior was discussed based on the calculated thermodynamics parameters.

2. Materials and methods

2.1 Materials

Styrene-divinylbenzene copolymer cation-exchange resin (Lewatit® Monoplus SP 112H) with sulfonic acid group and mean bead size of $6.7\times10^{-4} \pm 0.5\times10^{-4}$ m (Lanxess, Germany) was selected as representative of a strong acid cation exchange resin (SA-R). SA-R was dried in an oven at 383 K under vacuum for 2.16×10^{4} s and stored in a desiccator before being used in adsorption experiment. Prior to the adsorption experiment, SA-R was washed with methanol, n-propanol and n-hexane. Stigmasterol (Tama Biochemical Co. Ltd.) and n-heptane (AR grade, Apex Chemicals Co. Ltd.) were used in preparation of a model solution of sterol containing mixture. Cholesterol (Sigma-Aldrich Inc.) was used as an internal standard (ISTD) in quantitative analysis of stigmasterol. HPLC grade organic solvents (methanol, acetonitrile and water from RCI Labscan Ltd. and acetic acid from Merck Ltd.) were used in the quantification of stigmasterol.

2.2 Batch adsorption

To study kinetics, isotherm and thermodynamics of stigmasterol adsorptions on SA-R, isothermal batch adsorption was performed using a model solution of stigmasterol in n-heptane. This nonpolar solvent, n-heptane, was used in this experiment to avoid competitive adsorptions of stigmasterol and solvent in the adsorption system. Adsorption temperature and stigmasterol concentration were varied in the ranges of 298 – 313 K and 0.3×10^{-3} to 1.8×10^{-3} kg/kg-solution, respectively. The model solution (5.0×10^{-5} m^3) and the adsorbent (5 wt%) were heated and shaken in an orbital shaker (4000ic; IKA) at 3.33 rps for 7.2×10^{3} s. Before and after the adsorption, samples (2.0×10^{-7} m^3) were taken and filtered through a 4.5×10^{-7} m nylon filter and used for the quantitative analysis of stigmasterol content.

2.3 Quantitative analysis

The content of stigmasterol in the sample was analyzed using a high-performance liquid chromatography (HPLC) connected with a UV detector. An injection valve connected with a 2.0×10^{-8} m^3 of sample loop was used to introduce the sample into the HPLC. Peak separation was achieved using a reverse-phase column (Inertsil C8-3; 5.0×10^{-6} m particle diameter, 0.25 m length, 4.6×10^{3} m i.d., GL Sciences Inc, Japan). Composition of mobile phase and condition of analysis were adapted from the work reported by Chang et al. (2000). Mobile phase was a mixture of acetonitrile (85 %), methanol (5 %), and water containing 1% of acetic acid (10 %) and flowed at the rate of 2.16×10^{-8} m^3/s, the analysis was performed at the wavelength of 2.1×10^{-7} m. Since the sample was not dissolved well in the mobile phase, n-heptane in the sample was removed and an appropriate solvent was added to the solid sample as a solvent in the quantitative analysis. The solvent exchange was performed as follows; n-heptane was completely removed from the sample by evaporation at room temperature, methanol (8.0×10^{-7} m^3) was then added and the mixture was shaken in the orbital shaker at 3.33 rps for 3.6×10^{3} s. As an internal standard, cholesterol in methanol (4.0×10^{-3} kg/kg-solution, 2.0×10^{-7} m^3) was added in the sample. Amount of stigmasterol adsorbed on the adsorbent at time "*t*" (q_t) was calculated according to Eq(1).

$$q_t = \frac{(C_0 - C_t)W_{sol}}{W_{ads}} \quad (1)$$

where C_0 and C_t are liquid-phase concentration of stigmasterol at initial and at time *t*, respectively. W_{sol} is the weight of the solution and W_{ads} is the weight of adsorbent used.

3. Results and discussion

3.1 Adsorption capacity

Figure 1 shows the time dependence of adsorption capacity of SA-R at various initial concentrations of stigmasterol. The adsorption capacity increased with time until equilibrium was reached within 1.8×10^{3} s. Comparison of the profiles obtained at different initial concentrations revealed that the rates of adsorption on SA-R increased with the increase of concentration of stigmasterol. This is general behaviour of a process with positive order rate equation. The adsorption capacity at the equilibrium (q_e) increased from 2.4×10^{-3} to 9.2×10^{-3} kg/kg-adsorbent by increasing the initial concentration from 0.3×10^{-3} to 1.8×10^{-3} kg/kg-solution. In addition, the adsorption efficiency of SA-R was found in the range of 25 - 35 %, being higher at lower initial concentration.

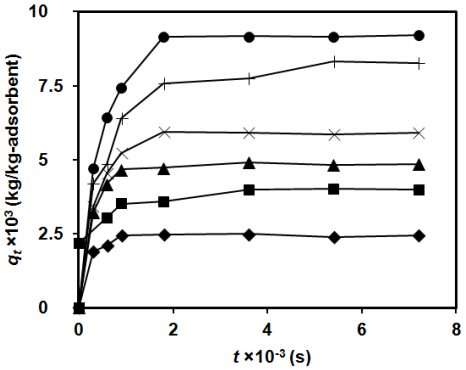

Figure 1: Capacities of SA-R for stigmasterol adsorption at various initial concentrations: (◆) 0.3×10^{-3}, (■) 0.6×10^{-3}, (▲) 0.9×10^{-3}, (×) 1.2×10^{-3}, (+) 1.5×10^{-3}, (●) 1.8 ×10^{-3} kg/kg-solution; at 303 K and 5 wt% SA-R

3.2 Adsorption kinetics

To study the kinetics of adsorption, the experimental data were comparatively analyzed based on pseudo-first-order and pseudo-second-order models which are expressed as Eq(2) and Eq(3).

$$\frac{dq_t}{dt} = k_1(q_e - q_t) \tag{2}$$

$$\frac{dq_t}{dt} = k_2(q_e - q_t)^2 \tag{3}$$

Where q_e and q_t are the amounts of stigmasterol adsorbed at equilibrium and at time t, respectively. k_1 and k_2 are the adsorption rate constant of pseudo-first-order and pseudo-second-order model. Linearized forms of these two models obtained by integrating Eq(2) and Eq(3) with the boundary conditions of $q_t = 0$ at $t = 0$ and $q_t = q_t$ at $t = t$ are expressed as Eq(4) and Eq(5).

$$\ln(q_e - q_t) = lnq_e - k_1 t \tag{4}$$

$$\frac{t}{q_t} = \frac{1}{k_2 q_e^2} + \frac{t}{q_e} \tag{5}$$

Linear plots corresponding to pseudo-first-order and pseudo-second-order models for SA-R are shown in Figure 2(a) and 2(b), respectively. The parameters, k and q_e, of each model were calculated from the slope and the y-intercept of the corresponding linear plot and summarized in Table 1. The correlation coefficients (R^2) of pseudo-second-order model were higher than pseudo-first-order model for all conditions. The lowest value of R^2 obtained from pseudo-second-order model was 0.9989 while the highest value of R^2 obtained from pseudo-first-order model was 0.9943. In addition, $q_{e,cal}$ from pseudo-second-order model agreed reasonably well with $q_{e,exp}$ ($\Delta q_e \leq 7.7\%$) while pseudo-first-order model could not well predict the value of $q_{e,exp}$., especially at initial concentration between 0.3×10^{-3} to 0.9×10^{-3} kg/kg-solution. Based on the correlation coefficients and Δq_e, pseudo-second-order model was selected to describe the kinetics of stigmasterol adsorption on SA-R. Considering the adsorption rate constant of pseudo-second-order model (k_2), the results show that k_2 depended on the initial concentration of stigmasterol (C_0). When C_0 was increased from 0.3×10^{-3} to 1.8×10^{-3} kg/kg-solution, k_2 decreased from 10.0313 to 0.4428 kg-adsorbent/(kg·s). This dependence of k_2 on initial concentration was previously reported in several adsorption systems (Ho and Mckay, 1999). Theoretical analysis by Azizian (2004)

clearly showed that k_2 is not an intrinsic rate constant of adsorption, but it is a complex function of adsorption rate constant, desorption rate constant and initial concentration of adsorbate.

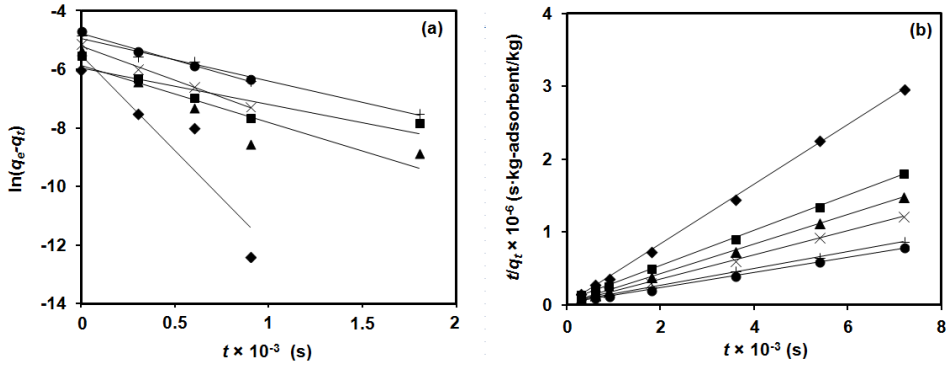

Figure 2: Linear plots of (a) pseudo-first-order and (b) pseudo-second-order kinetics models for various initial concentrations: (◆) 0.3×10^{-3}, (■) 0.6×10^{-3}, (▲) 0.9×10^{-3}, (×) 1.2×10^{-3}, (+) 1.5×10^{-3}, (●) 1.8 ×10^{-3} kg/kg-solution; at 303 K and 5 wt% SA-R

Table 1: Kinetic parameters of stigmasterol adsorptions on SA-R at 303 K with different initial concentrations

C_0	$q_{e,exp}$	Pseudo-first-order				Pseudo-second-order			
		k_1	$q_{e,cal}$	Δq_e (%)	R^2 (-)	k_2	$q_{e,cal}$	Δq_e (%)	R^2(-)
0.3	2.44	0.0065	3.93	61.3	0.8525	10.0313	2.45	0.4	0.9994
0.6	4.00	0.0012	2.60	35.2	0.8054	1.1144	4.14	3.5	0.9995
0.9	4.90	0.1161	2.80	42.8	0.8327	2.1669	4.93	0.6	0.9997
1.2	5.90	0.0023	5.54	6.1	0.9943	1.0602	6.06	2.7	0.9993
1.5	8.11	0.0015	7.13	12.1	0.9834	0.3139	8.73	7.6	0.9989
1.8	9.20	0.0018	8.51	7.2	0.9877	0.4428	9.57	4.0	0.9990

*Coefficient units: C_0×10^3 (kg/kg-solution); q_e×10^3 (kg/kg-adsorbent); k_1 (s^{-1}); k_2 (kg-adsorbent/(kg·s))

3.3 Adsorption isotherm

Adsorption isotherm was investigated at 298, 303, 308 and 313 K and discussed based on the data taken after 1 h of adsorption, which were reasonably considered as the performance at the equilibrium of adsorption according to the discussion in section of adsorption capacities. Figure 3 (a) shows dependence of adsorption capacity at the equilibrium (q_e) on concentration of stigmasterol at the equilibrium (C_e) at 303 K of SA-R. In the tested range of C_e, q_e increased with C_e and saturation of adsorption was not observed. Figure 3(b) shows effect of temperature on q_e for various initial concentrations. q_e decreased when the temperature was increased. This result indicated that stigmasterol adsorption was exothermic. This dependence was significant in the case of high initial concentration and became less significant when the initial concentration was lower.

Equilibrium adsorption data were analyzed based on Langmuir, Freundlich and linear isotherm models using the corresponding linearized form of each model, listed in Table 2. Langmuir model was considered as an inappropriate model for prediction of isotherm of stigmasterol adsorption for SA-R due to the value of R^2 was extremely low. At temperature of 298 and 313 K, q_m (saturated adsorption capacity) and K_{La} (adsorption equilibrium constant in Langmuir model) were negative, which had no physical meaning for adsorption process. Since R^2 of Freundlich model were larger than R^2 of linear model, except at 298 K. Freundlich model was considered as the most suitable model to be used to predict the performance of adsorption at the equilibrium for SA-R. However, the calculated values of 1/n were more than 1 for temperature of 298 and 313 K, indicating increase of hydrophobic surface characteristics after monolayer adsorption. The value of K_F was significantly influenced by adsorption temperature. The highest value of K_F was obtained at 298 K. Figure 3(a) shows good resemblances of the calculated curves and the experimental data for Freundlich model. Similar plots (not shown) were obtained at the other temperatures (298, 308 and 313 K) and showed good resemblances of the calculated curves and the experimental data, as well. Nonlinear regression analysis was performed for Freundlich model and gave the R^2 = 0.9782 higher than linear model (R^2 = 0.9652). Based on regression analysis, Freundlich model was the most suitable model for prediction of effect of C_e on q_e in the tested range of $0 \le C_e \le 1.38\times10^{-3}$ kg/kg-solution and $298 \le T \le 313$ K.

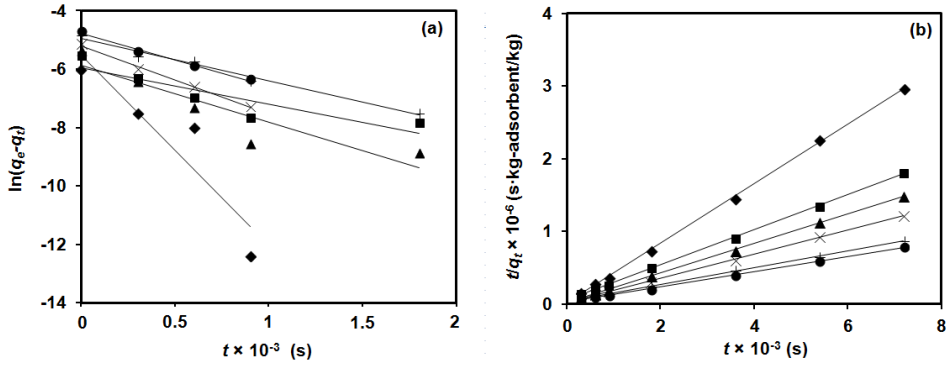

Figure 3: (a) Dependences of q_e on C_e calculated using Freundlich and linear models compared with the experimental data for adsorption of stigmasterol on SA-R (303 K, 5 wt% SA-R), (b) Effect of temperature on the adsorption capacity of SA-R at equilibrium (q_e) at various initial concentrations: (◆) 0.3×10^{-3}, (■) 0.6×10^{-3}, (▲) 0.9×10^{-3}, (×) 1.2×10^{-3}, (+) 1.5×10^{-3}, (●) 1.8×10^{-3} kg/kg-solution; T = 298 to 313 K, 5 wt% SA-R

Table 2: Parameters and correlation coefficients for Langmuir, Freundlich and linear models for isotherms of stigmasterol adsorption on SA-R

Models	Langmuir: $q_e = \frac{q_m K_{La} C_e}{1+K_{La} C_e}$			Freundlich: $q_e = K_F C_e^{1/n}$			Linear: $q_e = K_{Li} C_e$	
Linearized Equation; Parameters	$\frac{C_e}{q_e} = \frac{1}{K_{La} q_m} + \frac{1}{q_m} C_e$; K_{La}, q_m			$\log(q_e) = \log(K_F) + \frac{1}{n}\log(C_e)$; K_F, 1/n			$q_e = K_{Li} C_e$; K_{Li}	
T (K)	K_{La}	q_m	R^2 (-)	K_F	1/n (-)	R^2 (-)	K_{Li}	R^2 (-)
298	-197.35	-0.034	0.4696	29.785	1.180	0.9893	8.501	0.9899
303	490.36	0.021	0.6389	0.989	0.722	0.9686	6.734	0.9328
308	211.00	0.032	0.5156	1.837	0.841	0.9830	5.432	0.9797
313	-136.64	-0.024	0.4030	8.872	1.122	0.9825	3.953	0.9491

*Coefficient units: K_{La} (kg-solution/kg); q_m (kg/kg-adsorbent); K_F (kg/(kg-adsorbent(kg/kg-solution)$^{1/n}$)); K_{Li} (kg-solution/kg-adsorbent)

3.4 Adsorption thermodynamics

To obtain useful information for the design of adsorption process, thermodynamics parameters of adsorption (Gibb's free energy change: ΔG, enthalpy change: ΔH and entropy change: ΔS) were evaluated. Based on the discussion in section of adsorption isotherm, adsorption equilibrium constants at various temperatures were calculated using Freundlich model and ΔG and ΔS were calculated using Eq(6) and Eq(7), respectively.

$$\Delta G = -RT ln K_F \quad (6)$$

$$ln K_F = \frac{\Delta S}{R} - \frac{\Delta H}{RT} \quad (7)$$

From Eq(7), enthalpy change (ΔH) and entropy change (ΔS) were calculated from the slope and the y-intercept of the straight line plot between lnK_F and 1/T. As summarized in Table 3, adsorption had negative values of ΔG, ΔH and ΔS. The negative value of ΔG indicated that the adsorption was spontaneous and feasible. The increase of ΔG with respect to temperature indicated that the adsorption was more favorable at lower temperatures. Since the calculated values of ΔG was in the range of -20,000 to 0 J/mol, stigmasterol adsorption on SA-R could be considered as physical adsorption (Yu et al., 2001). The negative value of ΔH indicated that the adsorption was in section of adsorption isotherm. The negative value of ΔS indicated associative adsorption and decreased of the randomness between the solid/liquid interfaces due to the adsorption.

3.5 Feasibility of sterol recovery using adsorption technique

In conventional sterol recovery technique, vacuum distillation must be operated at temperature around 453 to 473 K, much higher than room temperature while cold crystallization usually be operated at 253 – 288 K, much lower than room temperature, and requires extremely long crystallization time (7.92 – 2.6 ×10^4 s). It should be noted that the adsorption using SA-R can be operated at the condition not far from ambient temperature and

pressure and the time required for adsorption to reach the equilibrium was extremely short compared with the crystallization time. Therefore, adsorption should be promising method in large scale operation for sterol recovery since it should reduce large amount of overall energy consumption in sterol recovery.

Table 3: Thermodynamics parameters of stigmasterol adsorption on SA-R

T (K)	ΔG (J/mol)	ΔH (J/mol)	ΔS (J/(mol·K))
298	-5,020.63	-49,339.43	-148.65
303	-4,277.40		
308	-3,534.17		
313	-2,790.94		

4. Conclusions

Analysis of kinetics, isotherm and thermodynamics of stigmasterol adsorption on commercial cation-exchange styrene-divinylbenzene resin with strong acid functional group (SA-R) revealed that SA-R was promising for separation of sterol from solution. Adsorption capacity at equilibrium of stigmasterol on SA-R increased with the increase of initial concentration of stigmasterol. The adsorption rate of stigmasterols on SA-R could be described by pseudo-second-order kinetics model. Equilibrium data was well fitted with Freundlich isotherm ($R^2 \geq 0.9686$) and better than Langmuir and linear isotherm models. The thermodynamics parameters indicated that the adsorption of stigmasterol on SA-R was exothermic and spontaneous processes.

Acknowledgments

Financial support from Thailand Research Fund (TRF) and King Mongkut's Institute of Technology Ladkrabang (KMITL) under Royal Golden Jubilee Ph.D. program (PHD/0021/2555) and National Research Council of Thailand (NRCT) are acknowledged.

References

Azizian S., 2004, Kinetic models of sorption: a theoretical analysis, Journal of Colloid and Interface Science, 276, 47-52.

Chang C.J., Chang Y.F., Lee H.Z., Lin J.Q., Yang P.W., 2000, Supercritical carbon dioxide extraction of high–value substances from soybean oil deodorizer distillate, Industrial & Engineering Chemistry Research, 39, 4521-4525.

Fernandes P., Cabral J.M.S., 2007, Phytosterols: Applications and recovery methods, Bioresource Technology, 98, 2335–2350.

Ho Y.S., Mckay G., 1999, Batch lead (II) removal from aqueous solution by peat: equilibrium and kinetics, Transactions of the Institution of Chemical Engineers, 77B, 165–173.

Khatoon S., Raja Rajan R.G., Gopala Krishna A.G., 2010, Physicochemical characteristics and composition of Indian soybean oil deodorizer distillate and the recovery of phytosterols, Journal of the American Oil Chemists' Society, 87, 321-326.

Moreira E.A., Baltanás M. A., 2004, Recovery of phytosterols from sunflower oil deodorizer distillates, Journal of the American Oil Chemists' Society, 81, 161-167.

Njimou J.R., Stoller M., Cicci A., Chianese A., Nanseu-Njiki C.P., Ngameni E., Bravi M., 2017, Adsorption of phenol/tyrosol from aqueous solutions on macro-reticular aromatic and macro-porous polystyrene cross-linked with divinylbenzene polymeric resins, Chemical Engineering Transactions, 57, 757-762.

Rohr R., 2003, Process for separation unsaponifiable valuable products from raw materials, US Patent, 2003/0120095 A1, USA.

Verleyen T., Verhe R., Garcia L., Dewettinck K., Huyghebaert A., Greyt W.D., 2001, Gas chromatographic characterization of vegetable oil deodorization distillate, Journal of Chromatography A, 921, 277–285.

Víctor-Ortega M.D., Ochando-Pulido J.M., Martínez-Ferez A., 2016, Equilibrium studies on phenol removal from industrial wastewater through polymeric resins, Chemical Engineering Transactions, 47, 253-258.

Wollmann G., Schwarzer J., Gutsche B., 2005, Processes for producing sterols from fatty acid production residues, US Patent, 6956125 B2, USA.

Yu Y., Zhuang Y.Y., Wang Z.H., 2001, Adsorption of water–soluble dye onto functionalized resin, Journal of Colloid and Interface Science, 242, 288–293.

Kinetics, isotherm and thermodynamics of sterol adsorption on styrene-divinylbenzene anion exchange resins

Chinakrit Ladadok[a], Takehiro Yamaki[b], Keigo Matsuda[c], Hideyuki Matsumoto[d], Duangkamol Na-Ranong[a]*

[a]Department of Chemical Engineering, Faculty of Engineering, King Mongkut's Institute of Technology Ladkrabang, 1, Chalongkrung 1, Ladkrabang, Bangkok 10520, Thailand
[b]National Institute of Advanced Industrial Science and Technology, Research Institute for Chemical Process Technology, 1-1-1 Higashi, Tsukuba, Ibaraki, Japan
[c]Department of Chemistry and Chemical Engineering, Graduate School of Science and Engineering, Yamagata University, 4-3-16, Jonan, Yonezawa-shi, Yamagata 992-8510, Japan
[d]Department of Chemical Science and Engineering, School of Materials and Chemical Technology, Tokyo Institute of Technology, 2-12-1 Ookayama, Meguro-ku, Tokyo 152-8552, Japan

* Corresponding author, e-mail: dnaranong@hotmail.com, duangkamol.na@kmitl.ac.th

ABSTRACT: Phytosterols can be recovered from natural resources using molecular distillation~~adsorption~~, cold crystallization, which require large energy consumption. Adsorption was considered as a feasible alternative methods. In this study, kinetics, isotherm and thermodynamics of phytosterols adsorption on styrene-divinylbenzene with two different functional groups, strong base (SB-R) and weak base (WB-R), were investigated using a model solution of stigmasterol in n-heptane. Isothermal adsorption experiments were performed in temperature range of 298-313 K and concentration range of 0.3 – 6.0 mg/g_{sol}. For both SB-R and WB-R cases, kinetics of adsorption were analyzed based on pseudo-first-order and pseudo-second-order models and the results revealed that pseudo-second-order model agreed with the experimental data much better than pseudo-first-order model. Analysis of isotherm data based on Langmuir, Freundlich and linear models showed that Freundlich was the best model that could predict behavior of sterol adsorption for both SB-R and WB-R cases. In addition, thermodynamics parameters (ΔG, ΔH and ΔS) indicated that the sterol adsorptions on these adsorbents were spontaneous, exothermic and favorable at low temperature.

KEYWORDS: phytosterols, separation, adsorption process

INTRODUCTION

Deodorizer distillate (DD) is a major byproduct from vegetable oil refining process. It consists of various hydrocarbons including free fatty acids (FFA), monoglycerides (MG), diglycerides (DG), triglycerides (TG) and small amount of some bioactive compounds [1]. The amount of FFA in DD varies around 25-82.5 wt% depending on type of vegetable oil, refining method and condition [2]. In recent years, large amount of DD has been annually generated due to high demand of biodiesel. Based on the amount of crude palm oil produced in 2014-2016 in Thailand, Indonesia and Malaysia (53 million ton per year), annually generated amount of palm fatty acid diatillate (PFAD) was about 3 million ton per year [3-9]. To make overall process of biodiesel production become more economical reasonable and environmental friendly, DD has been utilized as a low cost raw material for production of biodiesel [9] and as a natural resource of phytonutrients such as tocopherols, squalene and sterols [2]. Sterols were presented in varying concentrations in the DD such as campesterol (5.06 wt%), stigmasterol (4.1 wt%), and β-sitosterol (7.9 wt%) were found in soybean oil deodorizer distillate while brassicasterol was not found. Brassicasterol (1.64 wt%), campesterol (2.93 wt%), stigmasterol (0.01 wt%), and β-sitosterol (4.05 wt%) were found in rapeseed oil deodorizer distillate. Campesterol (0.45 wt%), stigmasterol (0.62 wt%), β-sitosterol (2.6 wt%), and other sterols (0.62 wt%) were found in sunflower oil deodorizer distillate while brassicasterol was not found [1].

Sterols have several beneficial bioactivities and have been therefore widely used in food, cosmetics and pharmaceutical industries [10]. As summarized in an excellent review [10], in an industrial scale production, sterols have been successfully recovered from DD by several methods. In general, these methods consisted of several steps of chemical and physical treatments. Since removal of undesired compounds (FFA and glycerides) from DD by distillation requires relatively high temperature and extremely low pressure, it is necessary to transform these undesired compounds to the forms that can be separated more easily. In one approach, FFA in DD was saponified and the resulted soap was removed from the obtained mixture by simple solid-liquid separation. In the last step, sterols were separated from the liquid mixture of unsaponifiable components by using either vacuum distillation or cold crystallization [11-13]. In the other approach, FFA and glycerides were chemically transformed to fatty acid alkyl esters (FAAE) by esterification and transesterification, respectively [14-18]. Then, either vacuum distillation or molecular distillation was applied to remove large fraction of FAAE. In this sterol preconcentration step, multiple steps of these physical treatments were usually applied to obtain high yield of sterol recovery and to reduce the size of the equipment

Formatted: Not Highlight

used in the downstream process. Similar to the former approach, cold crystallization was also applied as the last step of sterol isolation.

~~Moreira and Baltanás [16] focused on cold crystallization process and investigated effects of process variables on the quality and yield of sterol recovered from DD of sunflower oil. In their work, FFA and TG in DD were transformed to fatty acid ethyl esters (FAEE) and FAEE was removed by performing vacuum distillation at 1.3 mbar, ≤ 200 °C. Crystallization of the sterols in the obtained preconcentrated mixture was optimized by varying type of solvent (hexane single solvent, hexane with cosolvent), type of co-solvent (water, ethanol or both), mass ratio of solvent to preconcentrated mixture (3 to 5), cooling rate (-20 °C/h or brisk chilling from 40 to -5 °C), crystallization temperature (-20 to 0 °C) and ripening time (4 to 96 h). Based on the experimental results, the optimized yield (84%) with purity (36 %) of sterol was obtained at solvent to preconcentrated mixture mass ratio of 4 with cooling rate of -20°C/h to -5 °C and ripening time = 22 h using co-solvent of 2.5 wt% of ethanol in hexane.~~

~~Carmona et al [18] pointed that the preconcentration of sterol in FAME matrices required large amount of energy and also destroyed some sterols present in the matrices. Therefore, they proposed an alternative method for isolation of sterols from FAME matrices with no requirement of vacuum distillation. Crystallization was performed in FAME, which was formed from esterification and/or transesterification, without either additional FAME or partial distillation. The obtained isolated solid was then washed with hexane and gave the end-product of sterols. By using this proposed method, at the best condition of crystallization (-5 °C, 24 h), 35-42% of sterols were recovered from sunflower oil deodorizer distillate and had high purity of more than 92 %. In addition, some cases resulted in the end-product of sterols with the purity higher than 99 %.~~

Adsorption is widely used in separation of minor components from liquid or gas mixture under mild conditions. It was successfully applied to recovery of sterols from natural resources [23-25]. Barder et al [23-25] described an adsorption-desorption process using activated carbon, carbonaceous pyropolymer or magnesium silicate as an adsorbent and chlorobenzene, toluene or methyl-t-butyl ether as a desorbent. The described process could recover sterols from feed mixtures with wide range of sterol concentration (14-84 wt%), with high recovery portion (50-95%). The obtained sterols had reasonably high purity 58-78%, or even as high as 95% when the feed mixture was appropriately pretreated by liquid-liquid extraction.

Based on chemical resistance and simplicity of operation, two types of commercial grade styrene-divinylbenzene copolymer ion exchange resin were considered as attractive adsorbents in the sterol recovery process. As reported by Anasthas and Gaikar [26], sterol

Formatted: Tab stops: 1.25 cm, Left

adsorption on polymeric adsorbent occurred through a weak hydrogen bond between amino group on polymer matrix and hydroxyl group of sterol. Therefore, a strong base resin (SB-R) with quaternary amine functional group and a weak base resin (WB-R) with both quaternary and tertiary amine groups were selected in this study. The objective of this study was to comparatively investigate behavior of sterol adsorption on these resins. Isothermal batch adsorption was performed using stigmasterol in n-heptane as a model solution in order to evaluate adsorption capacities of SB-R and WB-R. Kinetics of sterol adsorption for both cases were evaluated based on pseudo-first-order and pseudo-second-order models. In addition, adsorption data at equilibrium were analyzed based on Langmuir, Freundlich and linear isotherms and three important thermodynamics parameters (i.e. Gibb's free energy change: ΔG, enthalpy change: ΔH and entropy change: ΔS) were calculated and the adsorption behavior was discussed based on the calculated thermodynamics parameters.

MATERIALS AND METHODS

Materials

To comparatively evaluate performance of phytosterol adsorption on a weak base and a strong base adsorbents, styrene-divinylbenzene copolymer anion-exchange resins with quaternary amine (Lewatit® Monoplus MP 800) and tertiary-quaternary amine (Lewatit® Monoplus MP 68) functional groups provided by Lanxess, Germany were selected as representatives of a weak- and a strong base ion exchange resins (WB-R and SB-R), respectively. Table 1 summarized characteristic properties of these two adsorbents. To remove moisture from the adsorbents, the adsorbents were dried in an oven at 60 °C under vacuum condition for 6 h and stored in a desiccator before being used in adsorption experiment. Prior to the adsorption experiment, the adsorbents were washed with n-propanol and n-hexane.

Formatted: Tab stops: 1.25 cm, Left

Stigmasterol supplied by Tama Biochemical Co. Ltd. and n-heptane (AR grade) supplied by Apex Chemicals Co. Ltd. were used in preparation of a model solution of phytosterol containing mixture. Cholesterol supplied from Sigma-Aldrich Inc. was used as an internal standard (ISTD) in quantitative an analysis of stigmasterol. HPLC grade organic solvents (methanol, acetonitrile and water supplied from RCI Labscan Ltd. and acetic acid supplied from Merck Ltd.) were used in the quantification of stigmasterol without purification.

Batch adsorption

To study kinetics, isotherm and thermodynamics of stigmasterol adsorptions on WB-R and SB-R, isothermal batch adsorption was performed using a model solution of stigmasterol in n-heptane. Adsorption temperature and stigmasterol concentration were varied in the ranges of 298 – 313 K and 0.3 - 6.0 mg/g_{sol}, respectively. The model solution (50 ml) and the adsorbent (5 wt%) were heated and shaken in an orbital shaker (4000ic; IKA) at 200 rpm for 2 h. Before and after the adsorption, samples (200 µl) were taken and filtered through a 0.45 µm nylon filter and used for the quantitative analysis of stigmasterol content.

Quantitative analysis

The content of stigmasterol in the sample was analyzed using a high performance liquid chromatograph (HPLC) connected with a UV detector. An injection valve connected with a 20 µl of sample loop was used to introduce the sample into the HPLC. Peak separation was achieved using a reverse-phase column (Inertsil C8-3; 5 µm particle diameter, 250 mm length, 4.6 mm i.d., GL Sciences Inc, Japan). Composition of mobile phase and condition of analysis were adapted from the work reported by Chang et al [27]. Mobile phase was a mixture of acetonitrile (85%), methanol (5%), and water containing 1% of acetic acid (10%) and flowed at the rate of 1.3 ml/min, the analysis was performed at the wavelength of 210 nm.

Since the sample was not dissolved well in the mobile phase, ~~n-heptane in the sample was removed and an appropriate solvent was added to the solid sample as a solvent in the quantitative analysis. The solvent exchange was performed as follows; n-heptane was completely removed from the sample by evaporation at room temperature, methanol (800µl) was then added and the mixture was shaken in the orbital shaker at 200 rpm for 1 h. As an internal standard, cholesterol in methanol (4.0 mg/g_{sol}, 200 µl) was added in the sample.~~ n-heptane was evaporated from sample in the first step and 800 µl of methanol was added. The sample was shaken at 200 rpm for 1 h, and then 200 µl of ISTD (cholesterol in methanol at 4.0 mg/g_{sol}) was added. 100 µl of the prepared sample was injected into the HPLC through the injection valve.

Amount of stigmasterol adsorbed on the adsorbent at time "*t*" (q_t) was calculated according to Eq. (1).

$$q_t = \frac{(C_0 - C_t)W_{sol}}{W_{ads}} \qquad (1)$$

Where C_0 and C_t are liquid-phase concentration of stigmasterol at initial and at time *t*, respectively. W_{sol} is the weight of the solution and W_{ads} is the weight of adsorbent used.

RESULTS AND DISCUSSION

Formatted: Left, Line spacing: 1.5 lines

Adsorption capacities

Fig. 1 shows time dependences of adsorption capacity of SB-R and WB-R at 303 K and 5 wt% of adsorbent loading for various initial concentrations of stigmasterol. For both SB-R and WB-R cases, adsorption rapidly occurred in the initial period and after 5 minutes of adsorption the rate of adsorption gradually decreased while the adsorption equilibrium was approached. In the tested range, adsorption reached the equilibrium within 30 min for all the initial concentrations. Comparison of the profiles obtained at different initial concentrations revealed that the rates of adsorption on both resins increased with the increase of concentration of stigmasterol. This observation could be explained as a result of the increase of concentration leading to increase in the driving force to overcome overall mass transfer resistance of adsorption process [28]. By increasing the initial concentration of stigmasterol from 0.3 to 6.0 mg/g_{sol}, in the case of SB-R, the adsorption capacity at the equilibrium (q_e) increased from 2.15 to 39.96 mg/g_{ads}. On the other hand, in the case of WB-R, q_e increased from 2.51 to 47.44 mg/g_{ads}. The adsorption capacity at the equilibrium of WB-R was approximately 1.2 times higher than SB-R.

Adsorption kinetics

To study the kinetics of adsorption, the experimental data were comparatively analyzed based on pseudo-first-order and pseudo-second-order models which are expressed as Eqs. (2) and (3), respectively [29, 30].

$$\frac{dq_t}{dt} = k_1(q_e - q_t) \qquad (2)$$

$$\frac{dq_t}{dt} = k_2(q_e - q_t)^2 \qquad (3)$$

Where q_e and q_t are the amounts of stigmasterol adsorbed at equilibrium and at time t, respectively. k_1 and k_2 are the adsorption rate constant of pseudo-first-order and pseudo-second-order model, respectively. Linearized forms of these two models obtained by integrating Eqs. (2) and (3) with the boundary conditions of $q_t = 0$ at $t = 0$ and $q_t = q_t$ at $t = t$ are expressed as Eqs. (4) and (5), respectively.

$$\ln(q_e - q_t) = \ln q_e - k_1 t \qquad (4)$$

$$\frac{t}{q_t} = \frac{1}{k_2 q_e^2} + \frac{t}{q_e} \qquad (5)$$

Linear plots corresponding to pseudo-first-order and pseudo-second-order models for SB-R are shown in Figs. 2(a) and 2(b), respectively. The parameters, k and q_e, of each model were calculated from the slope and the y-intercept of the corresponding linear plot and summarized

in Table 2. As shown in the table, the correlation coefficients (R^2) of pseudo-second-order model were higher than those of pseudo-first-order model for all conditions. The lowest value of R^2 obtained from pseudo-second-order model was 0.9986 while the highest value of R^2 obtained from pseudo-first-order model was 0.9899. Furthermore, $q_{e,cal}$ from pseudo-second-order model agreed reasonably well with $q_{e,exp}$ ($\Delta q_e < 7.5\%$) while pseudo-first-order model could not well predict the value of $q_{e,exp}$. Based on the correlation coefficients and Δq_e, pseudo-second-order model was selected to describe the kinetics of stigmasterol adsorption on SB-R. In the case of adsorption on WB-R, similar linear plots corresponding to the two kinetics models were obtained, as shown Fig. 3. The calculated parameters of each model were also summarized in Table 2. The results revealed that R^2 of pseudo-second-order model was higher than R^2 of pseudo-first-order model and $\Delta q_{e,\ pseudo\text{-}second\text{-}order}$ was less than $\Delta q_{e,pseudo\text{-}first\text{-}order}$ for all conditions. Therefore, pseudo-second-order model was selected as the suitable model for describing the kinetics of stigmasterol adsorption on WB-R as well.

For both SB-R and WB-R cases, k_2 depended on the initial concentration of stigmasterol (C_0). When C_0 was increased from 0.3 to 6.0 mg/g_{sol}, $k_{2,SB\text{-}R}$ decreased from 0.0585 to 0.0115 while $k_{2,WB\text{-}R}$ decreased from 0.1012 to 0.0115 g_{ads} /(mg min). This dependence of k_2 on initial concentration was previously reported in several adsorption systems [31-33]. Theoretically analysis by Azizian [34] clearly showed that k_2 is not an intrinsic rate constant of adsorption, but it is a complex function of adsorption rate constant, desorption rate constant and initial concentration of adsorbate.

Adsorption isotherm

Adsorption isotherm was investigated at 298, 303, 308 and 313 K and discussed based on the data taken after 1 h of adsorption, which were reasonably considered as the performance at the equilibrium of adsorption according to the discussion in section of adsorption capacities. Fig. 4 shows dependence of adsorption capacity at the equilibrium (q_e) on concentration of stigmasterol at the equilibrium (C_e) at 303 K. For both SB-R and WB-R, in the tested range of C_e, q_e increased with C_e and saturation of adsorption were not observed. Fig. 5 shows effect of temperature on q_e for various initial concentrations. For both SB-R and WB-R, q_e decreased when the temperature was increased. This result indicated that stigmasterol adsorption was exothermic for both SB-R and WB-R cases. It should be noted that this dependence was significant in the case of high initial concentration and became less significant when the initial concentration was lower.

Equilibrium adsorption data were analyzed based on Langmuir, Freundlich and linear isotherm models using the corresponding linearized form of each model, listed in Table 3. Langmuir model was considered as an inappropriate model for prediction of isotherm of stigmasterol adsorption for both SB-R and WB-R since the value of R^2 was extremely low, the obtained q_m (saturated adsorption capacity) and K_{La} (Adsorption equilibrium constant in Langmuir model, g_{sol}/mg) were negative, which had no physical meaning for adsorption process. Since R^2 of Freundlich model were larger than R^2 of linear model for all conditions, excepting SB-R at 313 K, Freundlich model was considered as the most suitable model to be used to predict the performance of adsorption at the equilibrium for both SB-R and WB-R. However, it should be noted that the calculated values of $1/n$ were nearly equal to 1 for all conditions, indicating that the concentration of stigmasterol in overall tested range in this study was low and the adsorption behaved like linear model. In addition, for both SB-R and WB-R cases, the calculated K_F (Adsorption equilibrium constant in Freundlich model, $mg/(g_{ads}(mg/g_{sol})^{1/n})$ decreased when the temperature of adsorption was increased.

Fig. 4 shows good resemblances of the calculated curves and the experimental data for both Freundlich and linear models. Similar plots (not shown) were obtained at the other temperatures (298, 308 and 313 K) and showed good resemblances of the calculated curves and the experimental data, as well. In the case of SB-R (Fig. 4a), nonlinear regression analysis was performed for both Freundlich and linear models and gave the same R^2 (0.9438). Based on regression analysis, Freundlich model was the most suitable model for prediction of effect of C_e on q_e in the tested range of $0 < C_e < 4.5$ mg/g_{sol} and $298 < T < 313$ K.

In the case of WB-R, similar results were obtained. Fig. 4b shows that both models show good resemblances of the calculated curves and the experimental data, as well. Regression analysis revealed that Freundlich model was slightly better than linear model (Freundlich model: $R^2 = 0.9706$; liner model: $R^2 = 0.9557$). Therefore, Freundlich model was also the most suitable model for prediction of effect of C_e on q_e in stigmasterol adsorption on WB-R.

Adsorption thermodynamics

In order to obtain useful information for the design of adsorption process, thermodynamics parameters of adsorption (Gibb's free energy change: ΔG, enthalpy change: ΔH and entropy change: ΔS) were evaluated for both SB-R and WB-R cases. Based on the discussion in section of adsorption isotherm, adsorption equilibrium constants at various temperatures were calculated using Freundlich model and ΔG and ΔS were calculated using Eqs. (6) and (7), respectively.

$$\Delta G = -RT \ln K_F \quad (6)$$

$$\ln K_F = \frac{\Delta S}{R} - \frac{\Delta H}{RT} \quad (7)$$

By performing linear regression analysis of the plot between $\ln K_F$ and $1/T$, as shown in Fig. 6, enthalpy change (ΔH) and entropy change (ΔS) were calculated from the slope and the y-intercept of the obtained straight line. As summarized in Table 4, for both SB-R and WB-R, adsorption had negative values of ΔG, ΔH and ΔS. The negative value of ΔG indicates that the adsorption is spontaneous and feasible. The increase of ΔG with respect to temperature indicates that the adsorption is more favorable at lower temperatures [35]. Since the calculated values of ΔG for both SB-R and WB-R cases were in the range of -20 to 0 kJ/mol, stigmasterol adsorption on SB-R and WB-R could be considered as physical adsorption [36]. The negative value of ΔH indicates that the adsorption is exothermic and agreed well with the effect of temperature on adsorption capacity at the equilibrium discussed in section of adsorption isotherm. Comparison of $\Delta H_{SB\text{-}R}$ (-24.97 kJ/mol) and $\Delta H_{WB\text{-}R}$ (-14.03 kJ/mol) indicates that the interaction between stigmasterol and SB-R is stronger than the interaction between stigmasterol and WB-R. The negative value of ΔS indicates associative adsorption and decrease of the randomness between the solid/liquid interface due to the adsorption [37, 38].

CONCLUSIONS

Analysis of kinetics, isotherm and thermodynamics of stigmasterol adsorption on commercial anion exchange styrene-divinylbenzene resin with strong and weak base functional group (SB-R and WB-R) revealed that both SB-R and WB-R were promising for separation of phytosterols from sterol containing mixture. Adsorption capacity at equilibrium of stigmasterol on WB-R was higher than SB-R. The adsorption rate of phytosterols on SB-R and WB-R could be described by pseudo-second-order kinetics model. Equilibrium data was well fitted with Freundlich isotherm ($R^2 \geq 0.9510$) and better than Langmuir and linear isotherm models. The thermodynamics parameters indicated that the adsorption on both resins were exothermic and spontaneous processes. In considering the possibility of reusing of resin, although desorption and reusability experiments of resin were not shown in this work. However, the thermodynamic values (ΔG and ΔH) for both SB-R and WB-R cases were indicated that the adsorption between sterol and resin occurred on the low interaction energy. It is relatively simple to separate sterol from resin after adsorption step. Therefore, resin should be able to reuse after desorption process due to it would decrease processing cost. However, the adsorption efficiency of the resin may be reduced by the number of reuse.

*Acknowledgement*s: Authors gratefully acknowledge financial supports from Thailand Research Fund (TRF) and King Mongkut's Institute of Technology Ladkrabang (KMITL) under Royal Golden Jubilee Ph.D. program (PHD/0021/2555) and from National Research Councils of Thailand (NRCT).

REFERENCES

1. Verleyen T, Verhe R, Garcia L, Dewettinck K, Huyghebaert A, Greyt WD (2001) Gas chromatographic characterization of vegetable oil deodorization distillate. *J Chromatogr A* **921**, 277–85.
2. Gunawan S, Ju YH (2009) Vegetable oil deodorizer distillate: characterization, utilization and analysis. *Sep Purif Rev* **38**, 207–41.
3. Wright T, Wiyono E (2014) Indonesia oilseed and products update July 2014. *United States Department of Agriculture* **ID1427**.
4. Abdi A, Wright T, Rahmanulloh A (2017) Oilseeds and products annual report 2017. United States Department of Agriculture **ID1705**.
5. Malaysian Palm Oil Board (2016) Overview of the Malaysian oil palm industry.
6. Malaysian Palm Oil Board (2017) Overview of the Malaysian oil palm industry.
7. Richey B, Preechajarn S (2015) Thailand palm oil production supply demand update. *United States Department of Agriculture* **TH5074**.
8. Santella R, Preechajarn S (2016) Thailand Oilseed and Product Annual 2016. *United States Department of Agriculture* **TH6049**.
9. Echim C, Verhé R, Greyt WD, Stevens C (2009) Production of biodiesel from side-stream refining products. *Energy Environ Sci* **2**, 1131–41.
10. Fernandes P, Cabral JMS (2007) Phytosterols: applications and recovery methods. *Biores Technol* **98**, 2335–50.
11. Yang H, Yan F, Wu D, Huo M, Li J, Cao Y, Jiang Y (2010) Recovery of phytosterols from waste residue of soybean oil deodorizer distillate. *Bioresour Technol* **101**, 1471–76.
12. Khatoon S, Rajan RGR, Krishna AGG (2010) Physicochemical characteristics and composition of Indian soybean oil deodorizer distillate and the recovery of phytosterols. *J Am Oil Chem Soc* **87**, 321–26.
13. Rohr R (2003) Process for separation unsaponifiable valuable products from raw materials. *US Patent* **2003/0120095 A1**.

14. Brown W, Smith FE (1964) Process for separating tocopherols and sterols from deodorizer sludge and the like. *US Patent* **3153055**.
15. Fizet C (1996) Process for tocopherols and sterols from natural sources. *US Patent* **5487817**.
16. Moreira EA, Baltanás MA (2004) Recovery of Phytosterols from sunflower oil deodorizer distillates. *JAOCS* **81**, 161-67.
17. Wollmann G, Schwarzer J, Gutsche B (2005) Processes for producing sterols from fatty acid production residues. *US Patent* **6956125 B2**.
18. Carmona MA, Jiménez C, Sanchidrián CJ, Peña F, Ruiz JR (2010) Isolation of sterols from sunflower oil deodorizer distillate. *J Food Eng* **101**, 210–13.
19. Watanabe Y, Nagao T, Hirota Y, Kitano M, Shimada Y (2004) Purification of tocopherols and phytosterols by a two-step *in situ* enzymatic reaction. *JAOCS* **81**, 339-45.
20. Yan F, Yang H, Li J, Wang H (2012) Optimization of phytosterols recovery from soybean oil deodorizer distillate. *J Am Oil Chem Soc* **89**, 1363–70.
21. Smith FE (1967) Separation of tocopherols and sterols from deodorizer sludge and the like. *US Patent* **3335154**.
22. Lin KM (2003) Separation of sterols from deodorizer distillate by crystallization. *J Food Lipids* **10**, 107-27.
23. Barder TJ (1989) Purification of sterols with activated carbon as adsorbent and chlorobenzene as desorbent. *US Patent* **4882065**.
24. Barder TJ, Johnson P (1989) Adsorption separation of sterols from tall oil pitch carbon adsorbent. *US Patent* **4849112**.
25. Barder TJ, Bedwell WB, Johnson SP (1990) Separation of sterols from low-acid feeds with magnesium silicate and methyl-tert-butyl ether desorbent. *US Patent* **4977243**.
26. Anasthas HM, Gaikar VG (1999) Adsorptive separations of alkylphenols using ion-exchange resins. *React Funct Polym* **39**, 227–37.
27. Chang CJ, Chang YF, Lee HZ, Lin JQ, Yang PW (2000) Supercritical carbon dioxide extraction of high–value substances from soybean oil deodorizer distillate. *Ind Eng Chem Res* **39**, 4521–5.
28. Aksu Z (2001) Biosorption of reactive dyes by dried activated sludge: equilibrium and kinetic modelling. *Biochem Eng J* **7**, 79–84.

29. Lin J, Wang L (2009) Comparison between linear and non-linear forms of pseudo-first-order and pseudo-second-order adsorption kinetic models for the removal of methylene blue by activated carbon. *Front Environ Sci Engin China* **33**, 320–24.
30. Ho YS, Mckay G (1999) Pseudo–second order model for sorption processes. *Process Biochem* **34**, 451–65.
31. Ho YS, Mckay G (1999) Batch lead (II) removal from aqueous solution by peat: equilibrium and kinetics. *Trans IChemE* **77**, 165–73.
32. Hameed BH, Ahmad AL, Latiff KNA (2007) Adsorption of basic dye (methylene blue) onto activated carbon prepared from rattan sawdust. *Dyes Pigm* **75**, 143–9.
33. Chen H, Zhao J (2009) Adsorption study for removal of congo red anionic dye using organo–attapulgite. *Adsorption* **15**, 381–9.
34. Azizian S (2004) Kinetic models of sorption: a theoretical analysis. *J Colloid Interf Sci* **276**, 47–52.
35. Chu BS, Baharin BS, Man YBC, Quek SY (2004) Separation of vitamin E from palm fatty acid distillate using silica: I equilibrium of batch adsorption. *J Food Eng* **62**, 97–103.
36. Yu Y, Zhuang YY, Wang ZH (2001) Adsorption of water–soluble dye onto functionalized resin. *J Colloid Interf Sci* **242**, 288–93.
37. Scheckel KG, Sparks DL (2001) Temperature effects on nickel sorption kinetics at the mineral–water interface. *Soil Sci Soc Am J* **65**, 719–28.
38. Rattanaphani S, Chairat M, Bremner JB, Rattanaphani V (2007) An adsorption and thermodynamic study of lac dyeing on cotton pretreated with chitosan. *Dyes Pigm* **72**, 88–96.

FIGURE LEGENDS

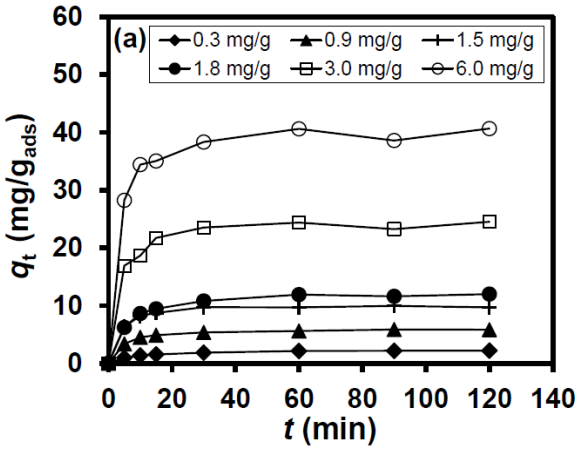

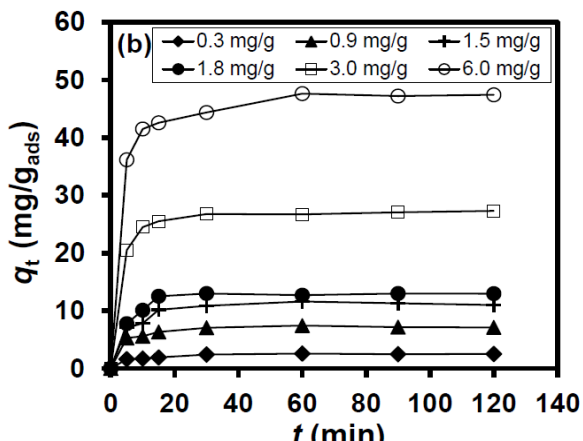

Fig. 1 Adsorption capacities of stigmasterol on (a) SB-R and (b) WB-R versus adsorption time at 303 K and 5 wt% of adsorbent loading for various initial stigmasterol concentrations.

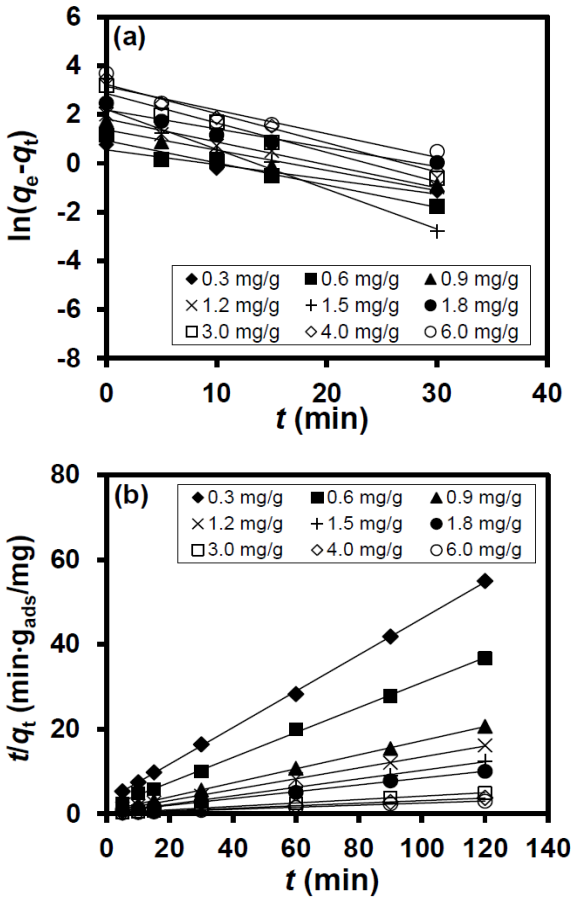

Fig. 2 Linear plots of (a) pseudo-first-order and (b) pseudo-second-order kinetics models for SB-R at 303 K and 5 wt% of adsorbent loading for various initial stigmasterol concentrations.

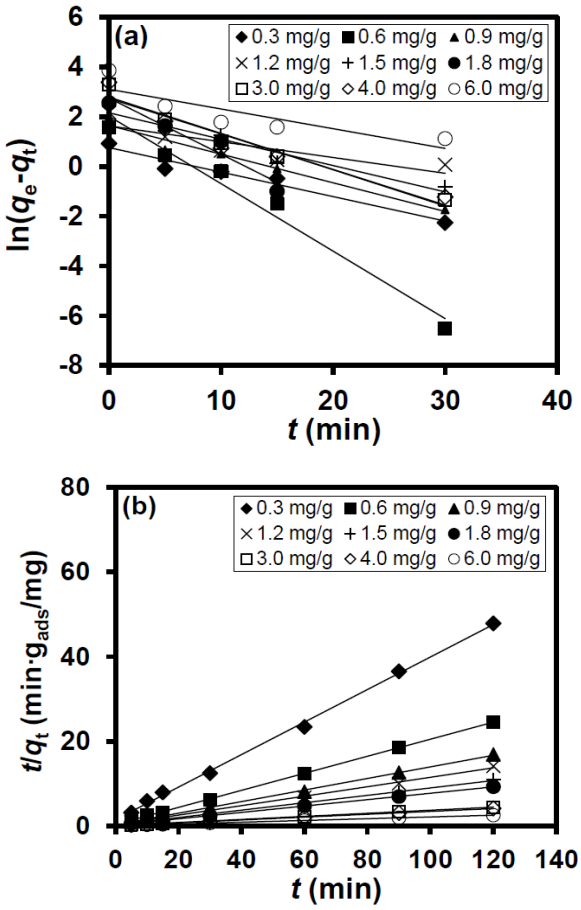

Fig. 3 Linear plots of (a) pseudo-first-order and (b) pseudo-second-order kinetics models for WB-R at 303 K and 5 wt% of adsorbent loading for various initial stigmasterol concentrations.

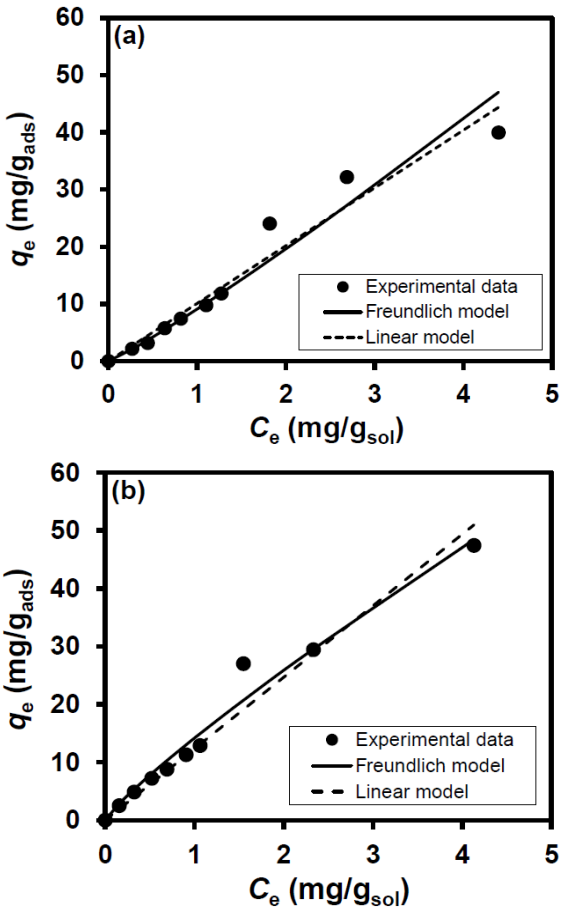

Fig. 4 Dependences of q_e on C_e calculated using Freundlich and linear model comparing with the experimental data for adsorption of stigmasterol on (a) SB-R and (b) WB-R, (T = 303 K, adsorbent loading = 5 wt%).

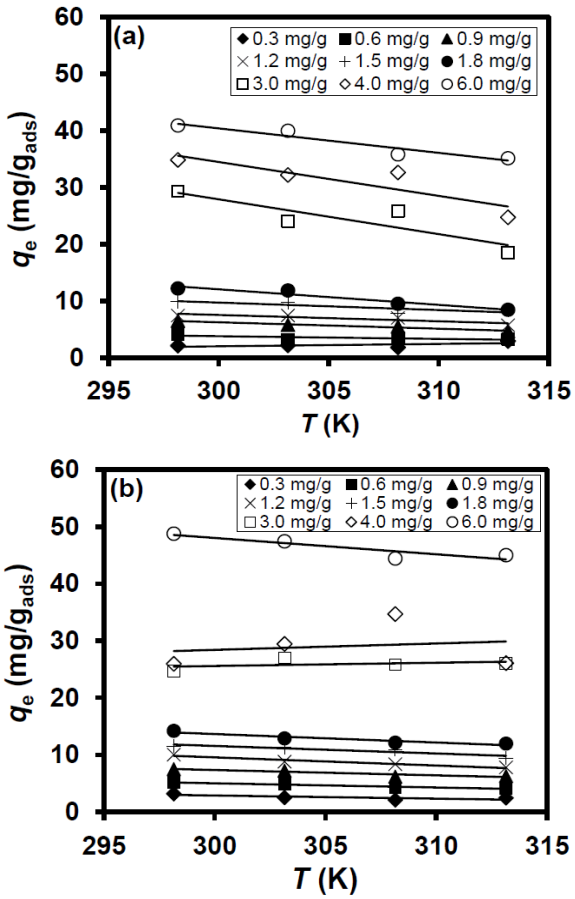

Fig. 5 Effect of temperature on the adsorption capacity of (a) SB-R and (b) WB-R at the equilibrium (q_e) for various initial stigmasterol concentrations, (T = 298–313 K, adsorbent loading = 5 wt%).

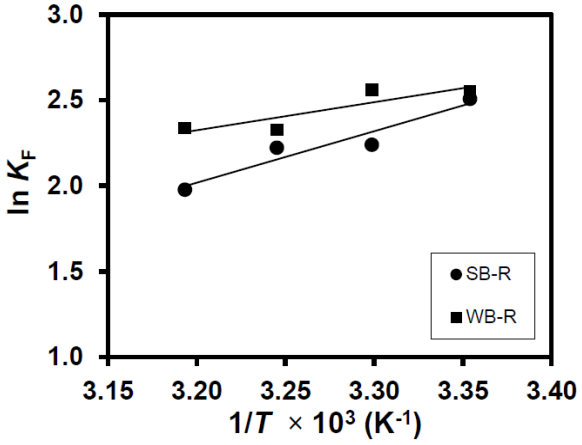

Fig. 6 Plot of lnK_F versus 1/T for SB-R and WB-R.

605
606
607
608
609
610
611
612
613
614
615
616
617
618
619
620
621
622
623
624

625 **TABLE LEGENDS**

626

627 **Table 1** Properties of adsorbents

Properties	SBA-R	WB-R
Commercial name	Lewatit® Monoplus MP 800	Lewatit® Monoplus MP 68
Type	Strong base macroporous	Weak base macroporous
Functional group	Quaternary amine, type I	Tertiary/quarternary amine
Matrix structure	Crosslinked polystyrene	Crosslinked polystyrene
Bead size (mm)	0.65 (± 0.05)	0.54 (± 0.05)
Total exchange capacity (min.eq/l)	0.8	1.3
Operating pH range	0 – 12	0 - 7
Operating temperature (max.°C)	70	70

628
629
630

646 **Table 2** Kinetic parameters of stigmasterol adsorptions on SB-R and WB-R at 303 K with different initial concentrations.

Adsorbents	C_0 (mg/g_{sol})	$q_{e,exp}$ (mg/g_{ads})	Pseudo-first-order				Pseudo-second-order			
			k_1 (min^{-1})	$q_{e,cal}$ (mg/g_{ads})	$\triangle q_e$ (%)	R^2	k_2 (g_{ads}/(mg min))	$q_{e,cal}$ (mg/g_{ads})	$\triangle q_e$ (%)	R^2
SB-R	0.3	2.1529	0.0605	1.7319	19.6	0.9475	0.0585	2.3272	7.5	0.9997
	0.6	3.1703	0.0911	2.5199	20.5	0.9628	0.0588	3.3898	6.5	0.9988
	0.9	5.7515	0.0832	3.9240	31.8	0.9121	0.0446	6.0168	4.4	0.9998
	1.2	7.4262	0.0943	6.1688	16.9	0.9804	0.0312	7.7640	4.4	0.9996
	1.5	9.7616	0.1637	9.0948	6.8	0.9899	0.0531	9.9502	1.9	0.9993
	1.8	11.8279	0.0772	8.8401	25.3	0.9413	0.0179	12.4069	4.7	0.9994
	3.0	24.0448	0.1209	17.4842	27.3	0.9694	0.0175	24.6914	2.6	0.9986
	4.0	32.1690	0.1200	25.4191	21.0	0.9829	0.0121	33.0033	2.5	0.9995
	6.0	39.9560	0.0970	23.3617	41.5	0.8892	0.0115	40.8163	2.1	0.9987
WB-R	0.3	2.5126	0.0984	2.1308	15.2	0.9607	0.1012	2.6001	3.4	0.9984
	0.6	4.8633	0.2711	7.5210	35.3	0.9765	0.1199	4.9628	2.0	0.9998
	0.9	7.2292	0.1151	5.1841	28.3	0.9623	0.0787	7.2939	0.9	0.9990
	1.2	8.8029	0.0635	5.0957	42.1	0.7450	0.0405	8.9445	1.6	0.9973
	1.5	11.2957	0.1059	8.6331	23.6	0.9437	0.0377	11.4286	1.2	0.9979
	1.8	12.8865	0.2255	15.5615	17.2	0.9333	0.0348	13.2450	2.7	0.9994
	3.0	27.0299	0.1458	16.2031	40.1	0.9529	0.0263	27.5482	1.9	0.9999
	4.0	29.4413	0.1429	15.4113	47.7	0.9208	0.0429	29.5858	0.5	0.9997
	6.0	47.4444	0.0792	22.2202	53.2	0.7337	0.0115	48.3092	1.8	0.9998

647

648

649

650

651

652 **Table 3** Parameters and correlation coefficients for Langmuir, Freundlich and linear models for isotherms of stigmasterol adsorption on SB-R
653 and WB-R.

Models		Langmuir: $q_e = \frac{q_m K_{La} C_e}{1 + K_{La} C_e}$			Freundlich: $q_e = K_F C_e^{1/n}$			Linear: $q_e = K_{Li} C_e$	
Linearized Equation; Parameters		$\frac{C_e}{q_e} = \frac{1}{K_{La} q_m} + \frac{1}{q_m} C_e$; K_{La}, q_m			$\log(q_e) = \log(K_F) + \frac{1}{n}\log(C_e)$; K_F, $1/n$			$q_e = K_{Li} C_e$; K_{Li}	
Adsorbents	T (K)	K_{La} (g_{sol}/mg)	q_m (mg/g_{ads})	R^2 (-)	K_F (mg/(g_{ads}(mg/g_{sol})$^{1/n}$))	$1/n$ (-)	R^2 (-)	K_{Li} (g_{sol}/g_{ads})	R^2 (-)
SB-R	298	-0.0094	-1,250.0	0.0055	12.11	1.0690	0.9698	11.91	0.8822
	303	-0.0552	-153.8	0.2036	9.30	1.1333	0.9794	10.09	0.9438
	308	-0.0524	-158.7	0.1732	9.12	1.1131	0.9744	9.89	0.9121
	313	-0.0491	-131.6	0.1356	7.10	1.0337	0.9510	7.88	0.9752
WB-R	298	0.0104	1,250.0	0.0142	12.83	0.9727	0.9887	12.87	0.9797
	303	0.0613	238.1	0.2782	13.48	0.9258	0.9836	12.34	0.9557
	308	-0.0785	-114.9	0.3173	10.25	1.1785	0.9845	11.53	0.9589
	313	-0.0452	-212.8	0.1966	10.35	1.0721	0.9811	11.20	0.9611

654
655
656
657
658

659 **Table 4** Thermodynamics parameters of stigmasterol adsorptions on SB-R and WB-R.

T (K)	SB-R			WB-R		
	Δ*G* (kJ/mol)	Δ*H* (kJ/mol)	Δ*S* (kJ/(mol K))	Δ*G* (kJ/mol)	Δ*H* (kJ/mol)	Δ*S* (kJ/(mol K))
298	-6.22	-24.97	-0.06	-6.20	-14.03	-0.03
303	-5.65			-6.43		
308	-5.69			-5.85		
313	-5.15			-5.97		

660
661

Author Biography

Name	Chinakrit Ladadok
Date of Birth	10 December 1986
Address	89, M. 6, Nikhom Sang Ton-Eng Lam Dom Noi Sub-district, Sirindhorn District, Ubon Ratchathani Province
Education	2009 Bachelor of Engineering (Chemical Engineering) Khon Kean University, Thailand 2012 Master of Engineering (Chemical Engineering) Khon Kean University, Thailand

Publications

- Chinakrit Ladadok, Sarawut Sinpichai, Nattawat Nonthanasin, Krittin Binabdullah, and Duangkamol Na-Ranong, "Synthesis of Moleculary Imprinted Polymer Originated from TFMAA and TRIM for Sterol Separation" *Chemical Engineering Transactions*, 70 (2018) 475-480.
- Chinakrit Ladadok, Takehiro Yamaki, Keigo Matsuda, Hideyuki Matsumoto, and Duangkamol Na-Ranong, "Kinetics, Isotherm, and Thermodynamics of Adsorption of Sterol on Strong Acid Ion Exchange Resin" *Chemical Engineering Transactions*, 70 (2018) 1075-1080.
- Chinakrit Ladadok, Takehiro Yamaki, Keigo Matsuda, Hideyuki Matsumoto, and Duangkamol Na-Ranong, "Kinetics, Isotherm, and Thermodynamics of sterol adsorption on styrene divinylbenzene anion exchange resins" *ScienceAsia* (accepted)

Conferences

- Chinakrit Ladadok and Duangkamol Na-Ranong "Separation of Phytosterols from Fatty Acid Methyl Esters Using Adsorption-Desorption Process" *RGJ-Ph.D. Congress 17*, 8-11 June 2016, Pattaya, Chonburi.
- Chinakrit Ladadok, Sarawut Sinpichai, Nattawat Nonthanasin, Krittin Binabdullah, and Duangkamol Na-Ranong, "Synthesis of Moleculary Imprinted Polymer Originated from TFMAA and TRIM for Sterol Separation" *23rd International Congress of Chemical and Process Engineering CHISA 2018*, 25-29 August 2018, Prague, Czech Republic.

- Chinakrit Ladadok, Takehiro Yamaki, Keigo Matsuda, Hideyuki Matsumoto, and Duangkamol Na-Ranong, “Kinetics, Isotherm, and Thermodynamics of Adsorption of Sterol on Strong Acid Ion Exchange Resin” *23rd International Congress of Chemical and Process Engineering CHISA 2018*, 25-29 August 2018, Prague, Czech Republic.